WSRC-TR-2002-00424
SRT-RPP-2002-00214

Key Words:
Hanford River Protection Project,
Waste Treatment Plant, Evaporation

Retention Period: Permanent

Key WTP R&T References:
Test Specification:
24590-WTP-TSP-RT-01-008, Rev. 0
Test Plan: WSRC-TR-2001-00408,
SRT-RPP-2001-00160, Rev. 0
Test Scoping Statement: S79

PHYSICAL PROPERTY MODELS OF CONCENTRATED CESIUM ELUATE SOLUTIONS

A. S. Choi
T. B. Edwards
R. A. Pierce

Issue Date: April 15, 2003

Westinghouse Savannah River Company
Savannah River Site
Aiken, SC 29808

Prepared for the U.S. Department of Energy Under Contract Number DE-AC09-96SR18500

SRS savannah river site ™

TABLE OF CONTENTS

Page

LIST OF FIGURES ..... **iii**
LIST OF EXHIBITS ..... **v**
LIST OF TABLES ..... **v**
LIST OF ACRONYMS ..... **vi**
ABSTRACT **1**
1.0 SUMMARY OF TESTING **1**
1.1. Objectives 1
1.2. Conduct of Testing 2
1.3. Results and Performance Against Objectives 3
1.4. Quality Requirements 5
1.5. Issues **5**
2.0 INTRODUCTION **5**
3.0 DISCUSSION **6**
3.1. Identification of Major Analytes and Their Bounding Concentration Ranges 6
3.2. Design of Computer Test Matrix 10
3.2.1. Definition of Factor Space 10
3.2.2. Definition of Mathematical Model 11
3.2.3. Selection of Candidate Design Points 12
3.2.4. Design Points for Phased Computer Runs 12
3.3. Semi-Batch Evaporation Model 15
3.4. Nitric Acid Database 17
3.5. Calculation of Physical Property Data 21
3.5.1. Model Bases 21
3.5.2. Model Results 22
3.6. Derivation of Physical Property Models 25
4.0 FUTURE WORK **36**
5.0 REFERENCES **37**
APPENDIX A. **A1**
APPENDIX B. **B1**
APPENDIX C. **C1**
APPENDIX D. **D1**
APPENDIX E. **E1**
APPENDIX F. **F1**

LIST OF FIGURES

Page

FIGURE 3.1. Scatter Plots of Initial (red closed squares) and Secondary (orange open squares) Design Points Using OLH Approach 13
FIGURE 3.2. Schematic of N^{th} Stage Evaporation of Cs Eluate Model. 16
FIGURE 3.3. Comparison of Calculated Heat Capacities of HNO_3-H_2O System vs. Literature Data at 20 ^oC 18
FIGURE 3.4. Calculated vs. Measured Equilibrium Pressures at 50 ^oC for HNO_3-H_2O System 19
FIGURE 3.5. Profiles of Concentration, Density, and VRF during Semi-Batch Evaporation of Cesium Eluate Matrix Feed #22 23
FIGURE 3.6. Profiles of Cumulative Condensate Acidity and Boilup Pressure during Semi-Batch Evaporation of Cesium Eluate Matrix Feed #22 23
FIGURE 3.7. Volume Reduction Factor vs. Feed Acidity during Semi-Batch Evaporation of Cesium Eluate Matrix Feed #22 24
FIGURE 3.8. Results from Fitting Density Model Using Phase 1 and 2 Data @ 80% Saturation - Actual vs. Predicted Densities (g/ml) 27
FIGURE 3.9. Results from Fitting Volume Reduction Factor (VRF) Model Using Phase 1 and 2 Data @ 80% Saturation - Actual vs. Predicted VRFs 28
FIGURE 3.10. Results from Fitting Viscosity Model Using Phase 1 and 2 Data @ 80% Saturation - Actual vs. Predicted Viscosities 29
FIGURE 3.11. Results from Fitting Heat Capacity Model Using Phase 1 and 2 Data @ 80% Saturation - Actual vs. Predicted Heat Capacities (cal/g/^oC). 30
FIGURE 3.12. Results from Fitting Solubility Model Using Phase 1 and 2 Data @ 100% Saturation - Actual vs. Predicted Solubilities (g TS/ml). 31
FIGURE 3.13. Results from Fitting Solubility Model Using Phase 1 and 2 Data @ 100% Saturation - Actual vs. Predicted Solubilities (g TS/1000 g H_2O). 32
FIGURE 3.14. Results from Fitting Density Model Using Phase 1 and 2 Data @ 100% Saturation - Actual vs. Predicted Densities (g/ml). 33
FIGURE 3.15. Results from Fitting Viscosity Model Using Phase 1 and 2 Data @ 100% Saturation - Actual vs. Predicted Viscosities (cP) 34
FIGURE 3.16. Results from Fitting Heat Capacity Model Using Phase 1 and 2 Data @ 100% Saturation - Actual vs. Predicted Heat Capacities (cal/g/^oC). 35
FIGURE D-1. Results from Fitting Density Model Using Phase 1 Data @ 80% Saturation – Actual vs. Predicted Densities (g/ml). D7
FIGURE D-2. Results from Fitting Volume Reduction Factor Model Using Phase 1 Data @ 80% Saturation – Actual vs. Predicted VRFs. D8
FIGURE D-3. Results from Fitting Viscosity Model Using Phase 1 Data @ 80% Saturation – Actual vs. Predicted Viscosities (cP). D9
FIGURE D-4. Results from Fitting Heat Capacity Model Using Phase 1 Data @ 80% Saturation – Actual vs. Predicted Heat Capacities (cal/g/^oC). D10
FIGURE D-5. Overlay Plot of Response versus Model Prediction with ± 15% Error Bands – Density (g/ml) @ 80% Saturation D11

LIST OF FIGURES *(Cont'd)*

Page

FIGURE D-6. Overlay Plot of Response versus Model Prediction with ± 15% Error Bands – Volume Reduction Factor @ 80% Saturation. D12
FIGURE D-7. Overlay Plot of Response versus Model Prediction with ± 15% Error Bands – Viscosity (cP) @ 80% Saturation. D13
FIGURE D-8. Overlay Plot of Response versus Model Prediction with ± 15% Error Bands – Heat Capacity (cal/g/^{o}C) @ 80% Saturation. D14
FIGURE E-1. Results from Fitting Solubility Model Using Phase 1 Data @ 100% Saturation – Actual vs. Predicted Solubilties (g TS/ml). E8
FIGURE E-2. Results from Fitting Solubility Model Using Phase 1 Data @ 100% Saturation – Actual vs. Predicted Solubilities.(g TS/1000 g H_2O) E9
FIGURE E-3. Results from Fitting Density Model Using Phase 1 Data @ 100% Saturation – Actual vs. Predicted Densities (g/ml). E10
FIGURE E-4. Results from Fitting Viscosity Model Using Phase 1 Data @ 80% Saturation – Actual vs. Predicted Viscosities (cP). E11
FIGURE E-5. Results from Fitting Heat Capacity Model Using Phase 1 Data @ 100% Saturation – Actual vs. Predicted Heat Capacities (cal/g/^{o}C). E12
FIGURE E-6. Overlay Plot of Response versus Model Prediction with ± 15% Error Bands – Solubility (g TS/ml) @ 80% Saturation.....E13
FIGURE E-7. Overlay Plot of Response versus Model Prediction with ± 15% Error Bands – Solubility (g TS/1000 g H_2O) @ 80% Saturation.....E14
FIGURE E-8. Overlay Plot of Response versus Model Prediction with ± 15% Error Bands – Density (g/ml) @ 100% Saturation.....E15
FIGURE E-9. Overlay Plot of Response versus Model Prediction with ± 15% Error Bands – Viscosity (cP) @ 100% Saturation. E16
FIGURE E-10. Overlay Plot of Response versus Model Prediction with ± 15% Error Bands – Heat Capacity (cal/g/^{o}C) @ 100% Saturation.....E17

LIST OF EXHIBITS

Page

EXHIBIT D-1. Responses of Interest @ 80% Saturation vs. Test Factors. D2
EXHIBIT E-1. Responses of Interest @ 100% Saturation vs. Test Factors. E2

LIST OF TABLES

Page

TABLE 1.1. Temperature and Concentration Ranges for Computer Test Matrix 3
TABLE 1.2. Coefficients of Eq. (1.1) Set by Statistical Analysis Using JMP® 4
TABLE 3.1. Analytical Data for Cesium Eluate Samples Used in Test Matrix Development (Data Taken from Ref. [2]). 7
TABLE 3.2. Major and Minor Species Selected for Computer Test Matrix. 9
TABLE 1.1. Temperature and Concentration Ranges for Computer Test Matrix. 11
TABLE 3.3. 31 OLH Design Points Selected for Phase 2 Computer Runs. 14
TABLE 3.4. 12 Design Points Selected for Phase 1 Computer Runs 15
TABLE 3.5. Comparison of Calculated Densities of 38 wt% HNO_3 in H_2O vs. Literature Data at 20 ^oC 17
TABLE 3.6. Measured vs. Calculated Solubilities and Densities of Ternary Systems Using Binary and Ternary HNO3DB 19
TABLE 3.7. Validation of 6-Component Nitric Acid Database 20
TABLE A-1. Assumed Organic Distribution in Cesium Eluate A3
TABLE A-2. Charge Balance Results for Tank AN-103 Cesium Eluate Sample Collected During an SRTC Bench-Scale IX Run A4
TABLE A-3. Charge Balance Results for Tank AN-102 Cesium Eluate Sample Collected During an SRTC Bench-Scale IX Run A5
TABLE A-4. Charge Balance Results for Tank AZ-102 Cesium Eluate Sample Collected During an SRTC Bench-Scale IX Run A6
TABLE A-5. Charge Balance Results for Tank AN-105 Cesium Eluate Sample Collected During an SRTC Bench-Scale IX Run A7
TABLE A-6. Charge Balance Results for Tank AN-107 Cesium Eluate Sample Collected During an SRTC Bench-Scale IX Run A8
TABLE A-7. Charge Balance Results for Tank AW-101 Cesium Eluate Sample Collected During a PNNL Bench-Scale IX Run A9
TABLE A-8. Charge Balance Results for Tank AN-107 Cesium Eluate Sample Collected During a PNNL Bench-Scale IX Run A10
TABLE B-1. 21 Design Points Generated for Mixture Response Surface Model in Scaled Weight Fractions (SWF). B2
TABLE B-2. 30 Design Points Selected for Phase 3 Computer Runs B3
TABLE B-3. Test Matrix for 3-Phase Computer Runs with Mixture Factors in Given Weight Fractions (WF) B4
TABLE C-1. Input Flows for Cesium Eluate Evaporation Model Run - Matrix 22 ..... C2
TABLE C-2. Calculated Physical Properties at 80% Saturation of $NaNO_3$ C3
TABLE C-3. Calculated Physical Properties at 100% Saturation of $NaNO_3$ C4

LIST OF ACRONYMS

EDTA	Ethylenediamine-N,N,N'N'-tetraacetic acid
ESP	Environmental Simulation Program
HEDTA	N-(2-Hydroxyethyl)-ethylenediamine-N,N',N'-triacetic acid
IDA	Iminodiacetic acid
IX	ion-exchange
NTA	Nitrilotriacetic acid
OLHs	Orthogonal Latin Hypercubes
PNNL	Pacific Northwest National Laboratory
RPP	River Protection Project
SRTC	Savannah River Technology Center
TFL	Thermal Fluids Lab
TOC	total organic carbon
TRU	Transuranic
V&V	verification and validation
VLE	vapor-liquid equilibrium
WTP	Waste Treatment Plant

This page left intentionally blank.

ABSTRACT

Major analytes expected to be present in the WTP cesium ion-exchange eluate solutions were identified from the available analytical data collected during radioactive bench-scale runs, and a test matrix of cesium eluate solutions was designed within the bounding concentration ranges of those major analytes. A computer model describing the semi-batch evaporation of cesium eluate solutions was built using the Environmental Simulation Program (ESP), licensed by OLI Systems, Inc., and was run to calculate the physical properties of each test matrix solution concentrated to the target endpoints of 80% and 100% bulk saturation. The calculated physical properties were then analyzed statistically and fitted into predetermined mathematical expressions for the bulk solubility, density, viscosity and heat capacity as a function of temperature and feed concentration of each species considered in the matrix. In addition, the volume reduction factor, which is defined as the ratio of total cumulative feed volume to that of the initial acid charge, was calculated and modeled for the 80% saturation case. The R^2 of the resulting physical property models ranged from 0.89 to 0.99. Validation of these physical property models against the true experimental data was not part of the current work scope; instead, the results of model validation will be discussed later in another report, after all the necessary data for model validation have been collected and analyzed.

1. SUMMARY OF TESTING

1.1. Objectives

The original scope of this task was to develop mathematical expressions for the bulk solubility, density and heat capacity of concentrated cesium eluate solutions as a function of temperature and concentrations of significant analytes present in the as-received Envelope A, B and C eluate feeds [1]. The task scope was later expanded to include the development of additional correlations for viscosity and the volume reduction factor that can be achieved at the prescribed evaporation endpoints. The bulk solubility is defined in this task as the point where the solution becomes just saturated with one or more of the major salt species present or supersaturated with other minor salt species to the extent that the total insoluble solids formed exclusively out of minor salt constituents would exceed 1.0 wt% of the entire solution.

The necessary data to develop such physical property models were to be calculated by the computer simulation of semi-batch cesium eluate evaporation using a statistically designed matrix of test solutions as the feed. The resulting physical property models or correlations will be used to support the design and operation of the RPP-WTP cesium eluate evaporator; specifically to (1) predict the heating/cooling duties and volume of concentrated eluate, (2) provide the evaporator operating parameters, and (3) provide the operating data and correlations for the RPP-WTP flowsheet model. The acceptance criterion for the physical property models was specified in the task plan as the relative difference of ±15% or less between the model predictions and the measured data during the upcoming bench-scale evaporation tests [1].

1.2. Conduct of Testing

The overall task to develop the physical property models of concentrated cesium eluate solutions was carried out in the following six steps:

A. *Identification of major analytes in cesium eluate solutions and their bounding concentration ranges* - Much of this was done in an earlier experimental work [2], but one major drawback of that work was that the most dominant species on a molar basis, hydronium ion or H^+, was not included as one of the matrix variables. So, a charge balance was performed in this task on each eluate data set to estimate the concentration of H^+, since it was not measured during the bench-scale runs, and the bounding concentration ranges of all major analytes, including H^+, were re-developed on a dry mass fraction basis.

B. *Statistical design of a test matrix of cesium eluate solutions* - A test matrix was designed for computer experimentation from the bounding concentration ranges determined in Step A and the temperature range between 20 and 60 ^oC. Each design point of the test matrix represented a test cesium eluate solution, whose physical properties were to be calculated at the prescribed endpoints using the semi-batch evaporation model developed in Step C. The minimum number of required design points was determined by the mathematical form of the physical property models defined in Step F.

C. *Development of semi-batch evaporation model* – The process model of semi-batch eluate evaporation was developed using the Environmental Simulation Program (ESP) version 6.5, licensed by OLI Systems, Inc. [3]. The evaporator pot was initially charged with 7.25 M nitric acid, and the required vacuum for the boilup at 50 ^oC was calculated by the model. The liquid level in the pot was maintained constant throughout the evaporation cycle by controlling the boilup rate or the vacuum. The OLI/ESP model was run in conjunction with two databases; the software default database called PUBLIC v6.5 and a private database called HNO3DB.

D. *Development of HNO3DB database* – It was found earlier that the PUBLIC database predicted neither the in-house nor the literature data on density and heat capacity of the nitric acid-water binary system adequately [4], and efforts to improve its predictability were already underway prior to the initiation of this task. However, it was later found during this study that the PUBLIC database would require a major overhaul of its thermodynamic and physical property parameters that had been used to describe the systems containing nitric acid. As a result, efforts to further improve the database for the ternary and higher-order nitric acid systems continued into this project, and the result was the development of a private database, called HNO3DB, optimized for the $NaNO_3$-KNO_3-$CsNO_3$-$Al(NO_3)_3$-HNO_3-H_2O system using both the SRTC in-house and literature data.

E. *Calculation of physical properties* – For each matrix feed defined in Step B, the semi-batch evaporation model was run in conjunction with the HNO3DB database until the 100% saturation limit was reached. It turned out that every test matrix feed became saturated with $NaNO_3$ well before any other salt species would precipitate out. The 80% bulk saturation was determined as the point where the calculated ion activity product of Na^+ and NO_3^- equaled 0.8 times the solubility product. Once the evaporation endpoints were determined, the density and viscosity of the final eluate solutions were recorded directly from the model output. The heat capacities were estimated from the enthalpies calculated at 0.5 ^oC increments within ±3 ^oC of each specified temperature using the OLI Express facility of the ESP software. The calculation of bulk solubility and volume reduction factor also required some manipulation of the model output.

F. *Development of physical property models* – The physical property data calculated in Step E were fitted into the model shown in Eq. (1.1) using JMP® statistical software and the least squares linear regression [5,6]:

$$\begin{aligned} \textit{Physical Property} \;=\; & \beta_1 \cdot [Al^{+3}] + \beta_2 \cdot [Ca^{+2}] + \beta_3 \cdot [Cs^+] \\ & + \beta_4 \cdot [H^+] + \beta_5 \cdot [K^+] + \beta_6 \cdot [Na^+] \\ & + \beta_7 \cdot [Al^{+3}] \cdot Temp + \beta_8 \cdot [Ca^{+2}] \cdot Temp \\ & + \beta_9 \cdot [Cs^+] \cdot Temp + \beta_{10} \cdot [H^+] \cdot Temp \\ & + \beta_{11} \cdot [K^+] \cdot Temp + \beta_{12} \cdot [Na^+] \cdot Temp \end{aligned} \qquad (1.1)$$

where β*'s* are the constants, *concentrations* in scaled weight fraction to those six cations only, and *Temp* is the temperature in degrees Celsius.

1.3. Results and Performance Against Objectives

The major analytes selected for inclusion in the physical property models and their bounding concentration ranges are shown in Table 1.1. The concentrations are given in terms of scaled weight fractions, i.e., the concentrations of the six major cations shown would add up to 1 for any matrix point. Nitrate, NO_3^-, was the only counter-balancing anion used. Besides those shown in Table 1.1, several minor cations such as Cr^{+3}, Fe^{+3}, and Zn^{+2} were also added to the model at fixed concentrations as the background species.

Table 1.1. Temperature and Concentration Ranges for Computer Test Matrix.

Al^{+3}	Ca^{+2}	Cs^+	H^+	K^+	Na^+	Temperature
wt fraction	wt fraction	wt fraction	Wt fraction	wt fraction	wt fraction	(^oC)
0.0017	0.0000	0.0036	0.0500	0.0141	0.5834	20
0.1243	0.1597	0.1983	0.3188	0.1309	0.7641	60

A test matrix consisting of 73 design points was constructed based on the concentration and temperature ranges given in Table 1.1. A phased approach was used to run the semi-batch evaporation simulation of these design points. In Phase I, the first 12 design points were run to provide the minimum necessary data to determine the values of the 12 coefficients of Eq. (1.1) that represented a particular physical property. In Phase 2, the next 31 design points were run to provide the "virtual experimental data," which were then used to evaluate the performance of the linear models. These Phase-2 design points were generated using the Orthogonal Latin Hypercubes (OLH) approach to ensure that the entire range of each input variable shown in Table 1.1 is fully represented. In Phase 3, the remaining 30 design points were to be run to determine if any additional terms need to be added to Eq. (1.1) in case the linear mixture models are found to be inadequate to explain all the variations seen in the model responses.

It turned out that the physical property models developed based on the first 12 design points would fit all 31 Phase 2 design points well within the task acceptance criterion of ±15% that it was deemed unnecessary to run the Phase 3 design points for further improvement of the models. Once validated against the OLH points, the final physical property models were then developed using all 43 design points of Phase 1 and 2. The resulting values for the 12 coefficients of Eq. (1.1) that best fit the design points are tabulated in Table 1.2 for the five physical properties of interest at 80% and 100% saturation. The applicable ranges of these coefficients or models are given in Table 1.1 in terms of scaled weight fractions of the six concentration variables and temperature. These physical property models will be validated later against the real experimental data. An example of how to apply Eq. (1.1) and the coefficients in Table 1.2 together for the property estimation is given in Appendix F, Sample Calculations.

TABLE 1.2. Coefficients of Eq. (1.1) Set by Statistical Analysis Using JMP®.

coefficients	80% Saturation				100% Saturation			
	density (g/ml)	viscosity (cP)	heat capacity (cal/g/°C)	VRF*	density (g/ml)	viscosity (cP)	heat capacity (cal/g/°C)	solubility (g TS/ml)
β_1	1.36176	6.11135	0.53721	139.01782	1.48886	12.72718	-0.03378	0.73699
β_2	1.44401	3.03668	0.57243	48.97029	1.47408	4.95164	0.38964	0.74161
β_3	1.34916	2.26934	0.58492	27.90272	1.50460	3.95236	0.49192	0.69789
β_4	1.30755	2.94761	0.85864	63.09169	1.31406	2.14149	0.84166	0.51292
β_5	1.37269	1.59566	0.59123	54.90814	1.42237	2.51310	0.46440	0.77862
β_6	1.24086	1.66923	0.78125	-11.80459	1.25453	1.38919	0.83926	0.42178
β_7	-0.00244	0.03731	-0.01159	-3.30647	-0.00619	-0.07447	0.00287	-0.01693
β_8	-0.00162	-0.04848	0.00036	-1.07174	-0.00111	-0.09208	0.00499	-0.00097
β_9	0.00389	0.00220	0.00178	0.58164	0.00147	-0.02821	0.00185	0.00599
β_{10}	0.00061	-0.03509	-0.00621	7.73972	0.00142	-0.00294	-0.00599	0.00356
β_{11}	0.00270	0.02265	-0.00271	-0.48689	0.00209	0.00172	0.00039	0.00590
β_{12}	0.00217	-0.00210	-0.00213	0.52935	0.00240	0.00758	-0.00426	0.00559

* Volume Reduction Factor (VRF) is defined as the ratio of cumulative feed volume to initial acid volume.

1.4. Quality Requirements

This work was conducted in accordance with the RPP-WTP QA requirements specified for work conducted by SRTC as identified in DOE IWO MOSRLE60. SRTC has provided matrices to WTP demonstrating compliance of the SRTC QA program with the requirements specified by WTP. Specific information regarding the compliance of the SRTC QA program with RW-0333P, Revision 10, NQA-1 1989, Part 1, Basic and Supplementary Requirements and NQA-2a 1990, Subpart 2.7 is contained in these matrices.

The quality assurance plan for the ESP software has been issued [7]. The most essential element of the software verification and validation (V&V) relevant to this work is on the development of the HNO3DB database, which is discussed later in this report. The results presented in this report satisfy the requirements outlined in the Task Technical and Quality Assurance Plan for this task [1]. The task plan specifies that all work described in this report does not invoke the additional RW-0333P QA requirements.

1.5. Issues

There are no open issues in this task.

2. INTRODUCTION

The Hanford River Protection Project (RPP) Waste Treatment Plant (WTP) is currently being built to extract radioisotopes from the vast inventory of Hanford tank wastes and immobilize them in a silicate glass matrix. The baseline flowsheet for the pretreatment of supernatant liquid includes removal of cesium and technetium using regenerative ion-exchange resins [8,9]. The loaded cesium ion-exchange columns will be eluted with 0.5 molar nitric acid, and the resulting eluate solution will be concentrated in a thermosiphon reboiler to reduce the storage volume and to recover the acid for reuse [10]. The reboiler pot is initially charged with a concentrated nitric acid solution and kept under a controlled vacuum during feeding so the pot contents would boil at 50 ^{o}C. The liquid level in the pot is maintained constant by controlling both feed and boilup rates. The feeding will continue with no bottom removal until the solution in the pot reaches the target endpoint of 80% saturation with respect to any one of the major salt species present.

This task is concerned with the prediction of physical properties of the cesium eluate solutions concentrated to a target endpoint via the semi-batch evaporation process just described. In an earlier work [4], the mathematical correlations for density, viscosity and heat capacity of 80% saturated Tank 241-AN-107 (will be abbreviated as Tank AN-107 hereafter) cesium and technetium eluate solutions were derived as a function of temperature only. The test specification for this task requires that physical property correlations or models be developed specifically for the concentrated Tank AZ-102 cesium eluate as a function of both

temperature and unevaporated eluate composition [11]. Tank AZ-102, categorized as an Envelope B tank, was chosen because it contains the highest level of soluble cesium among all the tanks to be processed during the first 10 years of WTP operation. However, the scope was later expanded in the task plan to develop a set of physical property models that can be applied to Envelopes A and C as well as Envelop B cesium eluate feeds simultaneously [1]. Such *a priori* predictive tools encompassing all waste envelopes would undoubtedly yield valuable information on the design and operation of the eluate evaporator and storage tanks, thereby supplementing or even replacing necessary experimental tests.

A unique feature of this task is that the physical property models presented in this report were developed based on the "virtual data" generated from the computer experiments. The overall approach taken to develop those models can be broken down into the following six steps:

- Identification of major analytes present in the available cesium eluate samples and their bounding concentration ranges,
- Design of a test matrix for computer experiments within the bounding concentration ranges of major analytes and temperature between 20 and 60 ^{o}C,
- Development of the semi-batch evaporation process model,
- Development of the OLI software database for the nitric acid systems,
- Calculation of physical properties for each test matrix solution concentrated to the target endpoints of 80% and 100% bulk saturation,
- Derivation of mathematical correlations that best fit calculated physical properties as a function of major analyte concentrations and temperature.

In essence, this report is a summary of the results from each of these six steps. As required in the test specification, the physical property models developed in this task will be validated against the experimental data when the on-going bench-scale tests with simulated cesium eluate solutions are completed. The test specification also calls for similar modeling work on the technetium eluate physical properties; this task was completed earlier [12].

3. DISCUSSION

All the bases and assumptions employed in this modeling study are discussed next along with the key results from each of the six task steps mentioned above.

3.1. Identification of Major Analytes and Their Bounding Concentration Ranges

Available analytical data on the cesium eluate samples were compiled and analyzed earlier, and the major cations were chosen as the variables for the solubility test matrix [2]. The data tabulated in Table 3.1 were collected during small-scale ion-exchange

tests at SRTC and PNNL using actual Hanford supernate samples from Tanks AN-102, AN-103, AN-105, AN-107 and AZ-102. Since the degree of salt dilution that occurred during the elution and resin-reconditioning cycles was not the same in all tests, the data given in Table 3.1 reflect the re-normalization of the respective raw data to a constant 13 column-volume elution. Those six major cations chosen for the solubility test matrix were Na^{+}, K^{+}, Cs^{+}, Al^{+3}, Ca^{+2}, and Fe^{+3}, while minor cations (Cu^{+2}, Mg^{+2}, and Zn^{+2}) were also included in the matrix as the background species [2].

TABLE 3.1. Analytical Data for Cesium Eluate Samples Used in Test Matrix Development (Data Taken from Ref. [2]).

Sample ID	AN-103	AN-102	AZ-102	AN-105	AN-107	AW-101	AN-107
Data Source	SRTC	SRTC	SRTC	SRTC	SRTC	PNNL	PNNL
elution volume (CV)	13	13	13	13	13	13	13
Cs (uCi/mL)	2500	511	10523	1938	998	3220	365
Cs (ug/mL)	115	24	485	89	46	148	4
ICP-ES (mg/L)							
Na	1060	1480	1626	6246	931	4460	708
Al	59	268	4	614	30	282	3
Si	<1	98	<1	33	16	104	12
Cr	15	10	42	37	8	7	4
Ni	<19	4.5	<1	2	35	6	68
Pb	<81	<9.3	<2	14	9	10	8
Ca	290	66	9	86	10	4	<3
Cu	8	30	<1	6	16	102	15
Fe	12	7	4	4	63	24	5
Mg	13	9	<1	9	3	<1	<1
Zn	21	4	<1	<1	2	24	<1
B	<1	223	<1	45	39	<1	<1
U	322	17	15	17	203	96	67
K (AA)	72	80	107	296	33	764	16
Carbon (mg/L)							
TOC	940	470	267	10769	9308	240	116
TIC	188	<21	324	222	169		
IC (mg/L)							
NO3-	19000	22400	21300	26500	28200	33000	24500
NO2-			952				
Cl- (by IC)	8300						
Cl- (by ISE)		<22	292	293		<100	<2
F- (by IC)	<81						
F- (by ISE)		<11				<100	<2
PO4(3-)			<100			18	
SO4(2-)							
C2O4(2-)			<100				
Calculated Results							
H+ (mg/L)	241	280	289	81	404	292	363
wt% total solids	2.14	2.58	2.47	3.40	3.00	3.97	2.58

However, one major drawback of that early work was that the most dominant species on a molar basis, hydronium ion or H^+, was not included as one of the matrix variables. Instead, the solubility of each matrix solution was to be measured at the preset acid concentration of 3, 4 or 5 M in order to account for the effect of varying acidity on the bulk solubility.

In this task, the concentration of H^+ was treated as one of the variables for the computer test matrix. However, since the acidity of eluate solutions was not measured during bench-scale tests, it had to be estimated by performing a charge balance on the same analytical data sets as compiled in Table 3.1 for the solubility test matrix development. The concentrations of H^+ thus estimated are also shown in Table 3.1; they ranged from 0.24 to 0.40 M except for the Tank AN-105 sample taken at SRTC. The low acidity of that sample was the result of an abnormally high concentration of sodium, which could very well have been due to analytical errors. For this reason, the Tank AN-105 data set was deleted from further considerations, and the test matrix for this task was developed based on the remaining six data sets.

The estimated acidity of these eluate samples was as much as 50% lower than the initial eluant acidity of 0.5 M, in part because they contained other effluents displaced during the elution and regeneration cycles such as the pre- and post-elution caustic rinse. Further lowering of acidity occurs due to the elution process itself, i.e., substitution of the metal ions occupying the resin sites with the free hydrogen ions in the eluant. However, during a recent pilot-scale run at the Thermal Fluids Lab (TFL) of SRTC, the cesium eluate solution was produced without such dilution, and the measured concentration of free acid in the resulting eluate was 0.52 M, which is essentially the same as the initial eluant acidity [16].

The results of charge balance are shown in Tables A-2 to A-8 in Appendix A along with several assumptions and adjustments made to the analytical data in Table 3.1. In essence, all the data given above detection limits, except for the halides and TOC/TIC, were entered into the charge balance, and the concentration of H^+ was adjusted until the molar concentration of total equivalent cations matched that of total equivalent anions.

Once the acidity of each cesium eluate sample was estimated, the major and minor species of the computer test matrix were next determined, as shown in Table 3.2. The six major cations chosen were Na^+, H^+, Cs^+, K^+, Al^{+3}, and Ca^{+2} in the order of decreasing average weight fractions, and they formed the test matrix variables along with temperature. The seven minor cations were also added to the test matrix but only as the background species, and their concentrations were fixed at their respective average values shown in Table 3.2. Therefore, the seven minor cations together made up for 4.67 wt% of the total cations in each test matrix solution, and the concentrations of the six major cations were varied within their bounding concentration ranges to account for the remaining 95.33 wt%. Nitrate was the only counterbalancing anion chosen, since it constituted practically all the anions detected in the samples, as shown in Table 3.1.

TABLE 3.2. Major and Minor Species Selected for Computer Test Matrix.

Sample ID	AN-103	AN-102	AZ-102	AN-107	AW-101	AN-107	Avg	Min	Max
Data Source	SRTC	SRTC	SRTC	SRTC	PNNL	PNNL	All Data	All Data	All Data
Major Cations									
Cs (wt%)	6.03	1.06	18.90	2.89	2.42	0.34	5.27	0.34	18.90
K	3.78	3.54	4.17	2.08	12.48	1.34	4.56	1.34	12.48
Na	55.62	65.42	63.36	58.57	72.84	59.31	62.52	55.62	72.84
Al	3.10	11.85	0.16	1.89	4.61	0.25	3.64	0.16	11.85
Ca	15.22	2.92	0.35	0.63	0.07	0.00	3.20	0.00	15.22
H+	12.64	12.37	11.28	25.39	4.77	30.39	16.14	4.77	30.39
Minor Cations									
Cr	0.79	0.44	1.64	0.50	0.11	0.34	0.64	0.11	1.64
Ni	0.00	0.20	0.00	2.20	0.10	5.70	1.37	0.00	5.70
Pb	0.00	0.00	0.00	0.57	0.16	0.67	0.23	0.00	0.67
Cu	0.42	1.33	0.00	1.01	1.67	1.26	0.95	0.00	1.67
Fe	0.63	0.31	0.16	3.96	0.39	0.42	0.98	0.16	3.96
Mg	0.68	0.40	0.00	0.19	0.00	0.00	0.21	0.00	0.68
Zn	1.10	0.18	0.00	0.13	0.39	0.00	0.30	0.00	1.10
total	100.00	100.00	100.00	100.00	100.00	100.00			
total (major)	96.38	97.15	98.21	91.44	97.17	91.62	95.33		
total (minor)	3.62	2.85	1.79	8.56	2.83	8.38	4.67		
wt% total solids	2.14	2.58	2.47	3.00	3.97	2.58	2.79		
Na+H	68.26	77.79	74.63	83.96	77.61	89.70	78.66		

Table 3.2 includes all the species whose reported concentrations were above detection limits in Table 3.1 except uranium, silica and boron. Exclusion of these three species is based on the following observations:

- Although the uranium levels shown in Table 3.1 are significant enough to warrant further consideration even as one of the major species for the test matrix, the high data were due to the fact that the Sr/TRU precipitation step was not performed on the cesium IX feed, as the WTP pretreatment flowsheet calls for [2]. So, uranium was excluded from the matrix completely.

- Silica and boron were deleted from the list of potential minor species of the matrix because it was suspected that their presence was mainly due to the leaching of glassware during the storage of strongly acidic samples.

It is also noted in Table 3.2 that the unit of the test matrix variables is given in weight percent based on the cations only, instead of the more conventional wet-basis units such as molar. Use of this dry-basis unit is simply to avoid the possibility of predicting multiple evaporation endpoints for essentially the same feeds, which can occur due to the requirement of the test specification that the physical property models be expressed in terms of feed composition, rather than that of the concentrated solution. To illustrate this point, a hypothetical case is considered next.

Suppose we have two solutions, each having exactly the same absolute quantities of constituent ions as in the other, and the only difference is that the volume of one solution is twice that of the other due to different amounts of water in each solution. So, the wet-basis concentrations in the solution with less water would be twice as high as those in the other solution with more water. Now, if we were to evaporate the two solutions side-by-side in separate pots until one of the major salts starts to precipitate, we would then find that the two solutions would come to exactly the same endpoint, provided water is the only volatile component, as in the technetium eluate evaporation. This means that if the correlations were expressed in terms of molar concentrations of the feed, they would predict two very different physical properties for the same final concentrated solution.

In the case of cesium eluate evaporation, water is not the only volatile component, so the problem of multiple evaporation endpoint predictions does not appear to be likely. In fact, one of the goals of cesium eluate evaporation is to recover nitric acid for re-use, which is possible due to the significant vapor pressure exerted by nitric acid under the WTP evaporator operating conditions. However, the problem of multiple evaporation endpoint predictions could still occur even to this system with two volatile components, if the concentrations of nitric acid in the bottom and the overhead happen to closely follow the same vapor-liquid equilibrium curve for the multi-electrolyte system. Therefore, the dry-basis concentration unit was chosen in this task in order to preclude any potential for multiple evaporation endpoint predictions.

3.2. Design of Computer Test Matrix

A detailed account of the statistical approaches taken to develop the test matrix for computer experiments was given earlier [5]. The test matrix defines the necessary data points where physical properties need to be calculated using the computer model. The number of necessary data points is determined by both the number of variables or factors in the matrix and the mathematical form of a particular physical property model to be fitted. Some of the key bases and results of the earlier study are described next.

3.2.1. Definition of Factor Space

The minimum and maximum concentration ranges of the six major cations given in Table 3.2 along with the temperature range between 20 and 60 ^{o}C formed the factor space of interest in the design of the test matrix. These six cations were considered as mixture variables, and only those combinations of weight fractions that satisfy the following constraint was considered to be valid:

$$Cs + K + Na + Al + Ca + H = 0.9533 \quad (3.1)$$

where the positive charge sign of each cation has been omitted for simplicity. To frame this in the more standard form of a mixture problem, a new constraint was derived by dividing both sides of Eq. (3.1) by 0.9533:

$$Cs + K + Na + Al + Ca + H \quad = \quad 1.0 \tag{3.2}$$

where the concentration of each cation now represents the scaled weight fraction, and the new design space is given in Table 1.1. Temperature is the 7th design factor and considered as the process variable. So, it is not impacted by the mixture constraint.

Table 1.1. Temperature and Concentration Ranges for Computer Test Matrix.

Al^{+3}	Ca^{+2}	Cs^{+}	H^{+}	K^{+}	Na^{+}	Temp
SWF	SWF	SWF	SWF	SWF	SWF	(^{o}C)
0.0017	0.0000	0.0036	0.0500	0.0141	0.5834	20
0.1243	0.1597	0.1983	0.3188	0.1309	0.7641	60

* The upper temperature bound initially used in the Reference [5] was 70 ^{o}C.

3.2.2. Definition of Mathematical Model

Models of interest can range from simple linear models to the more complex, response surface models. However, the forms of these models are restricted due to the mixture aspects of the problem as well as the presence of a process factor. The most complex model to be considered in this study is of the form given by Eq. (3.3):

$$\begin{aligned}
\text{Response}_{\text{model}} = {} & \beta_1 Al + \beta_2 Ca + \beta_3 Al \cdot Ca + \beta_4 Cs + \beta_5 Al \cdot Cs \\
& + \beta_6 Ca \cdot Cs + \beta_7 H + \beta_8 Al \cdot H + \beta_9 Ca \cdot H \\
& + \beta_{10} Cs \cdot H + \beta_{11} K + \beta_{12} Al \cdot K + \beta_{13} Ca \cdot K \\
& + \beta_{14} Cs \cdot K + \beta_{15} H \cdot K + \beta_{16} Na + \beta_{17} Al \cdot Na \\
& + \beta_{18} Ca \cdot Na + \beta_{19} Cs \cdot Na + \beta_{20} H \cdot Na + \beta_{21} K \cdot Na \\
& + \beta_{22} Al \cdot Temp + \beta_{23} Ca \cdot Temp + \beta_{24} Cs \cdot Temp \\
& + \beta_{25} H \cdot Temp + \beta_{26} K \cdot Temp + \beta_{27} Na \cdot Temp \\
& + \beta_{28} Al \cdot Ca \cdot Temp + \beta_{29} Al \cdot Cs \cdot Temp + \beta_{30} Ca \cdot Cs \cdot Temp \\
& + \beta_{31} Al \cdot H \cdot Temp + \beta_{32} Ca \cdot H \cdot Temp + \beta_{33} Cs \cdot H \cdot Temp \\
& + \beta_{34} Al \cdot K \cdot Temp + \beta_{35} Ca \cdot K \cdot Temp + \beta_{36} Cs \cdot K \cdot Temp \\
& + \beta_{37} H \cdot K \cdot Temp + \beta_{38} Al \cdot Na \cdot Temp + \beta_{39} Ca \cdot Na \cdot Temp \\
& + \beta_{40} Cs \cdot Na \cdot Temp + \beta_{41} H \cdot Na \cdot Temp + \beta_{42} K \cdot Na \cdot Temp
\end{aligned} \tag{3.3}$$

where the β's are unknown parameters that may or may not be significant in defining the function. Note that the impacts of the mixture variables and process variable are evident in equation (3.3) in that there is no intercept term and the temperature factor only appears in cross terms with the mixture variables. The minimum number of design points required to fit this model is 42.

3.2.3. Selection of Candidate Design Points

A total of 52 candidate design points in two sets were selected for the test matrix. The first set of 21 design points was generated using the coordinate exchange algorithm in the JMP® software and are optimal for a model consisting of the first 21 terms of Eq. (3.3). Note that these 21 design points, shown in Table B-1 in Appendix, address the mixture aspects of the problem only. The process aspects (temperature) can be handled by conducting the 21 mixture experiments both at the upper and lower temperature bounds, and this would provide the 42 data points necessary to fit the model given by Eq. (3.3).

The second set of 31 design points was generated using the Orthogonal Latin Hypercubes (OLH) approach [5]. Use of the OLH approach was facilitated by the unique feature of this problem; for a fixed set of input data, the output generated by the model runs would be deterministic, i.e., free of errors. The OLH approach ensures that the entire range of each input variable is fully represented, and it also guarantees that the estimates of quadratic effects and bilinear interaction effects are uncorrelated with those of linear effects, although the estimates of quadratic and bilinear interaction effects are correlated with each other.

In this problem, the mixture constraint given by Eq. (3.2) limited the effectiveness of the OHL approach in filling in the factor space somewhat, and Figure 3.1 reflects the resulting "space-filling" achieved after two successive OLH runs. In the initial run, the full ranges of the factor space defined in Table 1.1 were used to generate 13 design points, and the remaining 18 design points were generated in the secondary run using a reduced set of factor space ranges. The resulting 31 OLH points are given in Table 3.3.

3.2.4. Design Points for Phased Computer Runs

Instead of dealing with the full model defined by Eq. (3.3) right from the start, it was decided to make the necessary computer runs in phases, starting with a linear model in the mixture components of the following form:

$$\begin{aligned} \text{Response}_{\text{model}} = {} & \beta_1 \cdot Al + \beta_2 \cdot Ca + \beta_3 \cdot Cs + \beta_4 \cdot H + \beta_5 \cdot K + \beta_6 \cdot Na \\ & + \beta_7 \cdot Al \cdot Temp + \beta_8 \cdot Ca \cdot Temp + \beta_9 \cdot Cs \cdot Temp \\ & + \beta_{10} \cdot H \cdot Temp + \beta_{11} \cdot K \cdot Temp + \beta_{12} \cdot Na \cdot Temp \end{aligned} \tag{3.4}$$

where the coefficient β for each term has been re-sequenced from those shown in Eq. (3.3). This reduced model has a total of 12 coefficients, thus requiring at least 12 computer runs to generate the necessary data. For these Phase 1 runs, 6 design points were selected from the set of 21 candidate mixture design points given in Table B-1 using the D-optimal routine of JMP® software. These 6 design points were then run at both the upper and lower temperature bounds for a total of 12 design points in all, as shown in Table 3.4.

FIGURE 3.1. Scatter Plots of Initial (red closed squares) and Secondary (orange open squares) Design Points Using OLH Approach (Chemical Species are in Scaled Weight Fractions).

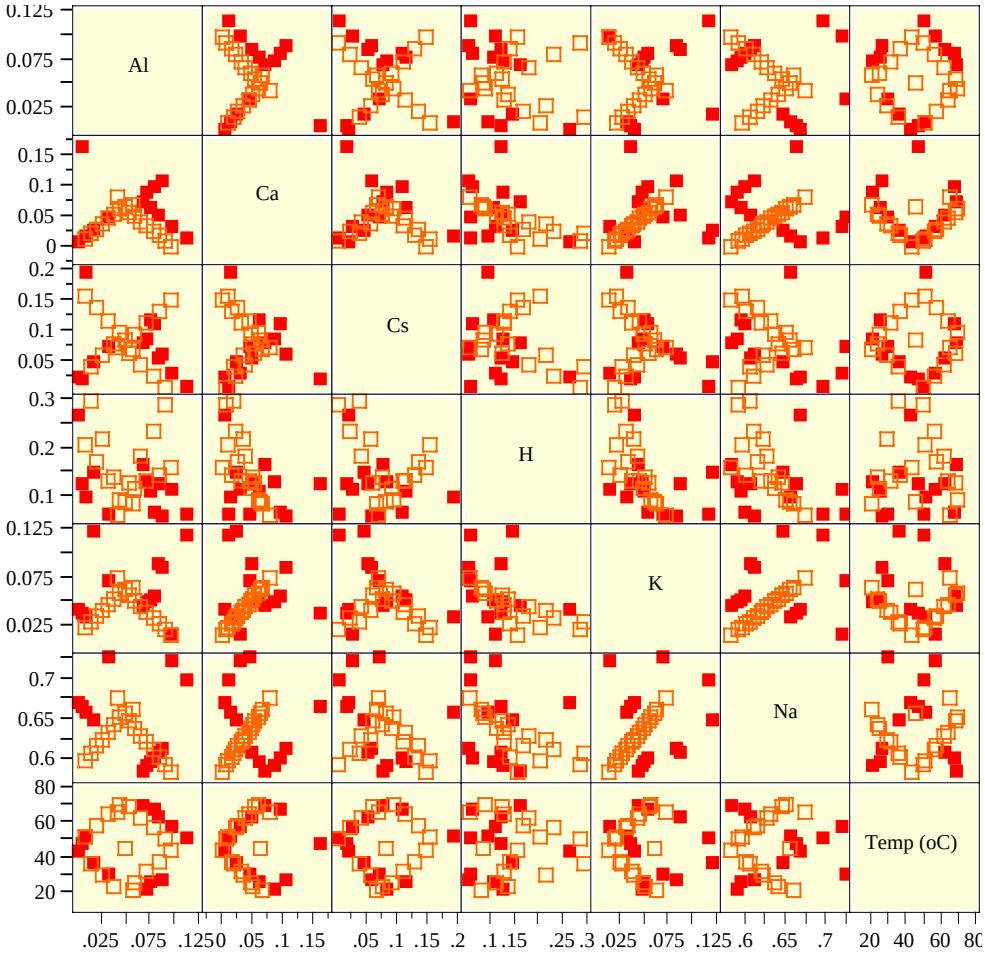

If the coefficients of each physical property model of interest could be fitted well with the data generated during Phase 1, the performance of these linear models were then to be evaluated against the "virtual experimental data" generated during Phase 2 computer runs using the 31 OLH design points shown in Table 3.3.

If models consisting only of those linear terms given by Eq. (3.4) appear to be inadequate to explain all the variations in model responses, Phase 3 computer runs were to be conducted to support the fitting of the full model given by Eq. (3.3). The design points for the Phase 3 runs would be the remaining 15 mixture points after the 6 mixture points were selected for Phase 1 from the 21 candidate design points shown in Table B-1. These 15 mixture points were then to be run at 20 and at 60 ºC to provide 30 design points in all. Together with the 12 design points selected earlier for Phase 1, these 30 additional design points given in Table B-2 would provide all the necessary data to fit the full model given by Eq. (3.3).

TABLE 3.3. 31 OLH Design Points Selected for Phase 2 Computer Runs.

Run ID	Al (SWF)	Ca (SWF)	Cs (SWF)	H (SWF)	K (SWF)	Na (SWF)	Temp (^{o}C)
NC13	0.06682	0.06985	0.07658	0.16003	0.04327	0.58345	59
NC14	0.07066	0.08482	0.08266	0.12585	0.04692	0.58909	20
NC15	0.07449	0.05987	0.11308	0.10725	0.05057	0.59474	24
NC16	0.07832	0.09480	0.10700	0.06528	0.05423	0.60038	57.5
NC17	0.08215	0.04989	0.05224	0.12260	0.08709	0.60603	54
NC18	0.08598	0.10477	0.05832	0.05581	0.08344	0.61167	25
NC19	0.09748	0.02994	0.02790	0.11170	0.01406	0.71892	49
NC20	0.11281	0.00998	0.00357	0.06100	0.11631	0.69634	44
NC21	0.03234	0.04490	0.07049	0.05887	0.06883	0.72457	27.5
NC22	0.01701	0.02495	0.04616	0.14639	0.11996	0.64554	32.5
NC23	0.00934	0.01497	0.19217	0.09437	0.03232	0.65683	45
NC24	0.00551	0.15966	0.01573	0.12066	0.03597	0.66248	41
NC25	0.00168	0.00499	0.02182	0.26377	0.03962	0.66812	37.5
NC26	0.05380	0.05588	0.06199	0.12670	0.05498	0.64665	59
NC27	0.05687	0.06785	0.06686	0.08448	0.06374	0.66020	20
NC28	0.05993	0.04790	0.09119	0.11423	0.04914	0.63761	24
NC29	0.06606	0.03991	0.04253	0.17962	0.04330	0.62857	54
NC30	0.07219	0.03193	0.11066	0.12822	0.03746	0.61954	29
NC31	0.07832	0.02395	0.02306	0.23254	0.03162	0.61051	49
NC32	0.08446	0.01597	0.13012	0.14221	0.02578	0.60147	34
NC33	0.09058	0.00798	0.00360	0.28546	0.01994	0.59244	44
NC34	0.09671	0.00000	0.14959	0.15620	0.01410	0.58340	39
NC35	0.05074	0.06386	0.08146	0.08744	0.06082	0.65568	40
NC36	0.04461	0.05987	0.09606	0.09040	0.05790	0.65116	60
NC37	0.04154	0.07983	0.07173	0.06065	0.07250	0.67375	56
NC38	0.03848	0.05189	0.07659	0.13885	0.05206	0.64213	22.5
NC39	0.03235	0.04390	0.11552	0.12891	0.04622	0.63309	55
NC40	0.02622	0.03592	0.05713	0.21629	0.04038	0.62406	27.5
NC41	0.02009	0.02794	0.13499	0.16742	0.03454	0.61502	50
NC42	0.01396	0.01996	0.03766	0.29373	0.02870	0.60599	32.5
NC43	0.00783	0.01197	0.15445	0.20593	0.02286	0.59695	45

If temperature did not appear to be a significant factor, the last 15 terms of Eq. (3.3), i.e., products of cross mixture terms and temperature, could be deleted from the models. In this case, the 15 mixture points selected for Phase 3 could be run at any single temperature between 20 and at 60 ºC. In either case, the Phase 2 computer runs made earlier with the 31 OLH design points would still provide the necessary data to assess the performance of the Phase 3 models.

Table B-3 provides the complete test matrix in the original weight fraction units, i.e., the sum of weight fractions of the six major cations equals 0.9533.

TABLE 3.4. 12 Design Points Selected for Phase 1 Computer Runs.

Run ID	Al (SWF)	Ca (SWF)	Cs (SWF)	H (SWF)	K (SWF)	Na (SWF)	Temp (^oC)
NC01	0.11065	0.15970	0.08215	0.05000	0.01410	0.58340	20
NC02	0.03306	0.00000	0.00360	0.31880	0.01410	0.63044	20
NC03	0.00170	0.15970	0.00360	0.12070	0.13090	0.58340	20
NC04	0.00170	0.15970	0.01040	0.05000	0.01410	0.76410	20
NC05	0.00170	0.00000	0.19830	0.05000	0.13090	0.61910	20
NC06	0.12430	0.00000	0.00360	0.05000	0.05800	0.76410	20
NC07	0.11065	0.15970	0.08215	0.05000	0.01410	0.58340	60
NC08	0.03306	0.00000	0.00360	0.31880	0.01410	0.63044	60
NC09	0.00170	0.15970	0.00360	0.12070	0.13090	0.58340	60
NC10	0.00170	0.15970	0.01040	0.05000	0.01410	0.76410	60
NC11	0.00170	0.00000	0.19830	0.05000	0.13090	0.61910	60
NC12	0.12430	0.00000	0.00360	0.05000	0.05800	0.76410	60

3.3. Semi-Batch Evaporation Model

The reboiler pot will be initially charged with a concentrated nitric acid solution and kept under vacuum so that boilup would occur at 50 ^oC while maintaining a constant liquid volume in the pot throughout the feeding cycle. The feeding will continue with no bottom withdrawal until the liquid in the pot reaches the target endpoint of 80% saturation with respect to any one of the major salt species present. As the feeding and boilup progress, the acid concentration in the pot will continuously decrease but the salt content will increase. As a result, the vapor-liquid equilibrium (VLE) of nitric acid solution in the pot will also change constantly. This section describes how this semi-batch evaporation process was modeled using the Environmental Simulation Program (ESP), licensed by OLI Systems, Inc.

The OLI/ESP software has a module, called DynaChem, which is used to simulate dynamic processes. However, its use as a full-scale dynamic flowsheet simulator is rather limited, since its library contains only three built-in "units" that can be used to model only a certain number of unit operations, and the software does not allow users to build any custom models. As a result, the main steady state module of the ESP software was used in this study to model the semi-batch evaporator by approximating it as a series of continuous still pots, as shown in Figure 3.2. The mass ratio of the initial acid charge-to-cesium eluate feed to the 1st stage was set at 5:1. Additional stages were then added to the existing model one-by-one at the same feed ratio of 5:1, until the concentrate from the final stage reaches the prescribed evaporation endpoint at 25 ^oC and 1 atm. Higher feed ratios of 10:1 and 100:1 were also tried and they were shown to have little impact on the overall vapor-liquid equilibria; only the required number of stages was increased proportionally. The validity of approximating the semi-batch evaporator as a series of continuous still pots was confirmed earlier against the batch distillation data collected at 1 atm [4].

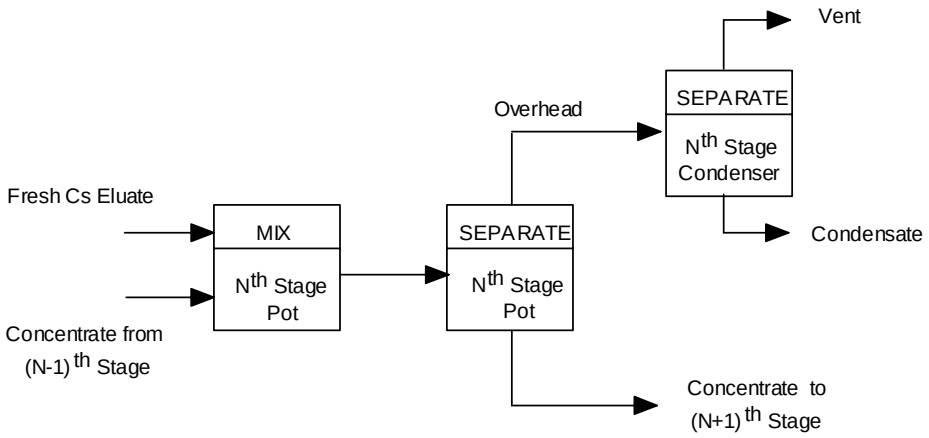

FIGURE 3.2. Schematic of N^{th} Stage Evaporation of Cs Eluate Model.

One key process constraint that must be adhered to during the execution of the model is to ensure that the liquid volume in the pot or the flow rate of concentrate from one stage to the next is maintained constant throughout the entire evaporation cycle. At a fixed feed rate, this was achieved in essence by controlling the boilup rate or the vacuum in the pot. It turned out that by maintaining the molar boilup rate very close to that of the feed it was possible to contain the volume fluctuations within ±2%. The design calls for charging the pot with a concentrated nitric acid prior to the initiation of feeding. The concentration of this initial acid charge was set at 7.25 M based on the observation that its equilibrium vapor concentration at 50 ^{o}C is ~0.5 M, which is the target acidity for the condensate.

The composition of concentrated eluate from each stage was checked for the presence of any solids. For the concentration ranges given in Table 1.1, the first-precipitating major salt is expected to be $NaNO_3$ for most cases, if not all. How accurately the model predicts which major salt would precipitate first at what concentration depends entirely on the accuracy of thermodynamic database(s) used in conjunction with the model. Every OLI/ESP model is built to run in conjunction with the software default database called PUBLIC. In this task, the PUBLIC database v6.5 was supplemented by a private database, called HNO3DB (also referred to as the nitric acid database hereafter), since the former alone could not adequately account for the observed vapor-liquid and solid-liquid equilibria of nitrated systems under strongly acidic conditions.

The nitric acid database was developed recently for the Na-K-Cs-Al-HNO_3-H_2O system using the binary and ternary experimental data from both SRTC and the open literature, and its use was truly instrumental to the success of this task. A brief account of its development history and the results of recent validation efforts are described next.

3.4 Nitric Acid Database

The nitric acid database used in this task was developed in several stages. First, prior to a full-blown simulation of the multi-electrolyte chemistry of cesium eluate solutions, it was deemed necessary to verify the capability of the PUBLIC database to accurately predict the VLE behavior of the base system involving HNO_3 and H_2O. This was done in an earlier study, which showed that there were significant discrepancies between the *P-x-y* equilibria predicted by PUBLIC v6.2 and the measured data from the literature, particularly for the liquid-phase (See Figure 3 in Ref. [4]).

Deficiencies were also found in the PUBLIC database's capability to accurately predict physical properties of the simple binary system. The calculated densities of 38 wt% nitric acid solution using PUBLIC v6.2 are compared in Table 3.5 to the literature data; it is evident that a significant bias is present in the calculated values at all temperatures. The calculated heat capacities of the HNO_3-H_2O system using PUBLIC v6.2 are also compared to the literature data in Figure 3.3, which shows a significant deviation of calculated values from the data starting at 4 m (molal) HNO_3 and higher. Considering the projection that the acidity in the cesium eluate evaporator pot will begin at above 7 M initially and decrease to a value between 3 and 5 M at the target endpoint of 80% saturation, the degree of discrepancy shown in Figure 3.3 for the same concentration range does not seem acceptable.

TABLE 3.5. Comparison of Calculated Densities of 38 wt% HNO_3 in H_2O vs. Literature Data at 20 ^oC.

T (^oC)	PUBLIC v6.2 (g/ml)	Perry's (g/ml)	% diff (decimals only)
0	1.3390	1.2513	35
10	1.3287	1.2428	35
20	1.3170	1.2335	36
30	1.3050	1.2245	36
40	1.2926	1.2150	36
50	1.2809	1.2054	37

Data regression is relatively straightforward for the new density parameters, but not for the heat capacity, since the latter requires evaluation of the second derivative of the activity coefficient. Therefore, with the revised heat capacity parameters, a new equilibrium speciation will result, and the parameters for the remaining properties including the density must be re-optimized based on the new speciation results. This means that in order to lessen the severity of deficiencies discussed earlier, all the thermodynamic and physical property parameters in the PUBLIC database that are related to the HNO_3-H_2O binary system had to be revised completely.

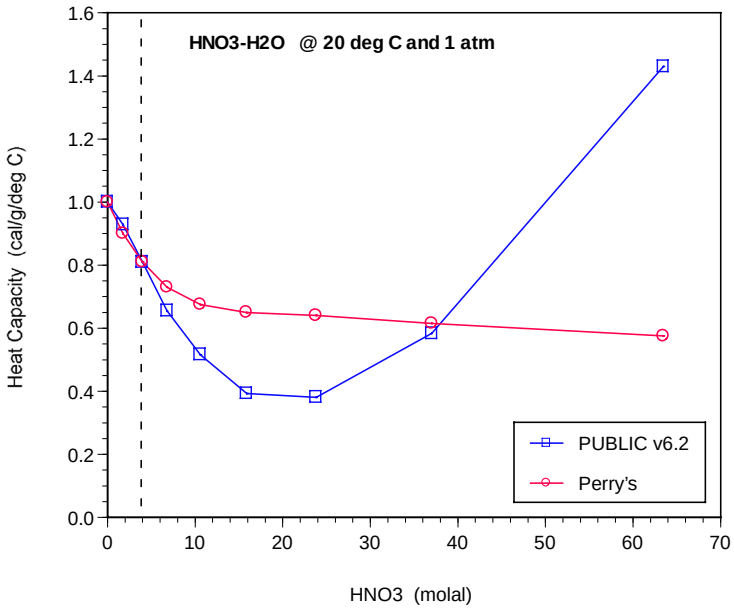

FIGURE 3.3. Comparison of Calculated Heat Capacities of HNO_3-H_2O System vs. Literature Data at 20 ^oC.

The revised parameters were then entered into the newly created binary database, called HNO3DB. In Figure 3.4, the *P-x-y* equilibria predicted by the binary HNO3DB are compared to the same data as referenced earlier [4], and the overall agreement is seen to be quite excellent.

The next step in the database development was to check the applicability of the binary HNO3DB to the ternary systems, and the results were not satisfactory at all. Solubilities and densities of three ternary systems, involving Na^+, K^+, and Cs^+ in nitric acid solutions, were calculated using the binary HNO3DB and PUBLIC v6.5, and the results are compared in Table 3.6 to the recent experimental data taken at SRTC [17]. The predicted solubility and density of each binary system, i.e., at 0 M HNO_3, are shown to be in good agreement with the data thanks to the improved PUBLIC v6.5. However, as the acidity is increased, the discrepancy between predicted and measured values becomes larger. At 6 M HNO_3, for example, the predicted solubility of the KNO_3-HNO_3-H_2O ternary system using the binary HNO3DB is less than 1/5 of the measured value. Although less pronounced, the discrepancies between the predicted and measured values for the $NaNO_3$-HNO_3-H_2O and $CsNO_3$-HNO_3-H_2O ternary systems are still quite substantial, i.e., the predictions being off by as much as 50% of the measured values.

These shortcomings led to the next stage of nitric acid database development to expand the binary HNO3DB to cover ternary, quaternary, and quinary nitric acid systems by adding $NaNO_3$, KNO_3, and $CsNO_3$ one by one. In order to determine the binary interaction parameters for Na^+, K^+, Cs^+, and their undissociated salts, the OLI personnel

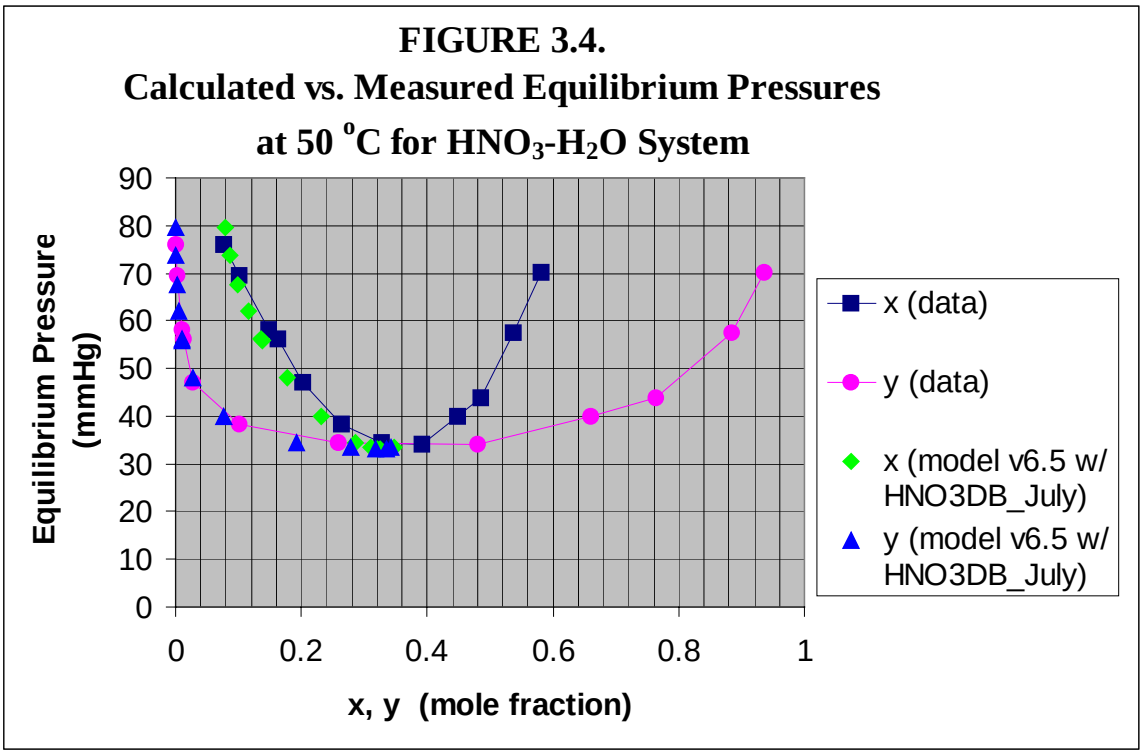

* x and y are the mole fractions of nitric acid in the liquid and vapor phases, respectively.

TABLE 3.6. Measured vs. Calculated Solubilities and Densities of Ternary Systems Using Binary and Ternary HNO3DB.

HNO3 (M)	measured solubility (M)	calc'd solubility Binary HNO3DB (M)	calc'd solubility Quinary HNO3DB (M)	measured density (g/ml)	calc'd density Binary HNO3DB (g/ml)	calc'd density Quinary HNO3DB (g/ml)
			Sat'd NaNO3-HNO3-H2O			
0	7.8	7.8	7.73	1.3785	1.4066	1.3849
4	3.5	2.5	3.45	1.3105	1.2621	1.2952
6	2.3	1.4	2.25	1.3046	1.2575	1.2945
8	1.6	0.8	1.45	1.3221	1.2809	1.3129
			Sat'd KNO3-HNO3-H2O			
0	2.93	2.94	2.91	1.1737	1.1804	1.1789
4	1.43	0.78	1.44	1.2130	1.1800	1.2165
6	1.55	0.30	1.52	1.2742	1.2120	1.2729
			Sat'd CsNO3-HNO3-H2O			
0	1.16	1.12	1.15	1.1644	1.1714	1.1631
4	0.80	0.56	0.80	1.2426	1.2339	1.2440
6	1.09	0.51	1.08	1.3490	1.2922	1.3481

assembled available binary and ternary data involving these alkali salts from two different sources: SRTC bench-scale tests (~35%) and the open literature (~65%). Solubilities and saturation densities of the three ternary systems were recalculated using the resulting quinary database for the $NaNO_3$-KNO_3-$CsNO_3$-HNO_3-H_2O system, and the overall improvements made over the binary database predictions are clearly evident in Table 3.6.

Once the nitric acid database was expanded to include Na^+, K^+ and Cs^+ in addition to H^+, it seemed then logical to further expand it by including the two remaining major cations in Table 3.2, namely, Al^{+3} and Ca^{+2}. However, inclusion of Ca^{+2} was not possible, since without sufficient data for optimization the resulting binary interaction parameters involving $Ca(NO_3)_2$ caused the entire database to behave erratically. In the end, the final version of the nitric acid database available for this task was optimized for the following 6-component system, $NaNO_3$-KNO_3-$CsNO_3$-$Al(NO_3)_3$-HNO_3-H_2O.

It is worth noting here that as the number of components in a particular database system increases, so does the difficulty of adding a new species to that database. This is due to a sharp increase in the number of possible combinations of binary interactions between the existing species and the new species just added. Speaking of the binary interactions, the thermodynamic framework of OLI software is based on the Bromley formulation, which considers the binary interactions between two opposite charges, i.e., between cations and anions, to be of greatest importance. For this 6-component nitric acid database, however, it was necessary to include additional binary interaction parameters for neutral-neutral species pairs and even for like-charge ion pairs with the use of the Pitzer formulation [18].

The final 6-component nitric acid database used in this task was next validated against the available experimental data. The OLI/ESP semi-batch evaporation model was run in conjunction with the database to simulate the solubility experiments conducted with two cesium eluate simulants, Tanks AZ-102 and AN-102 [17]. As shown in Table 3.7, the relative differences between the predicted and measured solubilities and saturation densities were all well within ±15%, thus satisfying the specified acceptance criterion for this task.

TABLE 3.7. Validation of 6-Component Nitric Acid Database.

Cs eluate		Data	HNO3DB	% difference
AZ-102	Density (g/ml)	1.3531	1.3610	2.2 *
	Solubility (g TS/ml)	0.6067	0.6290	3.7
AN-102	Density (g/ml)	1.3676	1.3444	6.3 *
	Solubility (g TS/ml)	0.6160	0.5770	6.5

* Based on decimals only

3.5. Calculation of Physical Property Data

The semi-batch evaporation model was run next in conjunction with the validated nitric acid database to calculate the required physical properties of each matrix solution at the target endpoints of 80% and 100% saturation. The key bases of the model and the calculated physical properties are presented in this section.

3.5.1 Model Bases

In order to conform to the OLI software input protocol, a composition vector was developed in a neutral species form for each of the design points defined in Tables 3.3, 3.4 and B-2. A sample input-vector is shown in Table C-1 in Appendix for the design point #22 (NC22). The actual inputs to the model were the full-scale molar flow rates given in the far right-hand column of the table. The physical properties of interest in this task are intensive properties, i.e., independent of the absolute flow rates chosen. Nevertheless, the full-scale flow rates were used in this task so that the resulting mass balance would reflect instantaneous flows required to satisfy the design basis Envelope B glass production rate of 60 metric tons per day at a sodium loading of 10 wt% Na_2O. The instantaneous sodium flow rate at this 100% glass attainment was calculated to be 185,484 g/hr. The corresponding instantaneous flow rate of cesium was calculated to be 119.14 g/hr based on the sodium-to-cesium mass ratio of 1,557, which was estimated from the SRTC analytical data for the AZ-102 supernate sample [13]. A conversion factor was calculated next by dividing this instantaneous cesium flow rate by the weight fraction of cesium and was applied to set the remaining flow rates of feed.

Furthermore, the bulk saturation limit of a multicomponent system was defined as the point where the solution would become just saturated with one or more of the major salt species present or supersaturated with other minor salt species to the extent that the total insoluble solids formed exclusively out of the minor salt constituents would exceed 0.5 wt% of the solution, whichever occurs first. These criteria were applied to the assumed eluate storage conditions of 25 ^{o}C and 1 atm. Experimentally, the determination of 0.5 wt% minor salt species-only presence will require both quantification and phase identification of filtered solids from a few samples taken beyond the formation of first solids. The precise determination of this limit may further require some degree of inter- or extrapolation of data.

Once the bulk saturation limit was determined for each matrix solution, the 80% saturation endpoint was determined as the point where the ionic product of the target salt constituents equaled 80% of its solubility product. Additional bases used in the model runs included:

- Initial acid charge = 7.25 M HNO_3.
- Evaporator operating temperature = 50 ^{o}C.
- Constant volume evaporation.
- Primary condenser operating temperature = 40 ^{o}C.

- No rectifier column was included.
- No pressure drop between the evaporator pot and the primary condenser.

3.5.2. Model Results

It will be shown in Section 3.5 that the linear model given by Eq. (3.4) could describe well all the physical property data generated from the first 43 computer runs of Phase 1 and 2 tests. It was, therefore, concluded that the additional Phase 3 computer runs would improve the fit only marginally, so they were omitted. All the calculated physical property data during the Phase 1 and 2 tests are tabulated in Tables C-2 and C-3 for the 80% and 100% saturation endpoints, respectively. In all 43 runs made, the first-precipitating major salt species always turned out to be $NaNO_3$. So, the model was run with each matrix feed, until the ionic product of Na^+ and NO_3^- equaled the solubility product of $NaNO_3$. The density, viscosity and heat capacity for each saturated solution were then calculated at that point.

Once the bulk solubility limit was determined for each matrix feed, the 80% saturation target was found by backing off to the point where the ionic product of Na^+ and NO_3^- equaled 80% of the solubility product of $NaNO_3$. The density, viscosity and heat capacity for each 80% saturated solution were then calculated along with the volume reduction factor (VRF), which is defined as the ratio of cumulative feed volume to that of the initial acid charge. The VRF, sometimes called a concentration factor, achievable at a given target endpoint should be a useful concept to the designers and process engineers of any evaporator systems.

Profiles of concentration, density, and volume reduction factor during the semi-batch evaporation of cesium eluate matrix feed #22 are shown in Figure 3.5. It is seen that throughout the feeding and boilup period the concentration of nitric acid in the pot decreased steadily from its initial value of 7.25 M to 1.85 M, at which point the solution became just saturated with $NaNO_3$. The 100% saturation is projected to occur at the 420^{th} stage of the model (see Figure 3.2 for the definition of a stage) or at VRF = 76, which is equivalent to saying, "when the cumulative volume of cesium eluate fed equals 76 times the volume of initial acid charge." If the actual cesium eluate feed had the same composition as the matrix feed #22, the VRF achievable at the operational target endpoint of 80% saturation would be 57. It is also seen that the concentration of Na^+ in the pot was increased linearly from zero initially to 4.9 M at saturation, and the linear increase was expected since the feed rate and the liquid volume were both kept constant throughout. As expected, the liquid density in the pot increased monotonically with increasing salt content from 1.2216 g/ml initially to 1.3744 g/ml at 100% saturation.

Profiles of cumulative condensate acidity and boilup pressure are shown in Figure 3.6 for the same matrix feed #22. It is seen that the cumulative condensate acidity started out high initially at near 0.6 M and then quickly fell to the asymptotic value of 0.4 M after the 150^{th} stage or VRF = 27. If it were desired to bring acidity

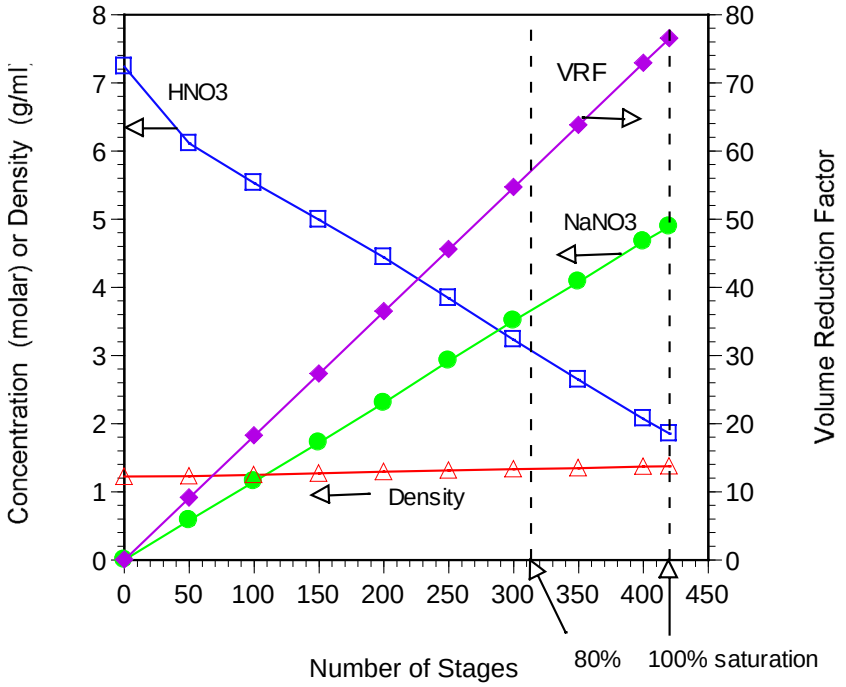

FIGURE 3.5. Profiles of Concentration, Density, and VRF during Semi-Batch Evaporation of Cesium Eluate Matrix Feed #22.

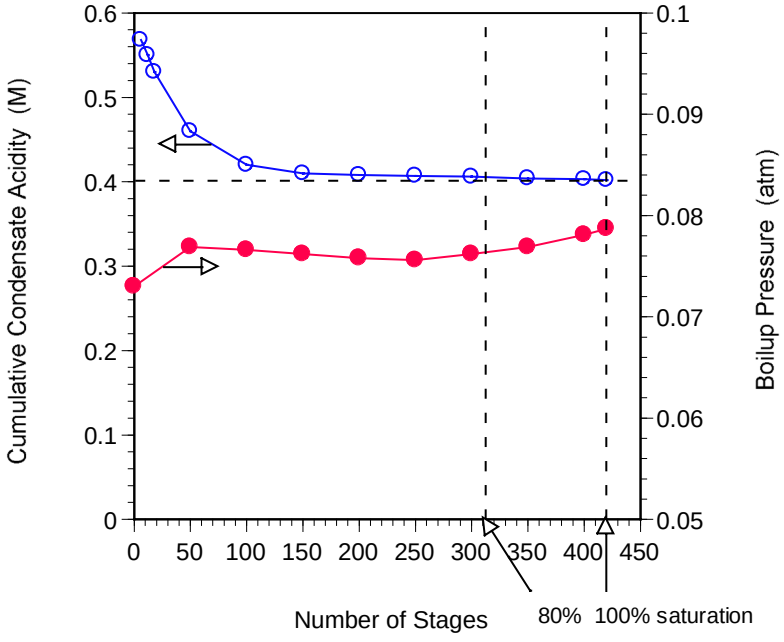

FIGURE 3.6. Profiles of Cumulative Condensate Acidity and Boilup Pressure during Semi-Batch Evaporation of Cesium Eluate Matrix Feed #22.

back up to 0.5 M for reuse in the elution, use of a rectifier column would achieve this easily. Preliminary calculations showed that for a given feed composition the higher the initial pot acidity, the higher the asymptotic acidity of cumulative condensate. This result is consistent with the overall acid balance, since the liquid in the pot was shown to reach the same acidity at 100% saturation regardless of the initial pot acidity; two different starting pot acidities of 7.25 and 8.56 M were run with the TFL cesium eluate feed using the OLI model, and the 100% saturation was found to occur at the same pot acidity of 4.8 M in both cases [20].

However, if the sodium concentration in the feed is varied, thereby impacting the evaporation endpoint, the asymptotic acidity of condensate will then depend on not only the initial pot acidity but the acidity of feed as well. For the matrix feed #22, both the sodium and acid concentrations were at near the midpoints of their respective matrix ranges. For all the matrix feeds considered in this task, a general trend is that the volume reduction factor achievable at 80% saturation increases with increasing feed acidity, as shown in Figure 3.7. Furthermore, the calculated boilup pressures remained relatively constant between 0.07 and 0.08 atm throughout this constant-volume, constant-temperature evaporation cycle.

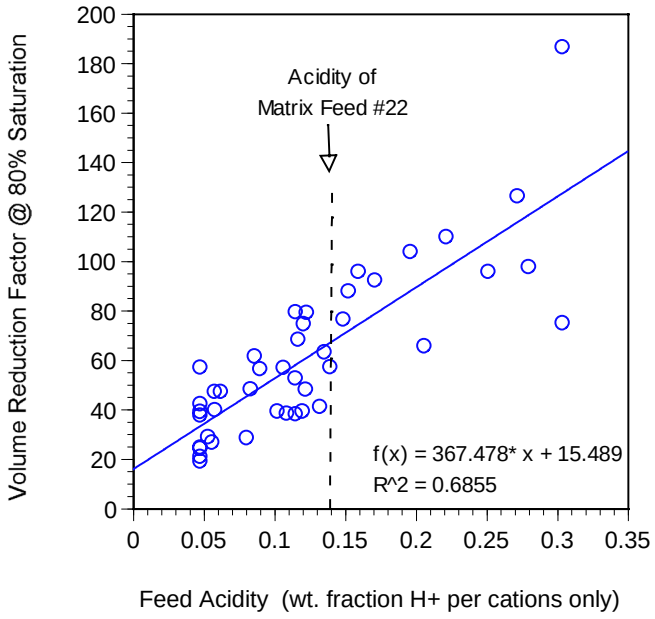

FIGURE 3.7. Volume Reduction Factor vs. Feed Acidity during Semi-Batch Evaporation of Cesium Eluate Matrix Feed #22.

3.6. Derivation of Physical Property Models

As stated earlier, a phased approach was taken for the development of physical property models from the data generated by the OLI/ESP model. The results of applying this phased approach to the model results at 80% and 100% saturation are discussed in this section. The data describing the relevant properties of the model results for the first two test phases are provided in Tables C-2 and C-3 for 80% and 100% saturation, respectively. For both target endpoints, the responses of interest were density, viscosity and heat capacity. In addition, for the 80% saturation case, the volume reduction factor (VRF) was also of interest and, for the 100% saturation case, the solubility expressed as grams of total solids (TS) per 1,000 grams of water or grams of total solids per milliliter was of interest. Tables 3.3 and 3.4 provide the test matrix for the first two test phases of this study. The statistical software package JMP® Version 5.0 was used to conduct the analyses presented in this section [19].

The first test phase (Phase 1) provided the necessary data to fit a linear mixture model in the concentration factors with and without the process factor, temperature, while the second test phase (Phase 2) provided a more thorough coverage of the factor space than Phase 1. The Phase 2 coverage was attained through the use of an Orthogonal Latin Hypercube (OLH) design approach, which was modified somewhat due to the mixture constraint imposed on the concentrations of the solution factors by Eq. (3.2).

Exhibit D-1 in Appendix D and Exhibit E-1 in Appendix E provide plots of the responses of interest versus each test factor for 80% and 100% saturation, respectively. In these and subsequent plots, small squares are used to represent the Phase 1 data, while the Phase 2 data are plotted using a combination of "pluses" and solid circles of different colors depending on the temperature (red for 20 ºC and green for 60 ºC). In general, a random scatter of data seen in both exhibits suggests that there are no dominating mixture factors or variables whose effects are clearly manifested on each of the mixture properties of interest for the entire matrix ranges considered in this task. However, there are two exceptions; definite linear correlations can be seen between the viscosity and the concentration of Al^{+3} at both saturation endpoints and between the VRF at 80% saturation and the concentration of H^{+}, as seen earlier in Figure 3.7. On the other hand, the effect of temperature is clearly shown on the density, bulk solubility and, a lesser degree, the heat capacity.

The first step in the phased approach was to fit a linear mixture model with temperature as a process variable. Figures D-1 to D-4 in Appendix D and Figures E-1 to E-5 in Appendix E provide the results of these statistical modeling efforts for the 80% and 100% saturation cases, respectively. Note that for each case, there are 12 Phase-1 data points and 12 model parameters. Thus, all of the variations in each set of response data are fully described by the fitted model for that response; there are no degrees of freedom remaining for error. It is also recalled that the response data were not experimentally generated; they were generated via a set of computer codes. Therefore, there are no experimental or random errors in any of the statistical models developed using the Phase 1 data. In fact, this is true of all the models developed in this task.

The response data from the OLH design points provided the mechanism to check for the performance of the models developed from the analysis of Phase 1 data. These data are shown on the plots of Figures D-1 to D-4 and Figures E-1 to E-5, although they were not used in fitting the model parameters. Overall, the OLH data points appear to be reasonably well predicted by the fitted models.

To provide some opportunity for improving the performance of these fitted models, a subset of the OLH data points were selected to participate in the model fitting process. Starting with the 15^{th} design point (NC15), every third design point was selected to be used in the model fitting (these points are represented by "plus" symbols), while the remaining OLH points continued to be used for model validation (these points are represented by solid circles). Although the resulting plots are not included in this report, these models could explain over 90 and 95% of the variations seen in the 80% and 100% saturation data, respectively.

Figures D-5 to D-8 in Appendix D and Figures E-6 to E-10 in Appendix E provide a series of plots involving these models based on the expanded data sets and the sensitivity lines at ±15% of their predictions. These sensitivity lines are provided in the plots to aid in assessing model performance. As stated previously, there is no random error in the data generated by these computer models. Any difference between the statistical model prediction and the computer result for a given set of factor levels represents a bias in the model. The sensitivity lines at ±15% of the model predictions provide an opportunity to assess the bias in the models over the points from the OLH design that were not used in the modeling effort. These are the enlarged points in these plots. Only the viscosity model developed for the 80% saturation case shows a computer generated result outside of the sensitivity lines, and this point was used in the model fitting; it is not enlarged in the plot.

Since the models based on the expanded data sets appeared to perform well for both the 80% and 100% saturation cases, the last step in the phased approach was to develop a final set of models using all 43 data points generated in both test phases. The results from these modeling efforts are provided in Figures 3.8 to 3.11 for 80% saturation and Figures 3.12 to 3.16 for 100% saturation. A review of these final models shows that the model parameters estimated using all 43 data points differ slightly from the earlier estimates, and it is recommended that these final models be used to relate the physical property predictions by the OLI/ESP model to the concentration and temperature ranges considered in this study.

FIGURE 3.8. Results from Fitting Density Model Using Phase 1 and 2 Data @ 80% Saturation - Actual vs. Predicted Densities (g/ml).

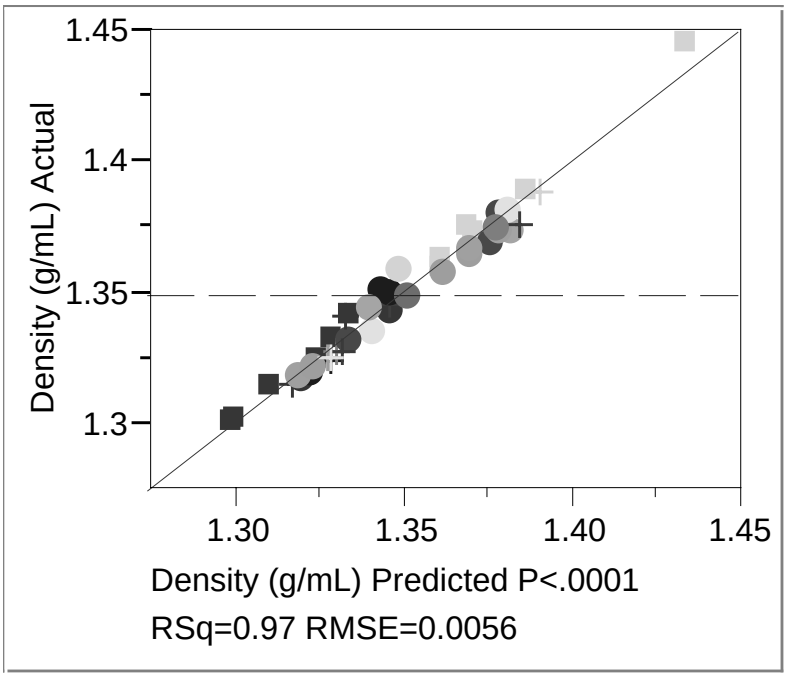

Summary of Fit

RSquare	0.972307
RSquare Adj	0.96248
Root Mean Square Error	0.005562
Mean of Response	1.348814
Observations (or Sum Wgts)	43

Analysis of Variance

Source	DF	Sum of Squares	Mean Square	F Ratio
Model	11	0.03366865	0.003061	98.9471
Error	31	0.00095894	0.000031	Prob > F
C. Total	42	0.03462759		<.0001

Tested against reduced model: Y=mean

Parameter Estimates

Term		Estimate	Std Error	t Ratio	Prob>|t|
Intercept	Zeroed	0	0	.	.
Al (swf)		1.3617618	0.068084	20.00	<.0001
Ca (swf)		1.4440109	0.044514	32.44	<.0001
Cs (swf)		1.3491631	0.048202	27.99	<.0001
H (swf)		1.3075459	0.033865	38.61	<.0001
K (swf)		1.3726865	0.071631	19.16	<.0001
Na (swf)		1.2408598	0.015567	79.71	<.0001
Al (swf)*Temp (oC)		-0.002437	0.001568	-1.55	0.1303
Ca (swf)*Temp (oC)		-0.001624	0.001019	-1.59	0.1211
Cs (swf)*Temp (oC)		0.0038915	0.001103	3.53	0.0013
H (swf)*Temp (oC)		0.0006061	0.000781	0.78	0.4436
K (swf)*Temp (oC)		0.0027002	0.001635	1.65	0.1087
Na (swf)*Temp (oC)		0.0021725	0.000356	6.10	<.0001

FIGURE 3.9. Results from Fitting Volume Reduction Factor (VRF) Model Using Phase 1 and 2 Data @ 80% Saturation - Actual vs. Predicted VRFs.

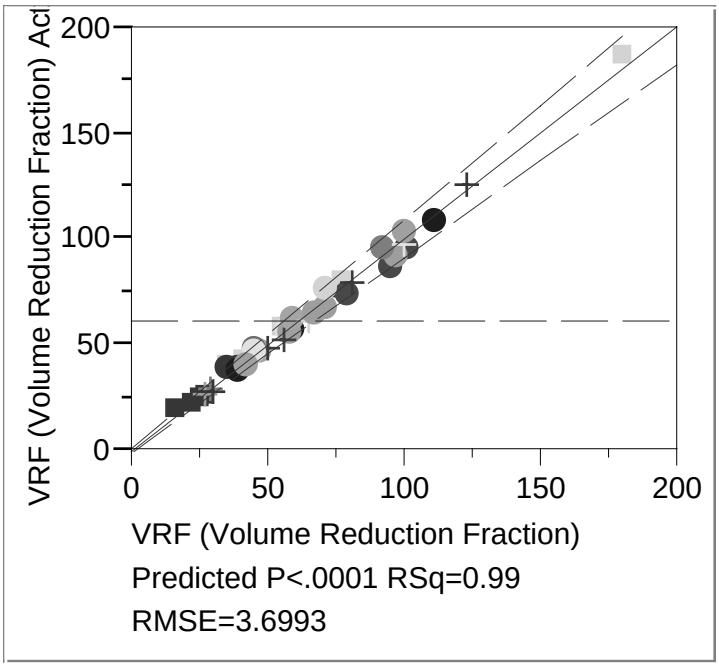

Summary of Fit

RSquare	0.990652
RSquare Adj	0.987335
Root Mean Square Error	3.699304
Mean of Response	61.20837
Observations (or Sum Wgts)	43

Analysis of Variance

Source	DF	Sum of Squares	Mean Square	F Ratio
Model	11	44956.693	4086.97	298.6493
Error	31	424.230	13.68	Prob > F
C. Total	42	45380.923		<.0001

Tested against reduced model: Y=mean

Parameter Estimates

Term		Estimate	Std Error	t Ratio	Prob>|t|
Intercept	Zeroed	0	0	.	.
Al (swf)		139.01782	45.28446	3.07	0.0044
Ca (swf)		48.970285	29.60751	1.65	0.1082
Cs (swf)		27.902718	32.06051	0.87	0.3908
H (swf)		63.091692	22.52485	2.80	0.0087
K (swf)		54.908142	47.64409	1.15	0.2579
Na (swf)		-11.80459	10.35409	-1.14	0.2630
Al (swf)*Temp (oC)		-3.306467	1.042908	-3.17	0.0034
Ca (swf)*Temp (oC)		-1.071743	0.67768	-1.58	0.1239
Cs (swf)*Temp (oC)		0.5816443	0.733539	0.79	0.4338
H (swf)*Temp (oC)		7.7397202	0.519498	14.90	<.0001
K (swf)*Temp (oC)		-0.486889	1.087257	-0.45	0.6574
Na (swf)*Temp (oC)		0.5293461	0.236774	2.24	0.0327

FIGURE 3.10. Results from Fitting Viscosity Model Using Phase 1 and 2 Data @ 80% Saturation - Actual vs. Predicted Viscosities.

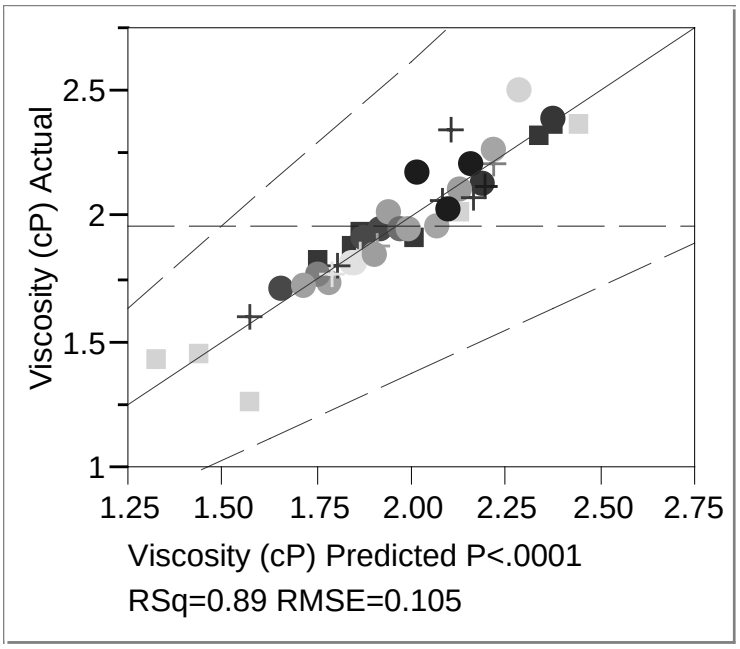

Summary of Fit

RSquare	0.88645
RSquare Adj	0.846158
Root Mean Square Error	0.104952
Mean of Response	1.96292
Observations (or Sum Wgts)	43

Analysis of Variance

Source	DF	Sum of Squares	Mean Square	F Ratio
Model	11	2.6657119	0.242337	22.0007
Error	31	0.3414640	0.011015	Prob > F
C. Total	42	3.0071758		<.0001

Tested against reduced model: Y=mean

Parameter Estimates

Term		Estimate	Std Error	t Ratio	Prob>|t|
Intercept	Zeroed	0	0	.	.
Al (swf)		6.111352	1.284756	4.76	<.0001
Ca (swf)		3.0366776	0.839989	3.62	0.0011
Cs (swf)		2.269341	0.909582	2.49	0.0181
H (swf)		2.9476053	0.639048	4.61	<.0001
K (swf)		1.5956633	1.351701	1.18	0.2468
Na (swf)		1.6692323	0.293754	5.68	<.0001
Al (swf)*Temp (oC)		0.0373055	0.029588	1.26	0.2168
Ca (swf)*Temp (oC)		-0.04848	0.019226	-2.52	0.0170
Cs (swf)*Temp (oC)		0.0021983	0.020811	0.11	0.9166
H (swf)*Temp (oC)		-0.035094	0.014739	-2.38	0.0236
K (swf)*Temp (oC)		0.0226456	0.030846	0.73	0.4684
Na (swf)*Temp (oC)		-0.002098	0.006717	-0.31	0.7569

FIGURE 3.11. Results from Fitting Heat Capacity Model Using Phase 1 and 2 Data @ 80% Saturation - Actual vs. Predicted Heat Capacities (cal/g/^{o}C).

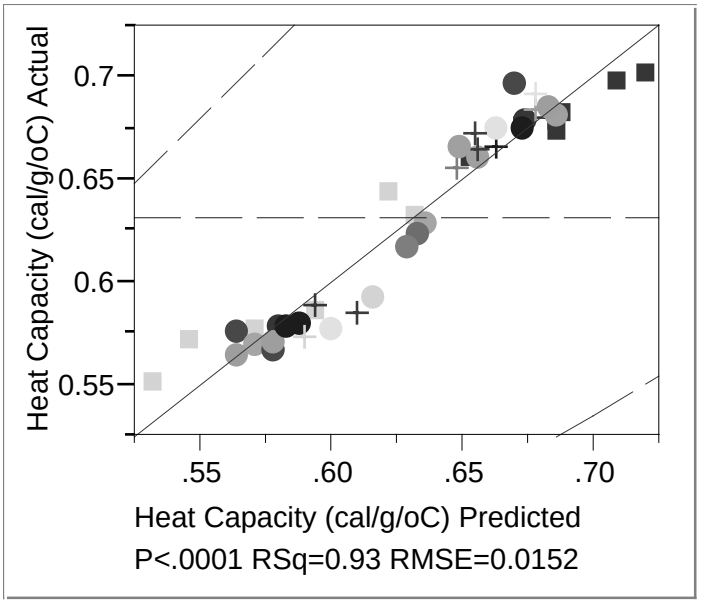

Summary of Fit

RSquare	0.931142
RSquare Adj	0.906708
Root Mean Square Error	0.015153
Mean of Response	0.631498
Observations (or Sum Wgts)	43

Analysis of Variance

Source	DF	Sum of Squares	Mean Square	F Ratio
Model	11	0.09625194	0.008750	38.1091
Error	31	0.00711787	0.000230	Prob > F
C. Total	42	0.10336981		<.0001

Tested against reduced model: Y=mean

Parameter Estimates

Term		Estimate	Std Error	t Ratio	Prob>|t|
Intercept	Zeroed	0	0	.	.
Al (swf)		0.5372078	0.185491	2.90	0.0069
Ca (swf)		0.5724292	0.121276	4.72	<.0001
Cs (swf)		0.5849211	0.131324	4.45	0.0001
H (swf)		0.8586404	0.092265	9.31	<.0001
K (swf)		0.5912291	0.195157	3.03	0.0049
Na (swf)		0.7812537	0.042412	18.42	<.0001
Al (swf)*Temp (oC)		-0.011593	0.004272	-2.71	0.0108
Ca (swf)*Temp (oC)		0.0003575	0.002776	0.13	0.8984
Cs (swf)*Temp (oC)		0.0017797	0.003005	0.59	0.5579
H (swf)*Temp (oC)		-0.006207	0.002128	-2.92	0.0065
K (swf)*Temp (oC)		-0.002709	0.004454	-0.61	0.5475
Na (swf)*Temp (oC)		-0.002128	0.00097	-2.19	0.0359

FIGURE 3.12. Results from Fitting Solubility Model Using Phase 1 and 2 Data @ 100% Saturation - Actual vs. Predicted Solubilities (g TS/ml).

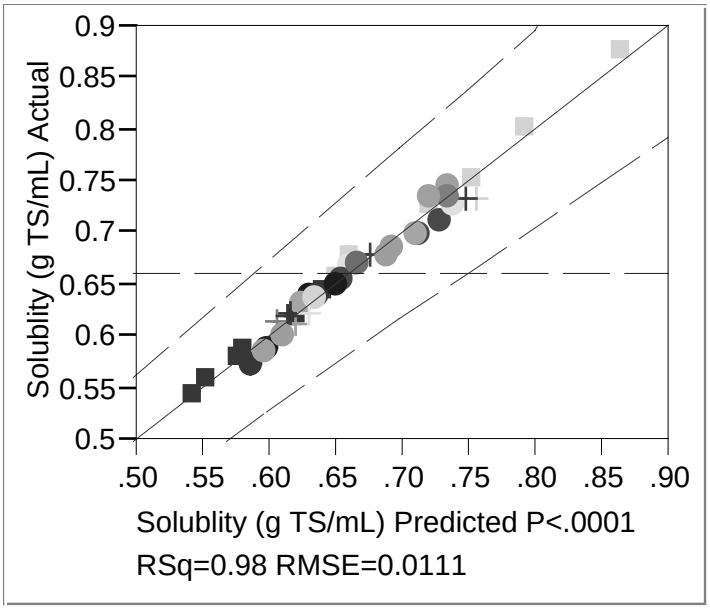

Summary of Fit

RSquare	0.981287
RSquare Adj	0.974646
Root Mean Square Error	0.011069
Mean of Response	0.6606
Observations (or Sum Wgts)	43

Analysis of Variance

Source	DF	Sum of Squares	Mean Square	F Ratio
Model	11	0.19917228	0.018107	147.7794
Error	31	0.00379825	0.000123	Prob > F
C. Total	42	0.20297054		<.0001

Tested against reduced model: Y=mean

Parameter Estimates

Term		Estimate	Std Error	t Ratio	Prob>|t|
Intercept	Zeroed	0	0	.	.
Al (swf)		0.7369865	0.1355	5.44	<.0001
Ca (swf)		0.7416068	0.088592	8.37	<.0001
Cs (swf)		0.6978888	0.095932	7.27	<.0001
H (swf)		0.5129244	0.067399	7.61	<.0001
K (swf)		0.7786191	0.142561	5.46	<.0001
Na (swf)		0.4217844	0.030982	13.61	<.0001
Al (swf)*Temp (oC)		-0.016925	0.003121	-5.42	<.0001
Ca (swf)*Temp (oC)		-0.00097	0.002028	-0.48	0.6358
Cs (swf)*Temp (oC)		0.005989	0.002195	2.73	0.0104
H (swf)*Temp (oC)		0.0035592	0.001554	2.29	0.0290
K (swf)*Temp (oC)		0.0059015	0.003253	1.81	0.0794
Na (swf)*Temp (oC)		0.0055875	0.000708	7.89	<.0001

FIGURE 3.13. Results from Fitting Solubility Model Using Phase 1 and 2 Data @ 100% Saturation - Actual vs. Predicted Solubilities (g TS/1000 g H_2O).

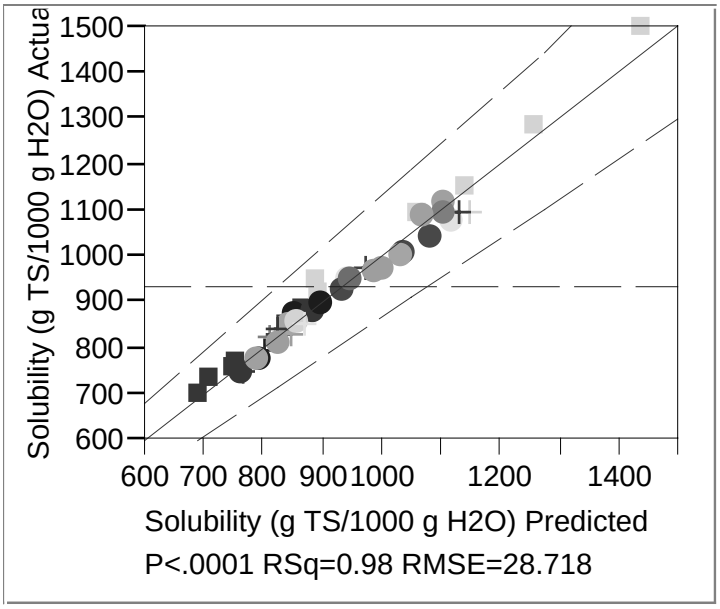

Summary of Fit

RSquare	0.976509
RSquare Adj	0.968173
Root Mean Square Error	28.71776
Mean of Response	933.4402
Observations (or Sum Wgts)	43

Analysis of Variance

Source	DF	Sum of Squares	Mean Square	F Ratio
Model	11	1062760.3	96614.6	117.1498
Error	31	25566.0	824.7	Prob > F
C. Total	42	1088326.3		<.0001

Tested against reduced model: Y=mean

Parameter Estimates

Term		Estimate	Std Error	t Ratio	Prob>|t|
Intercept	Zeroed	0	0	.	.
Al (swf)		1333.2607	351.544	3.79	0.0006
Ca (swf)		1053.5027	229.8436	4.58	<.0001
Cs (swf)		743.03475	248.8863	2.99	0.0055
H (swf)		617.11196	174.8608	3.53	0.0013
K (swf)		949.08223	369.8618	2.57	0.0153
Na (swf)		437.48135	80.37895	5.44	<.0001
Al (swf)*Temp (oC)		-48.49402	8.096112	-5.99	<.0001
Ca (swf)*Temp (oC)		-2.46527	5.260839	-0.47	0.6426
Cs (swf)*Temp (oC)		18.021038	5.694477	3.16	0.0035
H (swf)*Temp (oC)		7.0988419	4.032874	1.76	0.0882
K (swf)*Temp (oC)		22.20833	8.440394	2.63	0.0131
Na (swf)*Temp (oC)		12.222289	1.838084	6.65	<.0001

FIGURE 3.14. Results from Fitting Density Model Using Phase 1 and 2 Data @ 100% Saturation - Actual vs. Predicted Densities (g/ml).

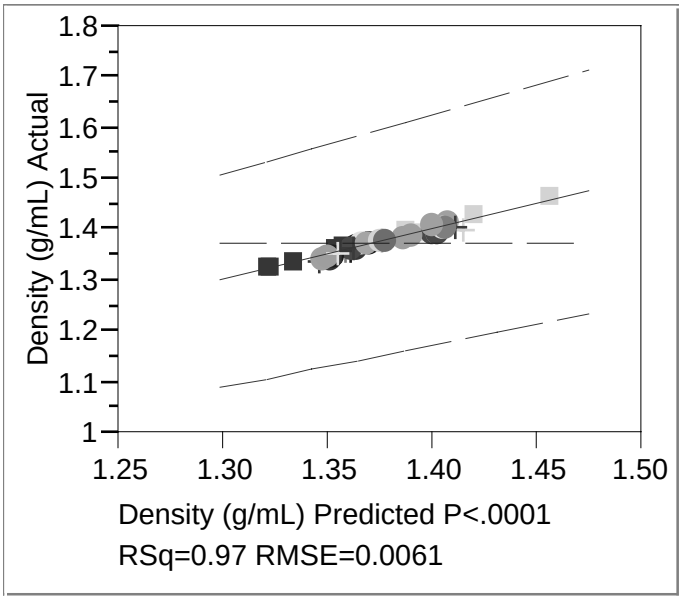

Summary of Fit

RSquare	0.966213
RSquare Adj	0.954224
Root Mean Square Error	0.006083
Mean of Response	1.375367
Observations (or Sum Wgts)	43

Analysis of Variance

Source	DF	Sum of Squares	Mean Square	F Ratio
Model	11	0.03280351	0.002982	80.5927
Error	31	0.00114708	0.000037	Prob > F
C. Total	42	0.03395059		<.0001

Tested against reduced model: Y=mean

Parameter Estimates

Term		Estimate	Std Error	t Ratio	Prob>|t|
Intercept	Zeroed	0	0	.	.
Al (swf)		1.4888566	0.074464	19.99	<.0001
Ca (swf)		1.4740819	0.048685	30.28	<.0001
Cs (swf)		1.5045988	0.052719	28.54	<.0001
H (swf)		1.314063	0.037039	35.48	<.0001
K (swf)		1.4223669	0.078344	18.16	<.0001
Na (swf)		1.2545259	0.017026	73.68	<.0001
Al (swf)*Temp (oC)		-0.006193	0.001715	-3.61	0.0011
Ca (swf)*Temp (oC)		-0.001105	0.001114	-0.99	0.3291
Cs (swf)*Temp (oC)		0.0014722	0.001206	1.22	0.2315
H (swf)*Temp (oC)		0.0014211	0.000854	1.66	0.1063
K (swf)*Temp (oC)		0.0020879	0.001788	1.17	0.2518
Na (swf)*Temp (oC)		0.0023975	0.000389	6.16	<.0001

FIGURE 3.15. Results from Fitting Viscosity Model Using Phase 1 and 2 Data @ 100% Saturation - Actual vs. Predicted Viscosities (cP).

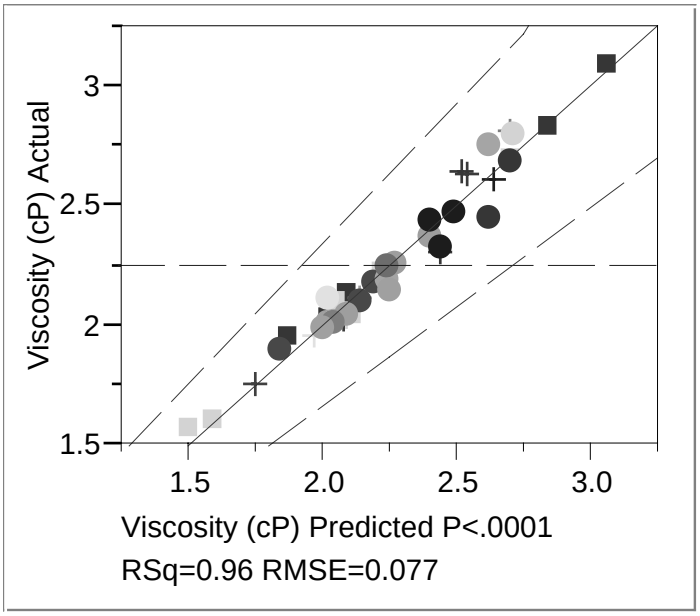

Summary of Fit

RSquare	0.963125
RSquare Adj	0.95004
Root Mean Square Error	0.076956
Mean of Response	2.24969
Observations (or Sum Wgts)	43

Analysis of Variance

Source	DF	Sum of Squares	Mean Square	F Ratio
Model	11	4.7950758	0.435916	73.6062
Error	31	0.1835904	0.005922	Prob > F
C. Total	42	4.9786662		<.0001

Tested against reduced model: Y=mean

Parameter Estimates

Term		Estimate	Std Error	t Ratio	Prob>|t|
Intercept	Zeroed	0	0	.	.
Al (swf)		12.727184	0.942048	13.51	<.0001
Ca (swf)		4.9516354	0.615922	8.04	<.0001
Cs (swf)		3.9523583	0.666952	5.93	<.0001
H (swf)		2.1414931	0.468582	4.57	<.0001
K (swf)		2.5131012	0.991136	2.54	0.0165
Na (swf)		1.3891874	0.215395	6.45	<.0001
Al (swf)*Temp (oC)		-0.074469	0.021696	-3.43	0.0017
Ca (swf)*Temp (oC)		-0.092077	0.014098	-6.53	<.0001
Cs (swf)*Temp (oC)		-0.028213	0.01526	-1.85	0.0740
H (swf)*Temp (oC)		-0.002939	0.010807	-0.27	0.7875
K (swf)*Temp (oC)		0.00172	0.022618	0.08	0.9399
Na (swf)*Temp (oC)		0.0075795	0.004926	1.54	0.1340

FIGURE 3.16. Results from Fitting Heat Capacity Model Using Phase 1 and 2 Data @ 100% Saturation - Actual vs. Predicted Heat Capacities (cal/g/^{o}C).

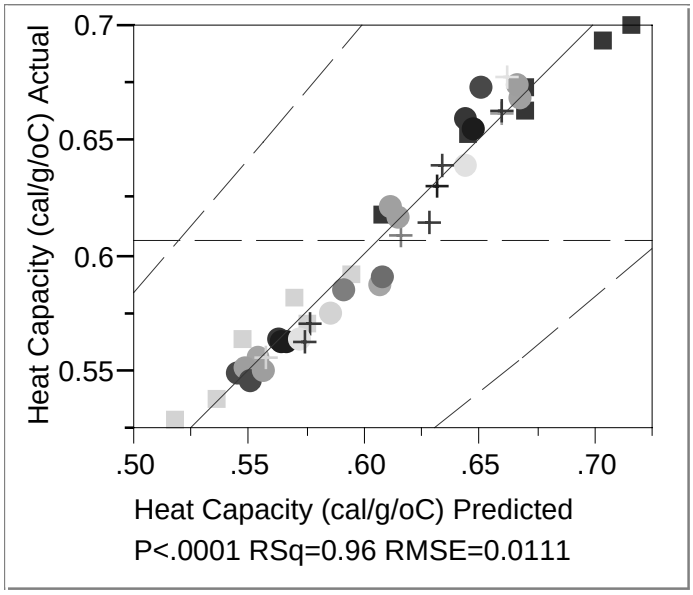

Summary of Fit

RSquare	0.96368
RSquare Adj	0.950792
Root Mean Square Error	0.011066
Mean of Response	0.607153
Observations (or Sum Wgts)	43

Analysis of Variance

Source	DF	Sum of Squares	Mean Square	F Ratio
Model	11	0.10072434	0.009157	74.7742
Error	31	0.00379622	0.000122	Prob > F
C. Total	42	0.10452057		<.0001

Tested against reduced model: Y=mean

Parameter Estimates

Term		Estimate	Std Error	t Ratio	Prob>|t|
Intercept	Zeroed	0	0	.	.
Al (swf)		-0.033781	0.135464	-0.25	0.8047
Ca (swf)		0.3896414	0.088568	4.40	0.0001
Cs (swf)		0.4919231	0.095906	5.13	<.0001
H (swf)		0.8416601	0.067381	12.49	<.0001
K (swf)		0.4644039	0.142523	3.26	0.0027
Na (swf)		0.8392561	0.030973	27.10	<.0001
Al (swf)*Temp (oC)		0.0028712	0.00312	0.92	0.3645
Ca (swf)*Temp (oC)		0.0049917	0.002027	2.46	0.0196
Cs (swf)*Temp (oC)		0.0018523	0.002194	0.84	0.4051
H (swf)*Temp (oC)		-0.005985	0.001554	-3.85	0.0006
K (swf)*Temp (oC)		0.0003942	0.003252	0.12	0.9043
Na (swf)*Temp (oC)		-0.004261	0.000708	-6.02	<.0001

4. FUTURE WORK

The physical property models derived in Section 3.5 will be validated against the data from on-going bench-scale tests with simulated cesium eluate solutions, and the results of model validation will be documented in another report. If the validation results show that the models need further improvement, the concentration ranges of major analytes given in Table 1.1, especially that of H^+, should be checked against the latest WTP flowsheet values and recent analytical data, before making any additional model runs. As stated in the task plan, this fine-tuning of models will be a major undertaking requiring significant levels of resources. This is because the task of developing these physical property models required a coherent plan for multi-faceted execution such as critical evaluation of analytical data, continual assessment and improvement of software database, development and execution of computer models, and finally statistical design and analysis of computer experiments and response data.

5. REFERENCES

[1] Choi, A. S., and Barnes, C. D., "Task Technical and Quality Assurance Plan for Cesium and Technetium Eluate Physical Property Modeling," **WSCR-TR-2001-00408, SRT-RPP-2001-00160, Rev. 0**, Westinghouse Savannah River Co., Aiken, SC, November 2001.

[2] Pierce, R. A., "Cesium Eluate Analytical Data Evaluation," **WSRC-TR-2001-00594, SRT-RPP-2001-00228**, Westinghouse Savannah River Co., Aiken, SC, December 2001.

[3] ESP Software, http://www.olisystems.com/, OLI Systems, Inc., Morris Plains, NJ (2002).

[4] Choi, A. S., "Estimation of Physical Properties of AN-107 Cesium and Technetium Eluate Blend," **WSCR-TR-2000-00527, SRT-RPP-2000-00061**, Westinghouse Savannah River Co., Aiken, SC, February 26, 2001.

[5] Edwards, T. B., "A Statistically Designed Test Matrix for a Computer Study of Cs Eluate Evaporation (U)," **SRT-SCS-2002-00034**, Westinghouse Savannah River Co., Aiken, SC, May 28, 2002.

[6] *JMP® Statistics and Graphics Guide*, Version 4, SAS Institute, Inc., Cary, NC, 2000.

[7] Choi, A. S., "Software Quality Assurance Plan for Hanford RPP-WTP Evaporator Modeling", **WSRC-RP-2001-00337**, Westinghouse Savannah River Co., Aiken, SC, December 18, 2001.

[8] Olson, J. W., "System Description for Cesium Removal Using Ion Exchange – System CXP," **24590-PTF-3YD-CXP-00001**, **Rev. A**, Bechtel National, Inc., Richland, Washington, December 14, 2001.

[9] Olson, J. W., "System Description for Technetium Removal Using Ion Exchange – System TXP," **24590-PTF-3YD-TXP-00001**, **Rev. A**, Bechtel National, Inc., Richland, WA, December 14, 2001.

[10] Woodworth, M., "System Description for Cesium Nitric Acid Recovery Process – System CNP," **24590-PTF-3YD-CNP-00001**, **Rev. B**, Bechtel National, Inc., Richland, WA, April 30, 2002.

[11] Longwell, R. L, "Eluate Physical Properties and Evaporation Test Specification", **24590-WTP-TSP-RT-01-008, Rev. 0**, Washington Group International, Richland, WA, August 30, 2001.

[12] Barnes, C.D., Edwards, T. B., and Choi, A. S., "Preliminary Modeling Results of Evaporated Tc-Eluate Physical Properties," **WSRC-TR-2002-00319, SRT-RPP-2002-00171**, Westinghouse Savannah River Co., Aiken, SC, September 26, 2002.

[13] Hassan, N. M., McCabe, D. J., King, W. D., and Crowder, M. L., "Small-Scale Ion Exchange Removal of Cesium and Technetium from Envelope B Hanford Tank 241-AZ-102," **BNF-003-98-0236, Revision 0**, Westinghouse Savannah River Co., Aiken, SC, August 28, 2000

[14] Schreiber, R. D., "Tank Characterization Report for Double-Shell Tank 241-AZ-102," **WHC-SD-WM-ER-411, Revision 0**, Westinghouse Hanford Co., Richland, WA, July 1995.

[15] Letter to S. T. Wach from M. E. Johnson, "TWRS-P Contract No. DE-AC06-96RL13308-W375-Approval of Envelope C Simulant Formulation for Sr/TRU Precipitation Tests," **BNFL Letter No. 000547**, BNFL Inc., Richland, WA, November 6, 1998.

[16] Pierce, R. A., and Choi, A. S., "Cesium Eluate Evaporation Solubility and Physical Property Behavior," **WSRC-TR-2002-0411, Rev. 0, SRT-RPP-2002-00206**, Westinghouse Savannah River Co., Aiken, SC, September 9, 2002.

[17] Pierce, R. A., and Edwards, T. B., "Cesium Eluate Evaporation Solubility and Physical Property Behavior," **WSRC-TR-2002-00273, Rev. 0, SRT-RPP-2002-00143**, Westinghouse Savannah River Co., Aiken, SC, June 11, 2002.

[18] Zemaitis, Jr., J. F., Clark, D. M., Rafal, M., and Scrivner, N. C., *Handbook of Aqueous Electrolyte Thermodynamics*, Design Institute for Physical Property Data (DIPPR), American Institute of Chemical Engineers, New York, NY (1986).

[19] *JMP® Statistics and Graphics Guide*, Version 5, SAS Institute Inc., Cary, NC, 2002.

[20] Choi, A. S., *Unpublished OLI Modeling Results of TFL Cesium Eluate Evaporation at 8.56 M Starting Pot Acidity*, Westinghouse Savannah River Co., Aiken, SC, September 2002.

APPENDIX A.

Charge Balance of Eluate Analytical Data

Assumptions and Results

For improved charge balance, the analytical data given in Table 3.1 were modified based on the following bases and assumptions:

- The concentrations of chloride and fluoride were deemed inaccurate when compared to the more recent data from the Thermal Fluids Lab (TFL) at SRTC. The TFL data showed that the measured concentrations of chloride and fluoride in all 11 different samples taken throughout the elution cycle were less than 2 mg/L. So, both chloride and fluoride were excluded from the charge balance and further deleted from considerations as the potential matrix variable [2].

- The TIC data reported for the SRTC samples were ignored because carbonate is not stable under the strongly acidic conditions prevailing in these eluate samples.

- The abnormally high TOC data for Tanks AN-105 and AN-107 samples by SRTC were attributed to the resin degradation products. For charge balance purposes, these TOC data were arbitrarily reduced to 200 mg/L each, which is more in line with the PNNL data.

- All the TOC data reported by SRTC were deemed high and further reduced by a factor of 0.2855, which was obtained based on the following data:

  The TOC level in the Tank AZ-102 filtrate was measured to be 6,040 mg/L at 2.65 M Na by SRTC [13]. As a comparison, the TOC level in the 1995 grab sample was reported to be 1,503 mg/L at 2.31M Na [14]. Comparison of these data yields:

$$\textit{Adjustment Factor} \;=\; \left(\frac{1{,}503}{6{,}040}\right)\left(\frac{2.65}{2.31}\right) \;=\; 0.2855$$

- Both adjusted and unadjusted TOC data were then distributed among various organic salts as follows:

  (a) The concentration of oxalate in each sample was arbitrarily set at 25 mg/L.

  (b) The concentration of formate in each sample was arbitrarily set at zero.

  (c) The remaining TOC data excluding oxalate and formate were distributed among the organic complexants found in the Tank AN-107 simulant shown in Table A-1 [15]. The organic acids thus added according to Table A-1 were next converted into the corresponding sodium salts.

  (d) Since HEDTA was not found in the OLI software database, it was assumed to be present as Na2EDTA.

  (e) Since the sodium salts of gluconic and iminodiacetic acids were not found in the OLI software database, they were added as NaOH and the corresponding acid.

TABLE A-1. Assumed Organic Distribution in Cesium Eluate.

Organic Constituent	Wt%
Na2EDTA	14.61
HEDTA	4.36
Sodium Gluconate	7.90
Glycolic Acid	37.95
Citric Acid	19.00
NTA	1.15
IDA	12.16
Sodium Acetate	2.88
Total	100.00

The results of charge balance are shown in Tables A-2 to A-8 for each cesium eluate sample. The full-scale flow rates given in these tables represent the required instantaneous flow rate of each cesium eluate feed to support the design basis Envelope B glass production rate of 60 metric tons per day at 10 wt% Na_2O.

TABLE A-2. Charge Balance Results for Tank AN-103 Cesium Eluate Sample Collected During an SRTC Bench-Scale IX Run.

	FW	Conc (mg/l)	Conc (M)	Equiv (M)
Anions				
NO2	46			
NO3	62	19000	0.306451613	0.306451613
OH	17	16.4592397	0.000968191	0.000968191
SO4	98.058			
C2O4	88.02	25	0.000284026	0.000568053
AlO2	58.98154			
F	19			
Cl	35.453			
CO3	60.009			
PO4	94.9714			
AsO4	138.9216			
B4O7	155.24			
CrO4	115.996	33.4629587	0.000288484	0.000576967
HgO(OH)	233.59			
MoO4	159.94			
RuO4	165.07			
Se	78.96			
SiO3	76.0855			
TcO4	162.9064			
CH3COO	59.0446	15.7061285	0.000266004	0.000266004
H2EDTA (-2)	290.247	130.212786	0.000448627	0.000897255
HEDTA (-3) **	275.2362			
COOH	45.0177			
OCH2COOH	75.042	284.193957	0.003787132	0.003787132
citrate (-1)	191.0962	143.475423	0.000750802	0.000750802
IDA (-2)	131.084			
NTA (-1)	190.116	8.66269315	4.55653E-05	4.55653E-05
Total Anions			0.313290445	0.314311582
Cations				
Na	22.99	1060	0.046107003	0.046107003
Ag	107.868			
Al	26.98154	59	0.00218668	0.006560041
Ba	137.33			
Ca	40.08	290	0.007235529	0.014471058
Cd	112.41			
Ce	140.12			
Cs	134.52	115	0.000854891	0.000854891
Cu	63.546	8	0.000125893	0.000251786
Fe	55.847	12	0.000214873	0.000644618
K	39.0983	72	0.001841512	0.001841512
La	138.906			
Mg	24.305	13	0.000534869	0.001069739
Mn	54.938			
Nd	144.24			
NH4	18			
Ni	58.71			
Pb	207.2			
Pu	244			
Sn	118.69			
Sr	87.62			
U	238.029			
Zn	65.38	21	0.000321199	0.000642398
Zr	91.22			
gluconic acid *	196.16	53.9455511	0.000275008	0.000275008
IDA *	133.084	92.2515216	0.000693183	0.000693183
H+	1	240.900345	0.240900345	0.240900345
Total Cations			0.05942245	0.314311582

Species	MW	Conc (M)	g/liter	full-scale flow (mole/hr)	TOC (g/liter)
NaNO2	69				
NaNO3	85	3.9215E-02	3.3333E+00	4.0627E+01	
NaOH	40.07	9.6819E-04	3.8795E-02	1.0030E+00	
Na2SO4	142.04				
Na2C2O4	134	2.8403E-04	3.8060E-02	2.9425E-01	6.8166E-03
NaAlO2	81.97154				
NaF	41.99				
NaCl	58.443				
Na2CO3	106				
Na3PO4	163.944				
Na3AsO4	207.8916				
Na2B4O7	201.22				
Na2CrO4	161.976	2.8848E-04	4.6727E-02	2.9887E-01	
Na(HgO(OH))	256.58				
Na2MoO4	205.92				
Na2RuO4	211.05				
Na2Se	101.95				
Na2SiO3	122.07				
NaTcO4	185.8964				
NaCH3COO	82.0346	2.6600E-04	2.1822E-02	2.7558E-01	6.3841E-03
Na2H2EDTA	336.227	4.4863E-04	1.5084E-01	4.6478E-01	5.3835E-02
Na3HEDTA	344.206				
NaCOOH	68.0077				
NaOCH2COOH	98.032	3.7871E-03	3.7126E-01	3.9235E+00	9.0891E-02
NaH2Citrate	214.086	7.5080E-04	1.6074E-01	7.7783E-01	5.4058E-02
Na2IDA	177.064				
NaH2NTA	213.106	4.5565E-05	9.7102E-03	4.7206E-02	3.2807E-03
HNO3	63	2.4090E-01	1.5177E+01	2.4957E+02	
AgNO3	169.868				
Al(NO3)3	212.98154	2.1867E-03	4.6572E-01	2.2654E+00	
Ba(NO3)2	261.33				
Ca(NO3)2	164.08	7.2355E-03	1.1872E+00	7.4960E+00	
Cd(NO3)2	236.41				
Ce(NO3)3	326.12				
CsNO3	196.52	8.5489E-04	1.6800E-01	8.8567E-01	
Cu(NO3)2	187.546	1.2589E-04	2.3611E-02	1.3043E-01	
Fe(NO3)3	241.847	2.1487E-04	5.1966E-02	2.2261E-01	
KNO3	101.0983	1.8415E-03	1.8617E-01	1.9078E+00	
La(NO3)3	324.906				
Mg(NO3)2	148.305	5.3487E-04	7.9324E-02	5.5412E-01	
Mn(NO3)2	178.938				
Nd(NO3)3	330.24				
NH4NO3	80				
Ni(NO3)2	182.71				
Pb(NO3)2	331.2				
Na2PuO2(OH)4	389.98				
Sn(OH)4	186.69				
Sr(NO3)2	211.62				
UO2(NO3)2	394.09				
Zn(NO3)2	189.38	3.2120E-04	6.0829E-02	3.3276E-01	
Zn(NO3)4	339.22				
gluconic acid *	196.16	2.7501E-04	5.3946E-02	2.8491E-01	1.9801E-02
IDA *	133.084	6.9318E-04	9.2252E-02	7.1814E-01	3.3273E-02
H2O	18.02	5.5122E+01	9.9330E+02	5.7107E+04	
Total			1.0150E+03	5.7419E+04	2.6834E-01

TABLE A-3. Charge Balance Results for Tank AN-102 Cesium Eluate Sample Collected During an SRTC Bench-Scale IX Run.

	FW	Conc (mg/l)	Conc (M)	Equiv (M)
Anions				
NO2	46			
NO3	62	22400	0.361290323	0.361290323
OH	17	8.01511317	0.000471477	0.000471477
SO4	98.058			
C2O4	88.02	25	0.000284026	0.000568053
AlO2	58.98154			
F	19			
Cl	35.453			
CO3	60.009			
PO4	94.9714			
AsO4	138.9216			
B4O7	155.24	800.613321	0.005157262	0.010314524
CrO4	115.996	22.3086391	0.000192322	0.000384645
HgO(OH)	233.59			
MoO4	159.94			
RuO4	165.07			
Se	78.96			
SiO3	76.0855	265.488562	0.003489345	0.00697869
TcO4	162.9064			
CH3COO	59.0446	7.64837256	0.000129536	0.000129536
H2EDTA (-2)	290.247	63.4093818	0.000218467	0.000436934
HEDTA (-3) **	275.2362			
COOH	45.0177			
OCH2COOH	75.042	138.393192	0.00184421	0.00184421
citrate (-1)	191.0962	69.8678536	0.000365616	0.000365616
IDA (-2)	131.084			
NTA (-1)	190.116	4.21844916	2.21888E-05	2.21888E-05
Total Anions			0.373464773	0.382806195
Cations				
Na	22.99	1480	0.064375816	0.064375816
Ag	107.868			
Al	26.98154	268	0.009932717	0.029798151
Ba	137.33			
Ca	40.08	66	0.001646707	0.003293413
Cd	112.41			
Ce	140.12			
Cs	134.52	24	0.000178412	0.000178412
Cu	63.546	30	0.000472099	0.000944198
Fe	55.847	7	0.000125342	0.000376027
K	39.0983	80	0.002046125	0.002046125
La	138.906			
Mg	24.305	9	0.000370294	0.000740588
Mn	54.938			
Nd	144.24			
NH4	18			
Ni	58.71	4.5	7.66479E-05	0.000153296
Pb	207.2			
Pu	244			
Sn	118.69			
Sr	87.62			
U	238.029	17	7.14199E-05	0.000428519
Zn	65.38	4	6.11808E-05	0.000122362
Zr	91.22			
gluconic acid *	196.16	26.2697248	0.00013392	0.00013392
IDA *	133.084	44.9234836	0.000337557	0.000337557
H+	1	279.877811	0.279877811	0.279877811
Total Cations			0.07935676	0.382806195

Species	MW	Conc (M)	g/liter	full-scale flow (mole/hr)	TOC (g/liter)
NaNO2	69				
NaNO3	85	4.3617E-02	3.7075E+00	2.1652E+02	
NaOH	40.07	4.7148E-04	1.8892E-02	2.3405E+00	
Na2SO4	142.04				
Na2C2O4	134	2.8403E-04	3.8060E-02	1.4100E+00	6.8166E-03
NaAlO2	81.97154				
NaF	41.99				
NaCl	58.443				
Na2CO3	106				
Na3PO4	163.944				
Na3AsO4	207.8916				
Na2B4O7	201.22	5.1573E-03	1.0377E+00	2.5602E+01	
Na2CrO4	161.976	1.9232E-04	3.1152E-02	9.5472E-01	
Na(HgO(OH))	256.58				
Na2MoO4	205.92				
Na2RuO4	211.05				
Na2Se	101.95				
Na2SiO3	122.07	3.4893E-03	4.2594E-01	1.7322E+01	
NaTcO4	185.8964				
NaCH3COO	82.0346	1.2954E-04	1.0626E-02	6.4304E-01	3.1089E-03
Na2H2EDTA	336.227	2.1847E-04	7.3454E-02	1.0845E+00	2.6216E-02
Na3HEDTA	344.206				
NaCOOH	68.0077				
NaOCH2COOH	98.032	1.8442E-03	1.8079E-01	9.1550E+00	4.4261E-02
NaH2Citrate	214.086	3.6562E-04	7.8273E-02	1.8150E+00	2.6324E-02
Na2IDA	177.064				
NaH2NTA	213.106	2.2189E-05	4.7286E-03	1.1015E-01	1.5976E-03
HNO3	63	2.7988E-01	1.7632E+01	1.3894E+03	
AgNO3	169.868				
Al(NO3)3	212.98154	9.9327E-03	2.1155E+00	4.9308E+01	
Ba(NO3)2	261.33				
Ca(NO3)2	164.08	1.6467E-03	2.7019E-01	8.1745E+00	
Cd(NO3)2	236.41				
Ce(NO3)3	326.12				
CsNO3	196.52	1.7841E-04	3.5062E-02	8.8567E-01	
Cu(NO3)2	187.546	4.7210E-04	8.8540E-02	2.3436E+00	
Fe(NO3)3	241.847	1.2534E-04	3.0314E-02	6.2222E-01	
KNO3	101.0983	2.0461E-03	2.0686E-01	1.0157E+01	
La(NO3)3	324.906				
Mg(NO3)2	148.305	3.7029E-04	5.4916E-02	1.8382E+00	
Mn(NO3)2	178.938				
Nd(NO3)3	330.24				
NH4NO3	80				
Ni(NO3)2	182.71	7.6648E-05	1.4004E-02	3.8049E-01	
Pb(NO3)2	331.2				
Na2PuO2(OH)4	389.98				
Sn(OH)4	186.69				
Sr(NO3)2	211.62				
UO2(NO3)2	394.09	7.1420E-05	2.8146E-02	3.5454E-01	
Zn(NO3)2	189.38	6.1181E-05	1.1586E-02	3.0371E-01	
Zr(NO3)4	339.22				
gluconic acid *	196.16	1.3392E-04	2.6270E-02	6.6480E-01	9.6422E-03
IDA *	133.084	3.3756E-04	4.4923E-02	1.6757E+00	1.6203E-02
H2O	18.02	5.4875E+01	9.8884E+02	2.7241E+05	
Total			1.0150E+03	2.7415E+05	1.3417E-01

TABLE A-4. Charge Balance Results for Tank AZ-102 Cesium Eluate Sample Collected During an SRTC Bench-Scale IX Run.

	FW	Conc (mg/l)	Conc (M)	Equiv (M)	Species	MW	Conc (M)	g/liter	full-scale flow (mole/hr)	TOC (g/liter)
Anions										
NO2	46	952	0.020695652	0.020695652	NaNO2	69	2.0696E-02	1.4280E+00	5.0839E+00	
NO3	62	21300	0.343548387	0.343548387	NaNO3	85	4.6574E-02	3.9588E+00	1.1441E+01	
OH	17	4.36796915	0.000256939	0.000256939	NaOH	40.07	2.5694E-04	1.0296E-02	6.3117E-02	
SO4	98.058				Na2SO4	142.04				
C2O4	88.02	25	0.000284026	0.000568053	Na2C2O4	134	2.8403E-04	3.8060E-02	6.9771E-02	6.8166E-03
AlO2	58.98154				NaAlO2	81.97154				
F	19				NaF	41.99				
Cl	35.453				NaCl	58.443				
CO3	60.009				Na2CO3	106				
PO4	94.9714				Na3PO4	163.944				
AsO4	138.9216				Na3AsO4	207.8916				
B4O7	155.24				Na2B4O7	201.22				
CrO4	115.996	93.6962843	0.000807754	0.001615509	Na2CrO4	161.976	8.0775E-04	1.3084E-01	1.9842E-01	
HgO(OH)	233.59				Na(HgO(OH))	256.58				
MoO4	159.94				Na2MoO4	205.92				
RuO4	165.07				Na2RuO4	211.05				
Se	78.96				Na2Se	101.95				
SiO3	76.0855				Na2SiO3	122.07				
TcO4	162.9064				NaTcO4	185.8964				
CH3COO	59.0446	4.16810776	7.05925E-05	7.05925E-05	NaCH3COO	82.0346	7.0593E-05	5.7910E-03	1.7341E-02	1.6942E-03
H2EDTA (-2)	290.247	34.5559967	0.000119057	0.000238114	Na2H2EDTA	336.227	1.1906E-04	4.0030E-02	2.9246E-02	1.4287E-02
HEDTA (-3) **	275.2362				Na3HEDTA	344.206				
COOH	45.0177				NaCOOH	68.0077				
OCH2COOH	75.042	75.4196706	0.001005033	0.001005033	NaOCH2COOH	98.032	1.0050E-03	9.8525E-02	2.4689E-01	2.4121E-02
citrate (-1)	191.0962	38.0756482	0.000199249	0.000199249	NaH2Citrate	214.086	1.9925E-04	4.2656E-02	4.8945E-02	1.4346E-02
IDA (-2)	131.084				Na2IDA	177.064				
NTA (-1)	190.116	2.29891399	1.20922E-05	1.20922E-05	NaH2NTA	213.106	1.2092E-05	2.5769E-03	2.9704E-03	8.7064E-04
Total Anions			0.366998783	0.368209621						
Cations										
Na	22.99	1626	0.070726403	0.070726403	HNO3	63	2.8940E-01	1.8232E+01	7.1090E+01	
Ag	107.868				AgNO3	169.868				
Al	26.98154	4	0.00014825	0.000444749	Al(NO3)3	212.98154	1.4825E-04	3.1574E-02	3.6417E-02	
Ba	137.33				Ba(NO3)2	261.33				
Ca	40.08	9	0.000224551	0.000449102	Ca(NO3)2	164.08	2.2455E-04	3.6844E-02	5.5161E-02	
Cd	112.41				Cd(NO3)2	236.41				
Ce	140.12				Ce(NO3)3	326.12				
Cs	134.52	485	0.003605412	0.003605412	CsNO3	196.52	3.6054E-03	7.0854E-01	8.8567E-01	
Cu	63.546				Cu(NO3)2	187.546				
Fe	55.847	4	7.16243E-05	0.000214873	Fe(NO3)3	241.847	7.1624E-05	1.7322E-02	1.7594E-02	
K	39.0983	107	0.002736692	0.002736692	KNO3	101.0983	2.7367E-03	2.7667E-01	6.7227E-01	
La	138.906				La(NO3)3	324.906				
Mg	24.305				Mg(NO3)2	148.305				
Mn	54.938				Mn(NO3)2	178.938				
Nd	144.24				Nd(NO3)3	330.24				
NH4	18				NH4NO3	80				
Ni	58.71				Ni(NO3)2	182.71				
Pb	207.2				Pb(NO3)2	331.2				
Pu	244				Na2PuO2(OH)4	389.98				
Sn	118.69				Sn(OH)4	186.69				
Sr	87.62				Sr(NO3)2	211.62				
U	238.029	15	6.30175E-05	0.000378105	UO2(NO3)2	394.09	6.3018E-05	2.4835E-02	1.5480E-02	
Zn	65.38				Zn(NO3)2	189.38				
Zr	91.22				Zr(NO3)4	339.22				
gluconic acid *	196.16	14.3161232	7.29819E-05	7.29819E-05	gluconic acid *	196.16	7.2982E-05	1.4316E-02	1.7928E-02	5.2547E-03
IDA *	133.084	24.4817992	0.000183957	0.000183957	IDA *	133.084	1.8396E-04	2.4482E-02	4.5189E-02	8.8300E-03
H+	1	289.397347	0.289397347	0.289397347	H2O	18.02	5.4932E+01	9.8988E+02	1.3494E+04	
Total Cations			0.077575949	0.368209621	Total			1.0150E+03	1.3584E+04	7.6220E-02

TABLE A-5. Charge Balance Results for Tank AN-105 Cesium Eluate Sample Collected During an SRTC Bench-Scale IX Run.

	FW	Conc (mg/l)	Conc (M)	Equiv (M)	Species	MW	Conc (M)	g/liter	full-scale flow (mole/hr)	TOC (g/liter)
Anions										
NO2	46	952	0.020695652	0.020695652	NaNO2	69	2.0696E-02	1.4280E+00	5.0839E+00	
NO3	62	21300	0.343548387	0.343548387	NaNO3	85	4.6574E-02	3.9588E+00	1.1441E+01	
OH	17	4.36796915	0.000256939	0.000256939	NaOH	40.07	2.5694E-04	1.0296E-02	6.3117E-02	
SO4	98.058				Na2SO4	142.04				
C2O4	88.02	25	0.000284026	0.000568053	Na2C2O4	134	2.8403E-04	3.8060E-02	6.9771E-02	6.8166E-03
AlO2	58.98154				NaAlO2	81.97154				
F	19				NaF	41.99				
Cl	35.453				NaCl	58.443				
CO3	60.009				Na2CO3	106				
PO4	94.9714				Na3PO4	163.944				
AsO4	138.9216				Na3AsO4	207.8916				
B4O7	155.24				Na2B4O7	201.22				
CrO4	115.996	93.6962843	0.000807754	0.001615509	Na2CrO4	161.976	8.0775E-04	1.3084E-01	1.9842E-01	
HgO(OH)	233.59				Na(HgO(OH))	256.58				
MoO4	159.94				Na2MoO4	205.92				
RuO4	165.07				Na2RuO4	211.05				
Se	78.96				Na2Se	101.95				
SiO3	76.0855				Na2SiO3	122.07				
TcO4	162.9064				NaTcO4	185.8964				
CH3COO	59.0446	4.16810776	7.05925E-05	7.05925E-05	NaCH3COO	82.0346	7.0593E-05	5.7910E-03	1.7341E-02	1.6942E-03
H2EDTA (-2)	290.247	34.5559967	0.000119057	0.000238114	Na2H2EDTA	336.227	1.1906E-04	4.0030E-02	2.9246E-02	1.4287E-02
HEDTA (-3) **	275.2362				Na3HEDTA	344.206				
COOH	45.0177				NaCOOH	68.0077				
OCH2COOH	75.042	75.4196706	0.001005033	0.001005033	NaOCH2COOH	98.032	1.0050E-03	9.8525E-02	2.4689E-01	2.4121E-02
citrate (-1)	191.0962	38.0756482	0.000199249	0.000199249	NaH2Citrate	214.086	1.9925E-04	4.2656E-02	4.8945E-02	1.4346E-02
IDA (-2)	131.084				Na2IDA	177.064				
NTA (-1)	190.116	2.29891399	1.20922E-05	1.20922E-05	NaH2NTA	213.106	1.2092E-05	2.5769E-03	2.9704E-03	8.7064E-04
Total Anions			0.366998783	0.368209621						
Cations										
Na	22.99	1626	0.070726403	0.070726403	HNO3	63	2.8940E-01	1.8232E+01	7.1090E+01	
Ag	107.868				AgNO3	169.868				
Al	26.98154	4	0.00014825	0.000444749	Al(NO3)3	212.98154	1.4825E-04	3.1574E-02	3.6417E-02	
Ba	137.33				Ba(NO3)2	261.33				
Ca	40.08	9	0.000224551	0.000449102	Ca(NO3)2	164.08	2.2455E-04	3.6844E-02	5.5161E-02	
Cd	112.41				Cd(NO3)2	236.41				
Ce	140.12				Ce(NO3)3	326.12				
Cs	134.52	485	0.003605412	0.003605412	CsNO3	196.52	3.6054E-03	7.0854E-01	8.8567E-01	
Cu	63.546				Cu(NO3)2	187.546				
Fe	55.847	4	7.16243E-05	0.000214873	Fe(NO3)3	241.847	7.1624E-05	1.7322E-02	1.7594E-02	
K	39.0983	107	0.002736692	0.002736692	KNO3	101.0983	2.7367E-03	2.7667E-01	6.7227E-01	
La	138.906				La(NO3)3	324.906				
Mg	24.305				Mg(NO3)2	148.305				
Mn	54.938				Mn(NO3)2	178.938				
Nd	144.24				Nd(NO3)3	330.24				
NH4	18				NH4NO3	80				
Ni	58.71				Ni(NO3)2	182.71				
Pb	207.2				Pb(NO3)2	331.2				
Pu	244				Na2PuO2(OH)4	389.98				
Sn	118.69				Sn(OH)4	186.69				
Sr	87.62				Sr(NO3)2	211.62				
U	238.029	15	6.30175E-05	0.000378105	UO2(NO3)2	394.09	6.3018E-05	2.4835E-02	1.5480E-02	
Zn	65.38				Zn(NO3)2	189.38				
Zr	91.22				Zr(NO3)4	339.22				
gluconic acid *	196.16	14.3161232	7.29819E-05	7.29819E-05	gluconic acid *	196.16	7.2982E-05	1.4316E-02	1.7928E-02	5.2547E-03
IDA *	133.084	24.4817992	0.000183957	0.000183957	IDA *	133.084	1.8396E-04	2.4482E-02	4.5189E-02	8.8300E-03
H+	1	289.397347	0.289397347	0.289397347	H2O	18.02	5.4932E+01	9.8988E+02	1.3494E+04	
Total Cations			0.077575949	0.368209621	Total			1.0150E+03	1.3584E+04	7.6220E-02

TABLE A-6. Charge Balance Results for Tank AN-107 Cesium Eluate Sample Collected During an SRTC Bench-Scale IX Run.

	FW	Conc (mg/l)	Conc (M)	Equiv (M)
Anions				
NO2	46			
NO3	62	28200	0.45483871	0.45483871
OH	17	3.16423197	0.000186131	0.000186131
SO4	98.058			
C2O4	88.02	25	0.000284026	0.000568053
AlO2	58.98154			
F	19			
Cl	35.453			
CO3	60.009			
PO4	94.9714			
AsO4	138.9216			
B4O7	155.24	140.017576	0.000901943	0.001803885
CrO4	115.996	17.8469113	0.000153858	0.000307716
HgO(OH)	233.59			
MoO4	159.94			
RuO4	165.07			
Se	78.96			
SiO3	76.0855	43.3450713	0.000569689	0.001139378
TcO4	162.9064			
CH3COO	59.0446	3.01944894	5.11384E-05	5.11384E-05
H2EDTA (-2)	290.247	25.0329582	8.62471E-05	0.000172494
HEDTA (-3) **	275.2362			
COOH	45.0177			
OCH2COOH	75.042	54.6353063	0.000728063	0.000728063
citrate (-1)	191.0962	27.5826543	0.000144339	0.000144339
IDA (-2)	131.084			
NTA (-1)	190.116	1.66537283	8.75977E-06	8.75977E-06
Total Anions			0.457952904	0.459948667
Cations				
Na	22.99	931	0.040495868	0.040495868
Ag	107.868			
Al	26.98154	30	0.001111871	0.003335614
Ba	137.33			
Ca	40.08	10	0.000249501	0.000499002
Cd	112.41			
Ce	140.12			
Cs	134.52	46	0.000341957	0.000341957
Cu	63.546	16	0.000251786	0.000503572
Fe	55.847	63	0.001128082	0.003384246
K	39.0983	33	0.000844026	0.000844026
La	138.906			
Mg	24.305	3	0.000123431	0.000246863
Mn	54.938			
Nd	144.24			
NH4	18			
Ni	58.71	35	0.000596151	0.001192301
Pb	207.2	9	4.34363E-05	8.68726E-05
Pu	244			
Sn	118.69			
Sr	87.62			
U	238.029	203	0.000852837	0.005117024
Zn	65.38	2	3.05904E-05	6.11808E-05
Zr	91.22			
gluconic acid *	196.16	10.3708458	5.28693E-05	5.28693E-05
IDA *	133.084	17.7350363	0.000133262	0.000133262
H+	1	403.65401	0.40365401	0.40365401
Total Cations			0.046069537	0.459948667

Species	MW	Conc (M)	g/liter	full-scale flow (mole/hr)	TOC (g/liter)
NaNO2	69				
NaNO3	85	3.9070E-02	3.3210E+00	1.0119E+02	
NaOH	40.07	1.8613E-04	7.4583E-03	4.8208E-01	
Na2SO4	142.04				
Na2C2O4	134	2.8403E-04	3.8060E-02	7.3563E-01	6.8166E-03
NaAlO2	81.97154				
NaF	41.99				
NaCl	58.443				
Na2CO3	106				
Na3PO4	163.944				
Na3AsO4	207.8916				
Na2B4O7	201.22	9.0194E-04	1.8149E-01	2.3360E+00	
Na2CrO4	161.976	1.5386E-04	2.4921E-02	3.9849E-01	
Na(HgO(OH))	256.58				
Na2MoO4	205.92				
Na2RuO4	211.05				
Na2Se	101.95				
Na2SiO3	122.07	5.6969E-04	6.9542E-02	1.4755E+00	
NaTcO4	185.8964				
NaCH3COO	82.0346	5.1138E-05	4.1951E-03	1.3245E-01	1.2273E-03
Na2H2EDTA	336.227	8.6247E-05	2.8999E-02	2.2338E-01	1.0350E-02
Na3HEDTA	344.206				
NaCOOH	68.0077				
NaOCH2COOH	98.032	7.2806E-04	7.1373E-02	1.8857E+00	1.7474E-02
NaH2Citrate	214.086	1.4434E-04	3.0901E-02	3.7384E-01	1.0392E-02
Na2IDA	177.064				
NaH2NTA	213.106	8.7598E-06	1.8668E-03	2.2688E-02	6.3070E-04
HNO3	63	4.0365E-01	2.5430E+01	1.0455E+03	
AgNO3	169.868				
Al(NO3)3	212.98154	1.1119E-03	2.3681E-01	2.8797E+00	
Ba(NO3)2	261.33				
Ca(NO3)2	164.08	2.4950E-04	4.0938E-02	6.4621E-01	
Cd(NO3)2	236.41				
Ce(NO3)3	326.12				
CsNO3	196.52	3.4196E-04	6.7201E-02	8.8567E-01	
Cu(NO3)2	187.546	2.5179E-04	4.7221E-02	6.5213E-01	
Fe(NO3)3	241.847	1.1281E-03	2.7282E-01	2.9217E+00	
KNO3	101.0983	8.4403E-04	8.5330E-02	2.1860E+00	
La(NO3)3	324.906				
Mg(NO3)2	148.305	1.2343E-04	1.8305E-02	3.1969E-01	
Mn(NO3)2	178.938				
Nd(NO3)3	330.24				
NH4NO3	80				
Ni(NO3)2	182.71	5.9615E-04	1.0892E-01	1.5440E+00	
Pb(NO3)2	331.2	4.3436E-05	1.4386E-02	1.1250E-01	
Na2PuO2(OH)4	389.98				
Sn(OH)4	186.69				
Sr(NO3)2	211.62				
UO2(NO3)2	394.09	8.5284E-04	3.3609E-01	2.2088E+00	
Zn(NO3)2	189.38	3.0590E-05	5.7932E-03	7.9229E-02	
Zr(NO3)4	339.22				
gluconic acid *	196.16	5.2869E-05	1.0371E-02	1.3693E-01	3.8066E-03
IDA *	133.084	1.3326E-04	1.7735E-02	3.4515E-01	6.3966E-03
H2O	18.02	5.4635E+01	9.8453E+02	1.4151E+05	
Total			1.0150E+03	1.4268E+05	5.7093E-02

TABLE A-7. Charge Balance Results for Tank AW-101 Cesium Eluate Sample Collected During a PNNL Bench-Scale IX Run.

	FW	Conc (mg/l)	Conc (M)	Equiv (M)
Anions				
NO2	46			
NO3	62	28200	0.45483871	0.45483871
OH	17	3.16423197	0.000186131	0.000186131
SO4	98.058			
C2O4	88.02	25	0.000284026	0.000568053
AlO2	58.98154			
F	19			
Cl	35.453			
CO3	60.009			
PO4	94.9714			
AsO4	138.9216			
B4O7	155.24	140.017576	0.000901943	0.001803885
CrO4	115.996	17.8469113	0.000153858	0.000307716
HgO(OH)	233.59			
MoO4	159.94			
RuO4	165.07			
Se	78.96			
SiO3	76.0855	43.3450713	0.000569689	0.001139378
TcO4	162.9064			
CH3COO	59.0446	3.01944894	5.11384E-05	5.11384E-05
H2EDTA (-2)	290.247	25.0329582	8.62471E-05	0.000172494
HEDTA (-3) **	275.2362			
COOH	45.0177			
OCH2COOH	75.042	54.6353063	0.000728063	0.000728063
citrate (-1)	191.0962	27.5826543	0.000144339	0.000144339
IDA (-2)	131.084			
NTA (-1)	190.116	1.66537283	8.75977E-06	8.75977E-06
Total Anions			0.457952904	0.459948667
Cations				
Na	22.99	931	0.040495868	0.040495868
Ag	107.868			
Al	26.98154	30	0.001111871	0.003335614
Ba	137.33			
Ca	40.08	10	0.000249501	0.000499002
Cd	112.41			
Ce	140.12			
Cs	134.52	46	0.000341957	0.000341957
Cu	63.546	16	0.000251786	0.000503572
Fe	55.847	63	0.001128082	0.003384246
K	39.0983	33	0.000844026	0.000844026
La	138.906			
Mg	24.305	3	0.000123431	0.000246863
Mn	54.938			
Nd	144.24			
NH4	18			
Ni	58.71	35	0.000596151	0.001192301
Pb	207.2	9	4.34363E-05	8.68726E-05
Pu	244			
Sn	118.69			
Sr	87.62			
U	238.029	203	0.000852837	0.005117024
Zn	65.38	2	3.05904E-05	6.11808E-05
Zr	91.22			
gluconic acid *	196.16	10.3708458	5.28693E-05	5.28693E-05
IDA *	133.084	17.7350363	0.000133262	0.000133262
H+	1	403.65401	0.40365401	0.40365401
Total Cations			0.046069537	0.459948667

Species	MW	Conc (M)	g/liter	full-scale flow (mole/hr)	TOC (g/liter)
NaNO2	69				
NaNO3	85	3.9070E-02	3.3210E+00	1.0119E+02	
NaOH	40.07	1.8613E-04	7.4583E-03	4.8208E-01	
Na2SO4	142.04				
Na2C2O4	134	2.8403E-04	3.8060E-02	7.3563E-01	6.8166E-03
NaAlO2	81.97154				
NaF	41.99				
NaCl	58.443				
Na2CO3	106				
Na3PO4	163.944				
Na3AsO4	207.8916				
Na2B4O7	201.22	9.0194E-04	1.8149E-01	2.3360E+00	
Na2CrO4	161.976	1.5386E-04	2.4921E-02	3.9849E-01	
Na(HgO(OH))	256.58				
Na2MoO4	205.92				
Na2RuO4	211.05				
Na2Se	101.95				
Na2SiO3	122.07	5.6969E-04	6.9542E-02	1.4755E+00	
NaTcO4	185.8964				
NaCH3COO	82.0346	5.1138E-05	4.1951E-03	1.3245E-01	1.2273E-03
Na2H2EDTA	336.227	8.6247E-05	2.8999E-02	2.2338E-01	1.0350E-02
Na3HEDTA	344.206				
NaCOOH	68.0077				
NaOCH2COOH	98.032	7.2806E-04	7.1373E-02	1.8857E+00	1.7474E-02
NaH2Citrate	214.086	1.4434E-04	3.0901E-02	3.7384E-01	1.0392E-02
Na2IDA	177.064				
NaH2NTA	213.106	8.7598E-06	1.8668E-03	2.2688E-02	6.3070E-04
HNO3	63	4.0365E-01	2.5430E+01	1.0455E+03	
AgNO3	169.868				
Al(NO3)3	212.98154	1.1119E-03	2.3681E-01	2.8797E+00	
Ba(NO3)2	261.33				
Ca(NO3)2	164.08	2.4950E-04	4.0938E-02	6.4621E-01	
Cd(NO3)2	236.41				
Ce(NO3)3	326.12				
CsNO3	196.52	3.4196E-04	6.7201E-02	8.8567E-01	
Cu(NO3)2	187.546	2.5179E-04	4.7221E-02	6.5213E-01	
Fe(NO3)3	241.847	1.1281E-03	2.7282E-01	2.9217E+00	
KNO3	101.0983	8.4403E-04	8.5330E-02	2.1860E+00	
La(NO3)3	324.906				
Mg(NO3)2	148.305	1.2343E-04	1.8305E-02	3.1969E-01	
Mn(NO3)2	178.938				
Nd(NO3)3	330.24				
NH4NO3	80				
Ni(NO3)2	182.71	5.9615E-04	1.0892E-01	1.5440E+00	
Pb(NO3)2	331.2	4.3436E-05	1.4386E-02	1.1250E-01	
Na2PuO2(OH)4	389.98				
Sn(OH)4	186.69				
Sr(NO3)2	211.62				
UO2(NO3)2	394.09	8.5284E-04	3.3609E-01	2.2088E+00	
Zn(NO3)2	189.38	3.0590E-05	5.7932E-03	7.9229E-02	
Zr(NO3)4	339.22				
gluconic acid *	196.16	5.2869E-05	1.0371E-02	1.3693E-01	3.8066E-03
IDA *	133.084	1.3326E-04	1.7735E-02	3.4515E-01	6.3966E-03
H2O	18.02	5.4635E+01	9.8453E+02	1.4151E+05	
Total			1.0150E+03	1.4268E+05	5.7093E-02

TABLE A-8. Charge Balance Results for Tank AN-107 Cesium Eluate Sample Collected During a PNNL Bench-Scale IX Run.

	FW	Conc (mg/l)	Conc (M)	Equiv (M)
Anions				
NO2	46			
NO3	62	24500	0.39516129	0.39516129
OH	17	6.87159292	0.000404211	0.000404211
SO4	98.058			
C2O4	88.02	25	0.000284026	0.000568053
AlO2	58.98154			
F	19			
Cl	35.453			
CO3	60.009			
PO4	94.9714			
AsO4	138.9216			
B4O7	155.24			
CrO4	115.996	8.92345565	7.6929E-05	0.000153858
HgO(OH)	233.59			
MoO4	159.94			
RuO4	165.07			
Se	78.96			
SiO3	76.0855	32.5088035	0.000427267	0.000854533
TcO4	162.9064			
CH3COO	59.0446	6.55717537	0.000111055	0.000111055
H2EDTA (-2)	290.247	54.3627332	0.000187298	0.000374596
HEDTA (-3) **	275.2362			
COOH	45.0177			
OCH2COOH	75.042	118.648565	0.001581095	0.001581095
citrate (-1)	191.0962	59.8997716	0.000313453	0.000313453
IDA (-2)	131.084			
NTA (-1)	190.116	3.61660089	1.90231E-05	1.90231E-05
Total Anions			0.398565649	0.399541169
Cations				
Na	22.99	708	0.030795998	0.030795998
Ag	107.868			
Al	26.98154	3	0.000111187	0.000333561
Ba	137.33			
Ca	40.08			
Cd	112.41			
Ce	140.12			
Cs	134.52	4	2.97354E-05	2.97354E-05
Cu	63.546	15	0.000236049	0.000472099
Fe	55.847	5	8.95303E-05	0.000268591
K	39.0983	16	0.000409225	0.000409225
La	138.906			
Mg	24.305			
Mn	54.938			
Nd	144.24			
NH4	18			
Ni	58.71	68	0.001158235	0.002316471
Pb	207.2	8	3.861E-05	7.72201E-05
Pu	244			
Sn	118.69			
Sr	87.62			
U	238.029	67	0.000281478	0.00168887
Zn	65.38			
Zr	91.22			
gluconic acid *	196.16	22.5218099	0.000114813	0.000114813
IDA *	133.084	38.5142275	0.000289398	0.000289398
H+	1	362.745187	0.362745187	0.362745187
Total Cations			0.033150049	0.399541169

Species	MW	Conc (M)	g/liter	full-scale flow (mole/hr)	TOC (g/liter)
NaNO2	69				
NaNO3	85	2.8023E-02	2.3820E+00	8.3468E+02	
NaOH	40.07	4.0421E-04	1.6197E-02	1.2039E+01	
Na2SO4	142.04				
Na2C2O4	134	2.8403E-04	3.8060E-02	8.4597E+00	6.8166E-03
NaAlO2	81.97154				
NaF	41.99				
NaCl	58.443				
Na2CO3	106				
Na3PO4	163.944				
Na3AsO4	207.8916				
Na2B4O7	201.22				
Na2CrO4	161.976	7.6929E-05	1.2461E-02	2.2913E+00	
Na(HgO(OH))	256.58				
Na2MoO4	205.92				
Na2RuO4	211.05				
Na2Se	101.95				
Na2SiO3	122.07	4.2727E-04	5.2156E-02	1.2726E+01	
NaTcO4	185.8964				
NaCH3COO	82.0346	1.1105E-04	9.1103E-03	3.3078E+00	2.6653E-03
Na2H2EDTA	336.227	1.8730E-04	6.2975E-02	5.5787E+00	2.2476E-02
Na3HEDTA	344.206				
NaCOOH	68.0077				
NaOCH2COOH	98.032	1.5811E-03	1.5500E-01	4.7093E+01	3.7946E-02
NaH2Citrate	214.086	3.1345E-04	6.7106E-02	9.3362E+00	2.2569E-02
Na2IDA	177.064				
NaH2NTA	213.106	1.9023E-05	4.0539E-03	5.6660E-01	1.3697E-03
HNO3	63	3.6275E-01	2.2853E+01	1.0804E+04	
AgNO3	169.868				
Al(NO3)3	212.98154	1.1119E-04	2.3681E-02	3.3117E+00	
Ba(NO3)2	261.33				
Ca(NO3)2	164.08				
Cd(NO3)2	236.41				
Ce(NO3)3	326.12				
CsNO3	196.52	2.9735E-05	5.8436E-03	8.8567E-01	
Cu(NO3)2	187.546	2.3605E-04	4.4270E-02	7.0307E+00	
Fe(NO3)3	241.847	8.9530E-05	2.1653E-02	2.6667E+00	
KNO3	101.0983	4.0922E-04	4.1372E-02	1.2189E+01	
La(NO3)3	324.906				
Mg(NO3)2	148.305				
Mn(NO3)2	178.938				
Nd(NO3)3	330.24				
NH4NO3	80				
Ni(NO3)2	182.71	1.1582E-03	2.1162E-01	3.4498E+01	
Pb(NO3)2	331.2	3.8610E-05	1.2788E-02	1.1500E+00	
Na2PuO2(OH)4	389.98				
Sn(OH)4	186.69				
Sr(NO3)2	211.62				
UO2(NO3)2	394.09	2.8148E-04	1.1093E-01	8.3838E+00	
Zn(NO3)2	189.38				
Zr(NO3)4	339.22				
gluconic acid *	196.16	1.1481E-04	2.2522E-02	3.4197E+00	8.2666E-03
IDA *	133.084	2.8940E-04	3.8514E-02	8.6197E+00	1.3891E-02
H2O	18.02	5.4874E+01	9.8882E+02	1.6344E+06	
Total			1.0150E+03	1.6462E+06	1.1600E-01

APPENDIX B.

Design of Computer Test Matrix

T ABLE B-1. 21 Design Points Generated for Mixture Response Surface Model in Scaled Weight Fractions (SWF).

Al SWF	Ca SWF	Cs SWF	H SWF	K SWF	Na SWF
0.11065	0.15970	0.08215	0.05000	0.01410	0.58340
0.03306	0.00000	0.00360	0.31880	0.01410	0.63044
0.08193	0.05458	0.01027	0.05667	0.03245	0.76409
0.00170	0.15970	0.00360	0.12070	0.13090	0.58340
0.00170	0.00000	0.13804	0.07038	0.02578	0.76410
0.00170	0.00000	0.18952	0.21128	0.01410	0.58340
0.00170	0.04970	0.00360	0.05000	0.13090	0.76410
0.06300	0.00000	0.00360	0.11764	0.13090	0.68486
0.00170	0.01852	0.00360	0.19798	0.01410	0.76410
0.00170	0.15250	0.19830	0.05000	0.01410	0.58340
0.12430	0.00000	0.11140	0.05000	0.13090	0.58340
0.05934	0.00000	0.11701	0.19535	0.04489	0.58340
0.00170	0.13957	0.00360	0.25763	0.01410	0.58340
0.11754	0.00000	0.00360	0.21128	0.08418	0.58340
0.12430	0.00000	0.19830	0.05000	0.01410	0.61330
0.00170	0.15970	0.01040	0.05000	0.01410	0.76410
0.12430	0.09582	0.00360	0.05000	0.07250	0.65378
0.00170	0.00000	0.19830	0.05000	0.13090	0.61910
0.00170	0.00000	0.04152	0.24248	0.13090	0.58340
0.12430	0.00000	0.00360	0.05000	0.05800	0.76410
0.12430	0.00000	0.04886	0.16144	0.01410	0.65130

TABLE B-2. 30 Design Points Selected for Phase 3 Computer Runs.

Run ID	Al (SWF)	Ca (SWF)	Cs (SWF)	H (SWF)	K (SWF)	Na (SWF)	Temp (^{o}C)
NC44	0.08193	0.05458	0.01027	0.05667	0.03245	0.76409	20
NC45	0.00170	0.00000	0.13804	0.07038	0.02578	0.76410	20
NC46	0.00170	0.00000	0.18952	0.21128	0.01410	0.58340	20
NC47	0.00170	0.04970	0.00360	0.05000	0.13090	0.76410	20
NC48	0.06300	0.00000	0.00360	0.11764	0.13090	0.68486	20
NC49	0.00170	0.01852	0.00360	0.19798	0.01410	0.76410	20
NC50	0.00170	0.15250	0.19830	0.05000	0.01410	0.58340	20
NC51	0.12430	0.00000	0.11140	0.05000	0.13090	0.58340	20
NC52	0.05934	0.00000	0.11701	0.19535	0.04489	0.58340	20
NC53	0.00170	0.13957	0.00360	0.25763	0.01410	0.58340	20
NC54	0.11754	0.00000	0.00360	0.21128	0.08418	0.58340	20
NC55	0.12430	0.00000	0.19830	0.05000	0.01410	0.61330	20
NC56	0.12430	0.09582	0.00360	0.05000	0.07250	0.65378	20
NC57	0.00170	0.00000	0.04152	0.24248	0.13090	0.58340	20
NC58	0.12430	0.00000	0.04886	0.16144	0.01410	0.65130	20
NC59	0.08193	0.05458	0.01027	0.05667	0.03245	0.76409	60
NC60	0.00170	0.00000	0.13804	0.07038	0.02578	0.76410	60
NC61	0.00170	0.00000	0.18952	0.21128	0.01410	0.58340	60
NC62	0.00170	0.04970	0.00360	0.05000	0.13090	0.76410	60
NC63	0.06300	0.00000	0.00360	0.11764	0.13090	0.68486	60
NC64	0.00170	0.01852	0.00360	0.19798	0.01410	0.76410	60
NC65	0.00170	0.15250	0.19830	0.05000	0.01410	0.58340	60
NC66	0.12430	0.00000	0.11140	0.05000	0.13090	0.58340	60
NC67	0.05934	0.00000	0.11701	0.19535	0.04489	0.58340	60
NC68	0.00170	0.13957	0.00360	0.25763	0.01410	0.58340	60
NC69	0.11754	0.00000	0.00360	0.21128	0.08418	0.58340	60
NC70	0.12430	0.00000	0.19830	0.05000	0.01410	0.61330	60
NC71	0.12430	0.09582	0.00360	0.05000	0.07250	0.65378	60
NC72	0.00170	0.00000	0.04152	0.24248	0.13090	0.58340	60
NC73	0.12430	0.00000	0.04886	0.16144	0.01410	0.65130	60

TABLE B-3. Test Matrix for 3-Phase Computer Runs with Mixture Factors in Given Weight Fractions (WF).

Test Stage	Run ID	Al (WF)	Ca (WF)	Cs (WF)	H (WF)	K (WF)	Na (WF)	Temp (^{o}C)
1	NC01	0.10548	0.15224	0.07831	0.04767	0.01344	0.55616	20
1	NC02	0.03152	0.00000	0.00343	0.30391	0.01344	0.60100	20
1	NC03	0.00162	0.15224	0.00343	0.11506	0.12479	0.55616	20
1	NC04	0.00162	0.15224	0.00991	0.04767	0.01344	0.72842	20
1	NC05	0.00162	0.00000	0.18904	0.04767	0.12479	0.59019	20
1	NC06	0.11850	0.00000	0.00343	0.04767	0.05529	0.72842	20
1	NC07	0.10548	0.15224	0.07831	0.04767	0.01344	0.55616	60
1	NC08	0.03152	0.00000	0.00343	0.30391	0.01344	0.60100	60
1	NC09	0.00162	0.15224	0.00343	0.11506	0.12479	0.55616	60
1	NC10	0.00162	0.15224	0.00991	0.04767	0.01344	0.72842	60
1	NC11	0.00162	0.00000	0.18904	0.04767	0.12479	0.59019	60
1	NC12	0.11850	0.00000	0.00343	0.04767	0.05529	0.72842	60
2	NC13	0.06370	0.06659	0.07300	0.15256	0.04125	0.55620	59
2	NC14	0.06736	0.08086	0.07880	0.11997	0.04473	0.56158	20
2	NC15	0.07101	0.05707	0.10780	0.10224	0.04821	0.56697	24
2	NC16	0.07466	0.09037	0.10200	0.06223	0.05170	0.57234	57.5
2	NC17	0.07831	0.04756	0.04980	0.11687	0.08302	0.57773	54
2	NC18	0.08196	0.09988	0.05560	0.05320	0.07954	0.58311	25
2	NC19	0.09293	0.02854	0.02660	0.10648	0.01340	0.68535	49
2	NC20	0.10754	0.00951	0.00340	0.05815	0.11088	0.66382	44
2	NC21	0.03083	0.04280	0.06720	0.05612	0.06562	0.69073	27.5
2	NC22	0.01622	0.02378	0.04400	0.13955	0.11436	0.61539	32.5
2	NC23	0.00890	0.01427	0.18320	0.08996	0.03081	0.62616	45
2	NC24	0.00525	0.15220	0.01500	0.11503	0.03429	0.63154	41
2	NC25	0.00160	0.00476	0.02080	0.25145	0.03777	0.63692	37.5
2	NC26	0.05129	0.05327	0.05910	0.12078	0.05241	0.61645	59
2	NC27	0.05421	0.06468	0.06374	0.08053	0.06076	0.62937	20
2	NC28	0.05713	0.04566	0.08693	0.10890	0.04685	0.60783	24
2	NC29	0.06297	0.03805	0.04054	0.17123	0.04128	0.59922	54
2	NC30	0.06882	0.03044	0.10549	0.12223	0.03571	0.59061	29
2	NC31	0.07466	0.02283	0.02198	0.22168	0.03014	0.58200	49
2	NC32	0.08052	0.01522	0.12404	0.13557	0.02458	0.57338	34
2	NC33	0.08635	0.00761	0.00343	0.27213	0.01901	0.56477	44
2	NC34	0.09219	0.00000	0.14260	0.14891	0.01344	0.55616	39
2	NC35	0.04837	0.06088	0.07766	0.08336	0.05798	0.62506	40
2	NC36	0.04253	0.05707	0.09157	0.08618	0.05520	0.62075	60
2	NC37	0.03960	0.07610	0.06838	0.05782	0.06911	0.64229	56
2	NC38	0.03668	0.04947	0.07301	0.13237	0.04963	0.61214	22.5
2	NC39	0.03084	0.04185	0.11013	0.12289	0.04406	0.60352	55
2	NC40	0.02500	0.03424	0.05446	0.20619	0.03849	0.59492	27.5
2	NC41	0.01915	0.02664	0.12869	0.15960	0.03293	0.58630	50
2	NC42	0.01331	0.01903	0.03590	0.28001	0.02736	0.57769	32.5
2	NC43	0.00746	0.01141	0.14724	0.19631	0.02179	0.56907	45

TABLE B-3. (Cont'd)

Test Stage	Run ID	Al (WF)	Ca (WF)	Cs (WF)	H (WF)	K (WF)	Na (WF)	Temp (^{o}C)
3	NC44	0.07810	0.05203	0.00979	0.05402	0.03093	0.72841	20
3	NC45	0.00162	0.00000	0.13159	0.06709	0.02458	0.72842	20
3	NC46	0.00162	0.00000	0.18067	0.20141	0.01344	0.55616	20
3	NC47	0.00162	0.04738	0.00343	0.04767	0.12479	0.72842	20
3	NC48	0.06006	0.00000	0.00343	0.11215	0.12479	0.65288	20
3	NC49	0.00162	0.01766	0.00343	0.18873	0.01344	0.72842	20
3	NC50	0.00162	0.14538	0.18904	0.04767	0.01344	0.55616	20
3	NC51	0.11850	0.00000	0.10620	0.04767	0.12479	0.55616	20
3	NC52	0.05657	0.00000	0.11155	0.18623	0.04279	0.55616	20
3	NC53	0.00162	0.13305	0.00343	0.24560	0.01344	0.55616	20
3	NC54	0.11205	0.00000	0.00343	0.20141	0.08025	0.55616	20
3	NC55	0.11850	0.00000	0.18904	0.04767	0.01344	0.58466	20
3	NC56	0.11850	0.09135	0.00343	0.04767	0.06911	0.62325	20
3	NC57	0.00162	0.00000	0.03958	0.23116	0.12479	0.55616	20
3	NC58	0.11850	0.00000	0.04658	0.15390	0.01344	0.62088	20
3	NC59	0.07810	0.05203	0.00979	0.05402	0.03093	0.72841	60
3	NC60	0.00162	0.00000	0.13159	0.06709	0.02458	0.72842	60
3	NC61	0.00162	0.00000	0.18067	0.20141	0.01344	0.55616	60
3	NC62	0.00162	0.04738	0.00343	0.04767	0.12479	0.72842	60
3	NC63	0.06006	0.00000	0.00343	0.11215	0.12479	0.65288	60
3	NC64	0.00162	0.01766	0.00343	0.18873	0.01344	0.72842	60
3	NC65	0.00162	0.14538	0.18904	0.04767	0.01344	0.55616	60
3	NC66	0.11850	0.00000	0.10620	0.04767	0.12479	0.55616	60
3	NC67	0.05657	0.00000	0.11155	0.18623	0.04279	0.55616	60
3	NC68	0.00162	0.13305	0.00343	0.24560	0.01344	0.55616	60
3	NC69	0.11205	0.00000	0.00343	0.20141	0.08025	0.55616	60
3	NC70	0.11850	0.00000	0.18904	0.04767	0.01344	0.58466	60
3	NC71	0.11850	0.09135	0.00343	0.04767	0.06911	0.62325	60
3	NC72	0.00162	0.00000	0.03958	0.23116	0.12479	0.55616	60
3	NC73	0.11850	0.00000	0.04658	0.15390	0.01344	0.62088	60

This page left intentionally blank.

APPENDIX C.

Model Execution and Data Generation

TABLE C-1. Input Flows for Cesium Eluate Evaporation Model Run - Matrix 22.

Matrix Run Number = NC22
Temperature (^{o}C) = 32.5

Cations	FW	wt fraction	Species	MW	full-scale (g/hr)	wt frac dry	wt frac total	full-scale (mole/hr)
Cs	134.52	0.044	CsNO3	196.52	1.7405E+02	0.00544	0.00015	8.856676E-01
K	39.0983	0.11436	KNO3	101.0983	8.0069E+02	0.02502	0.00070	7.919927E+00
Na	22.99	0.61539	NaNO3	85	6.1608E+03	0.19250	0.00537	7.247970E+01
Al	26.98154	0.01622	Al(NO3)3	212.98154	3.4668E+02	0.01083	0.00030	1.627755E+00
Ca	40.08	0.02378	Ca(NO3)2	164.08	2.6360E+02	0.00824	0.00023	1.606531E+00
H+	1	0.13955	HNO3	63	2.3805E+04	0.74383	0.02075	3.778633E+02
Cr	51.996	0.00636	Cr(NO3)3	237.996	7.8871E+01	0.00246	0.00007	3.313952E-01
Cu	63.546	0.00946	Cu(NO3)2	187.546	7.5581E+01	0.00236	0.00007	4.030018E-01
Fe	55.847	0.00978	Fe(NO3)3	241.847	1.1470E+02	0.00358	0.00010	4.742479E-01
Mg	24.305	0.00211	Mg(NO3)2	148.305	3.4934E+01	0.00109	0.00003	2.355543E-01
Ni	58.71	0.01366	Ni(NO3)2	182.71	1.1509E+02	0.00360	0.00010	6.299268E-01
Pb	207.2	0.00233	Pb(NO3)2	331.2	1.0096E+01	0.00032	0.00001	3.048454E-02
Zn	65.38	0.00299	Zn(NO3)2	189.38	2.3483E+01	0.00073	0.00002	1.239987E-01
			H2O	18.02	1.1151E+06		0.97210	6.188073E+04
total cations		1.00000	total dry		3.2004E+04	1.00000		
total (major)		0.95330	total		1.1471E+06		1.00000	6.234534E+04
total (minor)		0.04670						

Basis:

wt% total solids (avg of all eluates) = 2.79
full-scale Cs flow (g/hr) = 119.14
conversion factor to full-scale = 2707.72727

TABLE C-2. Calculated Physical Properties at 80% Saturation of $NaNO_3$.

Test Phase	Run ID	density (g/ml)	VRF (volume reduction factor)	viscosity (cP)	heat capacity (cal/g/deg C)
1	NC01	1.3239	24.56	2.35651	0.6598
1	NC02	1.3018	74.84	1.90369	0.7012
1	NC03	1.3325	37.98	1.87207	0.6721
1	NC04	1.3137	18.94	1.82157	0.6971
1	NC05	1.3408	24.12	1.92658	0.6814
1	NC06	1.2999	20.80	2.32014	0.6756
1	NC07	1.3749	39.03	2.00905	0.5713
1	NC08	1.3628	186.43	1.25107	0.5762
1	NC09	1.3887	79.24	1.44975	0.5851
1	NC10	1.3732	42.12	1.42459	0.6310
1	NC11	1.4452	56.93	1.88911	0.6437
1	NC12	1.3589	37.46	2.36148	0.5498
2	NC13	1.3698	87.66	1.94915	0.5759
2	NC14	1.3179	39.13	2.13674	0.6791
2	NC15	1.3246	39.14	2.12742	0.6669
2	NC16	1.3736	47.05	1.96573	0.5694
2	NC17	1.3653	68.18	2.11518	0.5638
2	NC18	1.3273	28.78	2.21545	0.6561
2	NC19	1.3516	56.81	2.21169	0.5794
2	NC20	1.3428	39.68	2.39944	0.5787
2	NC21	1.3253	26.60	1.88832	0.6838
2	NC22	1.3353	57.03	1.81992	0.6758
2	NC23	1.3738	56.22	1.74001	0.6613
2	NC24	1.3452	52.49	1.60684	0.6721
2	NC25	1.3319	95.56	1.72056	0.6969
2	NC26	1.3802	74.44	1.92146	0.5666
2	NC27	1.3153	28.38	2.06438	0.6809
2	NC28	1.3201	38.28	2.03242	0.6759
2	NC29	1.3583	92.06	2.01758	0.5708
2	NC30	1.3278	48.00	2.07489	0.6648
2	NC31	1.3502	109.65	2.17709	0.5781
2	NC32	1.3439	63.06	2.27149	0.6293
2	NC33	1.3411	126.16	2.34801	0.5883
2	NC34	1.3587	76.36	2.50250	0.5924
2	NC35	1.3486	48.12	1.95071	0.6237
2	NC36	1.3887	61.36	1.85783	0.5733
2	NC37	1.3821	47.05	1.81376	0.5773
2	NC38	1.3182	41.00	1.94940	0.6822
2	NC39	1.3759	79.01	1.80660	0.5844
2	NC40	1.3215	65.50	1.85307	0.6862
2	NC41	1.3753	95.55	1.77557	0.6175
2	NC42	1.3253	97.58	1.77838	0.6926
2	NC43	1.3671	103.62	1.72835	0.6666

TABLE C-3. Calculated Physical Properties at 100% Saturation of $NaNO_3$.

Test Phase	Run ID	HNO3 (M)	density (g/ml)	solubility (g TS/1000 g H2O)	solubility (g TS/liter)	viscosity (cP)	heat capacity (cal/g/deg C)
1	NC01	1.02	1.3616	753.76	585.20	3.08986	0.6171
1	NC02	4.02	1.3203	732.15	558.07	2.04760	0.6991
1	NC03	3.37	1.3564	844.26	620.95	2.02118	0.6618
1	NC04	3.57	1.3345	763.12	577.62	1.95084	0.6926
1	NC05	3.30	1.3726	880.67	642.76	2.12925	0.6721
1	NC06	1.64	1.3239	693.43	542.10	2.82510	0.6523
1	NC07	0.34	1.3953	945.31	678.04	2.21971	0.5625
1	NC08	0.88	1.3920	1093.02	726.93	2.03144	0.5374
1	NC09	0.79	1.4253	1281.42	800.57	1.59326	0.5699
1	NC10	0.65	1.4032	1150.69	750.75	1.55916	0.5911
1	NC11	0.48	1.4603	1495.54	875.11	2.09719	0.5807
1	NC12	0.30	1.3755	913.89	656.80	2.69121	0.5276
2	NC13	0.60	1.3936	1011.31	700.71	2.18237	0.5498
2	NC14	2.29	1.3429	747.21	574.30	2.45503	0.6599
2	NC15	1.54	1.3574	793.54	600.57	2.60969	0.6311
2	NC16	0.44	1.3967	1004.33	699.86	2.19394	0.5560
2	NC17	0.52	1.3894	976.38	686.41	2.37852	0.5513
2	NC18	0.96	1.3605	823.64	614.47	2.81767	0.6087
2	NC19	0.57	1.3712	878.62	641.28	2.47674	0.5628
2	NC20	0.45	1.3650	883.46	640.28	2.68629	0.5636
2	NC21	2.27	1.3529	828.75	613.10	2.11901	0.6626
2	NC22	1.85	1.3744	950.34	669.72	2.11002	0.6395
2	NC23	1.01	1.4149	1118.51	747.04	2.00942	0.6165
2	NC24	1.61	1.3780	974.90	680.24	1.75794	0.6391
2	NC25	2.40	1.3641	925.37	655.60	1.89628	0.6732
2	NC26	0.60	1.3928	1045.63	711.95	2.10771	0.5459
2	NC27	2.67	1.3379	750.39	573.55	2.31077	0.6635
2	NC28	2.22	1.3465	775.42	588.09	2.33170	0.6556
2	NC29	0.63	1.3822	969.04	680.22	2.26229	0.5505
2	NC30	1.16	1.3659	832.18	620.38	2.63778	0.6144
2	NC31	0.67	1.3718	901.55	650.38	2.44276	0.5630
2	NC32	0.85	1.3743	855.04	633.46	2.75489	0.5882
2	NC33	0.70	1.3612	842.90	622.60	2.64472	0.5708
2	NC34	0.70	1.3779	860.58	637.33	2.80698	0.5748
2	NC35	0.84	1.3782	949.28	671.19	2.24790	0.5910
2	NC36	0.57	1.4016	1095.23	732.66	2.03761	0.5557
2	NC37	0.52	1.4073	1076.24	729.49	2.01319	0.5645
2	NC38	3.00	1.3414	775.25	585.80	2.15153	0.6694
2	NC39	0.68	1.4028	1095.15	733.26	2.02454	0.5625
2	NC40	2.85	1.3471	809.61	602.67	2.04711	0.6742
2	NC41	0.84	1.4066	1098.69	736.36	2.01659	0.5852
2	NC42	2.70	1.3534	850.25	621.93	1.95990	0.6782
2	NC43	1.21	1.4100	1091.88	735.98	1.99000	0.6219

APPENDIX D.

Derivation of Physical Property Models

@ 80% Saturation

EXHIBIT D-1. Responses of Interest @ 80% Saturation vs. Test Factors (Analyte Concentrations in Scaled Weight Fractions).

Density (g/mL) By Al

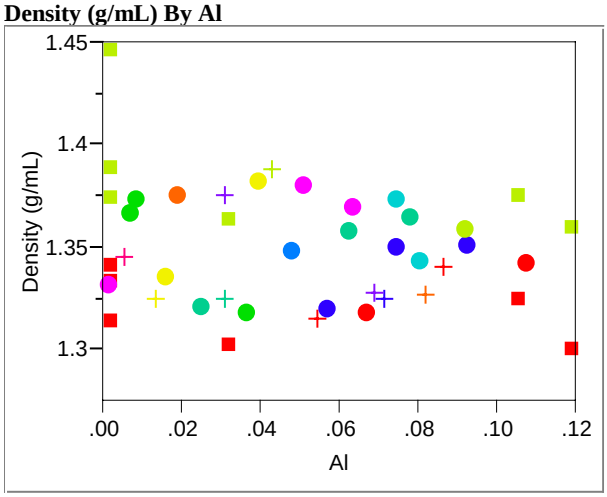

Heat Capacity (cal/g/oC) By Al

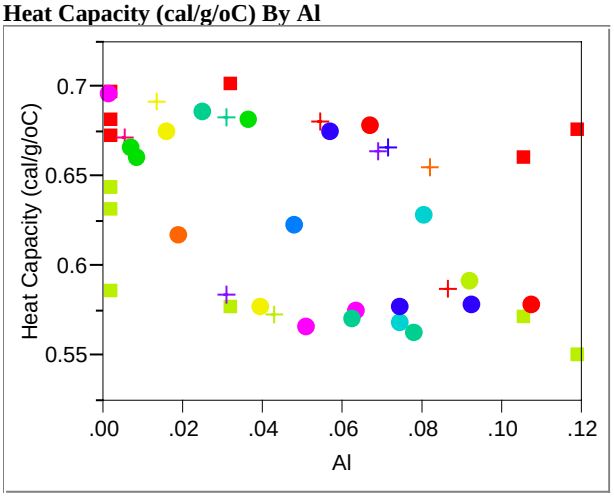

VRF (Volume Reduction Fraction) By Al

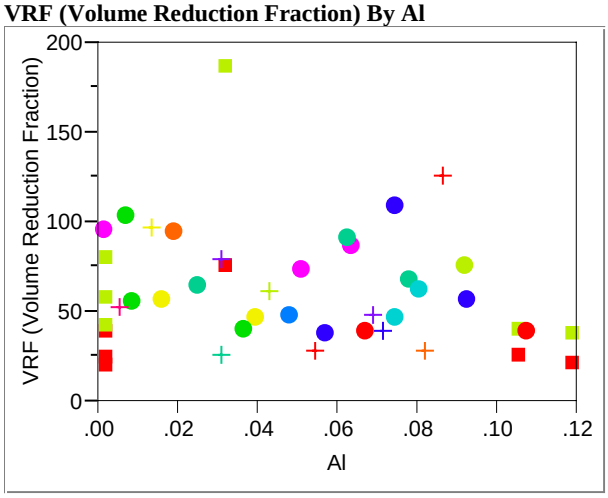

Density (g/mL) By Ca

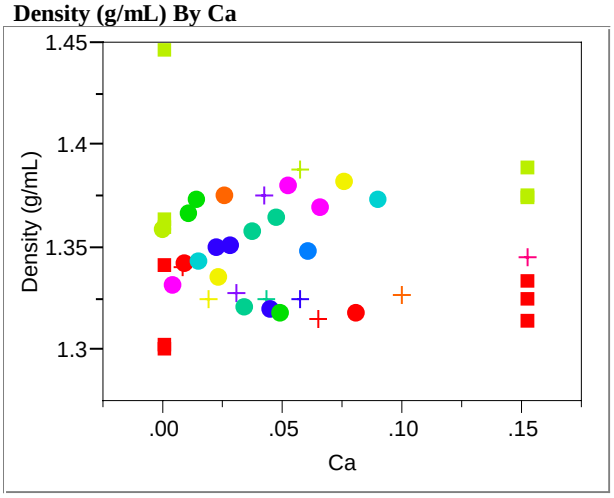

Viscosity (cP) By Al

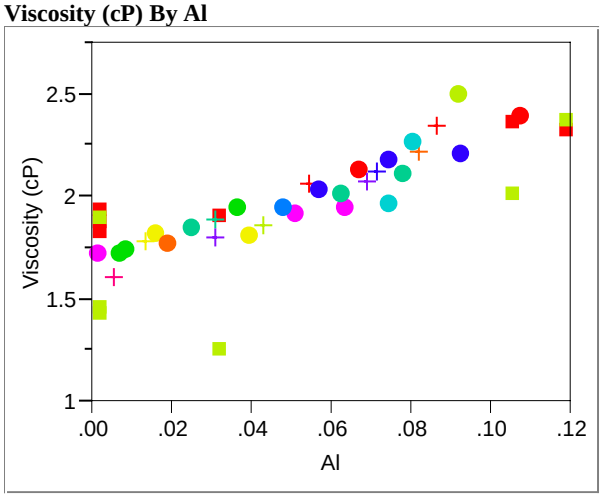

VRF (Volume Reduction Fraction) By Ca

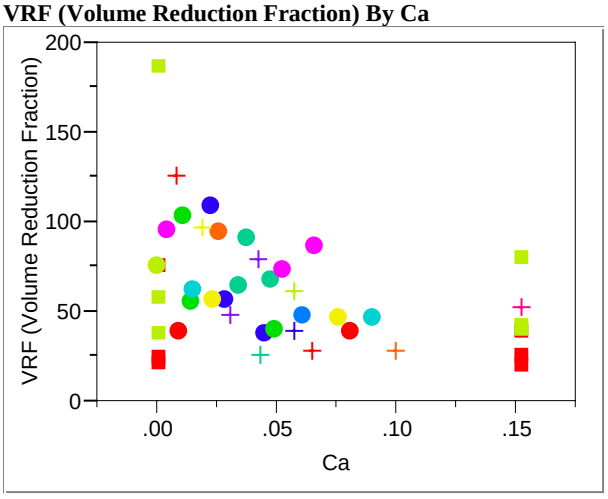

EXHIBIT D-1. Responses of Interest @ 80% Saturation vs. Test Factors *(continued)*
(Analyte Concentrations in Scaled Weight Fractions).

Viscosity (cP) By Ca

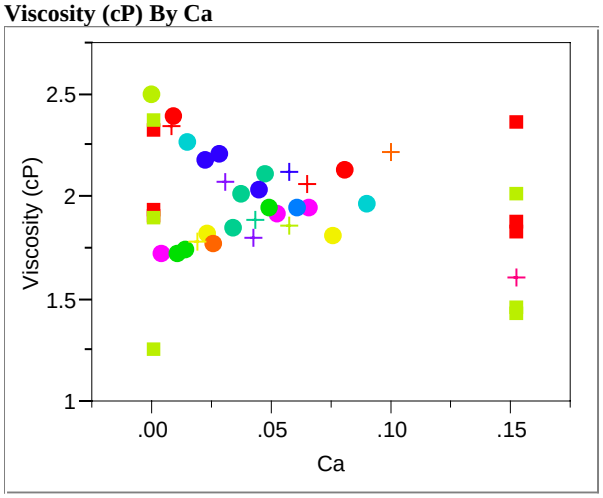

VRF (Volume Reduction Fraction) By Cs

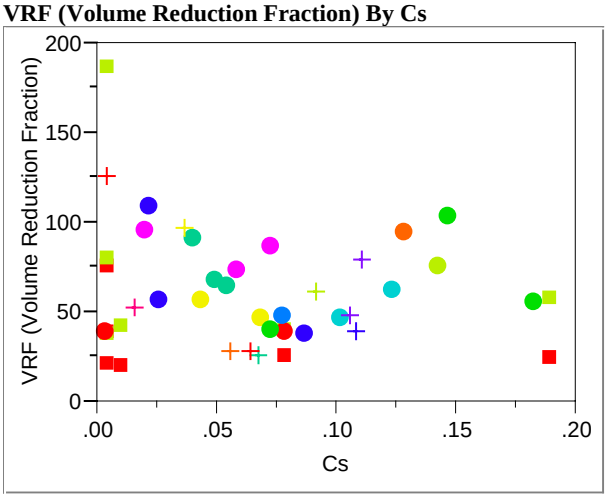

Heat Capacity (cal/g/oC) By Ca

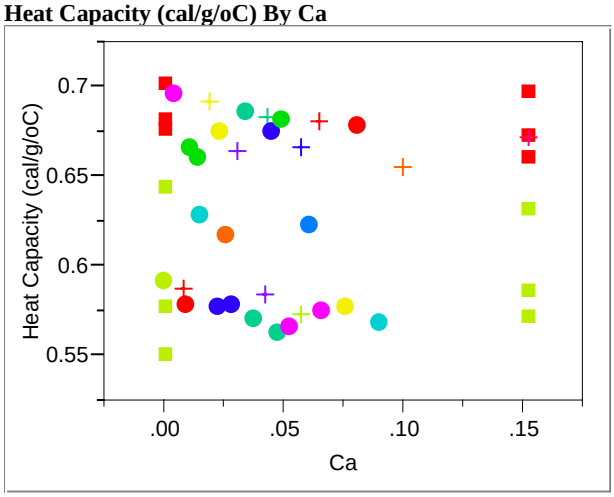

Viscosity (cP) By Cs

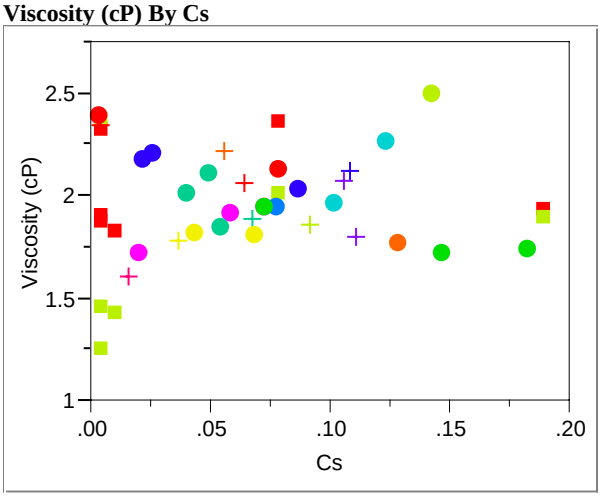

Density (g/mL) By Cs

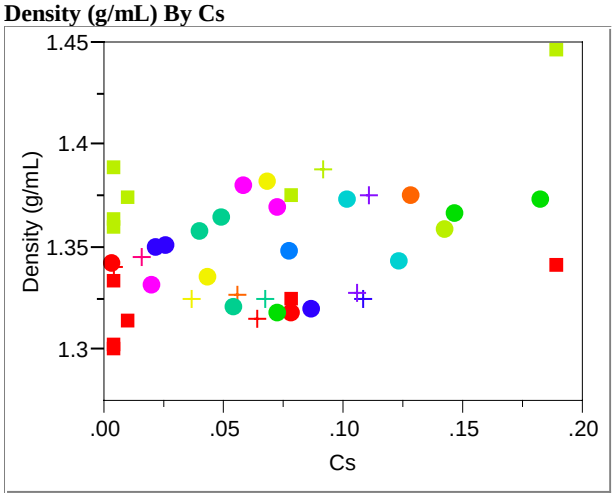

Heat Capacity (cal/g/oC) By Cs

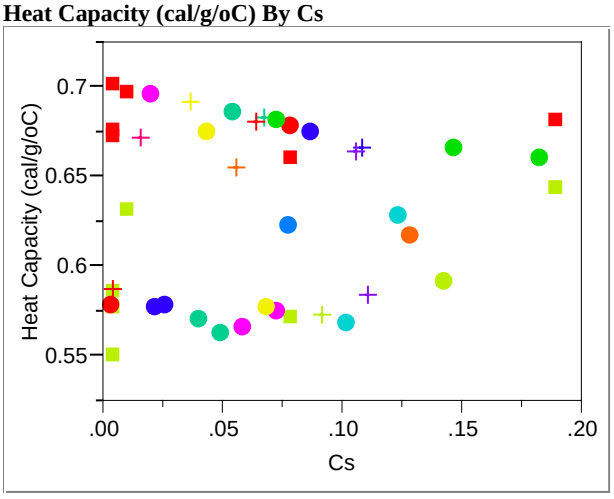

EXHIBIT D-1. Responses of Interest @ 80% Saturation vs. Test Factors *(continued)* (Analyte Concentrations in Scaled Weight Fractions).

Density (g/mL) By H

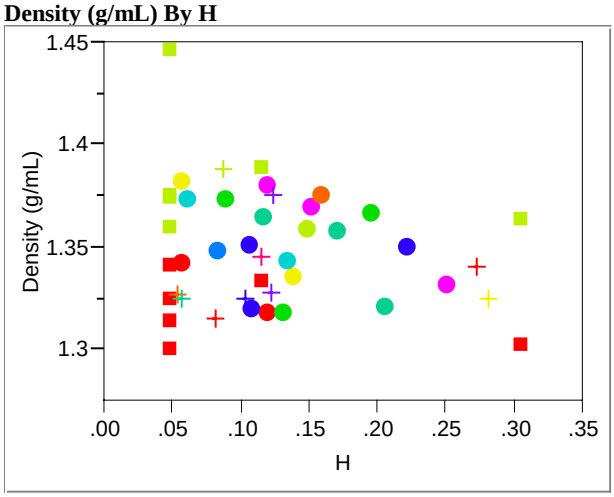

Heat Capacity (cal/g/oC) By H

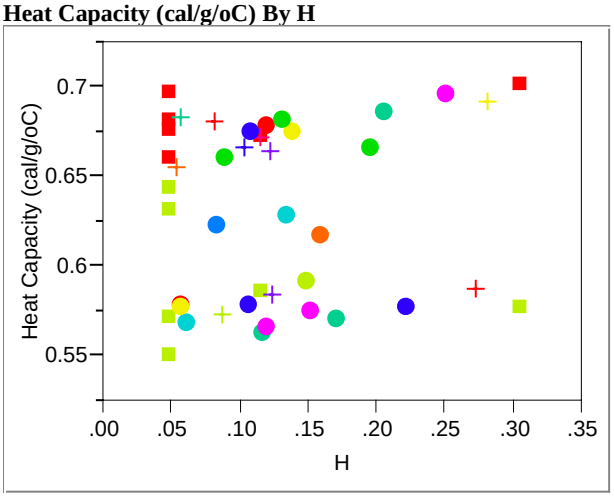

VRF (Volume Reduction Fraction) By H

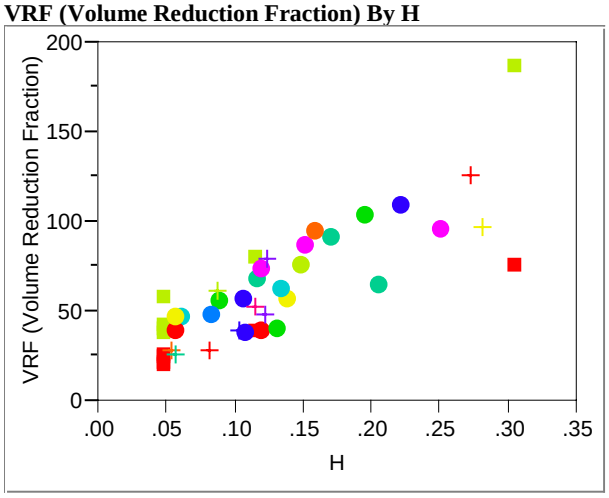

Density (g/mL) By K

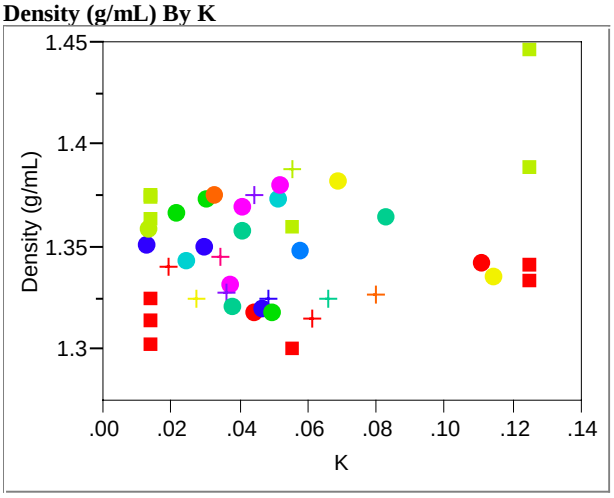

Viscosity (cP) By H

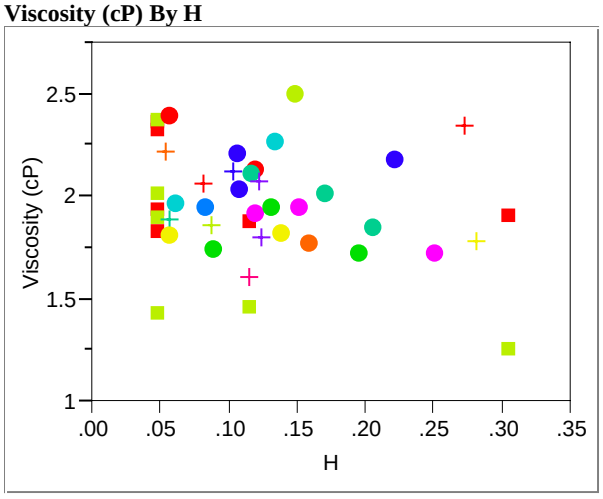

VRF (Volume Reduction Fraction) By K

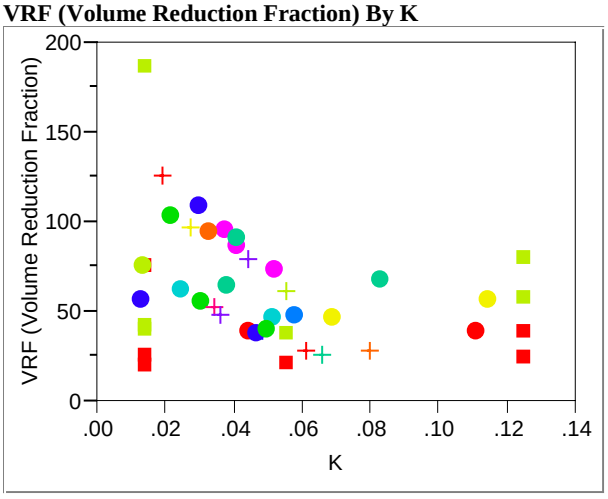

EXHIBIT D-1. Responses of Interest @ 80% Saturation vs. Test Factors *(continued)*
(Analyte Concentrations in Scaled Weight Fractions).

Viscosity (cP) By K

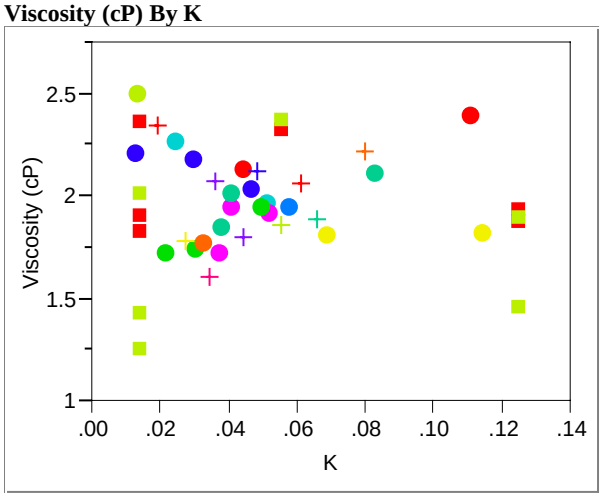

VRF (Volume Reduction Fraction) By Na

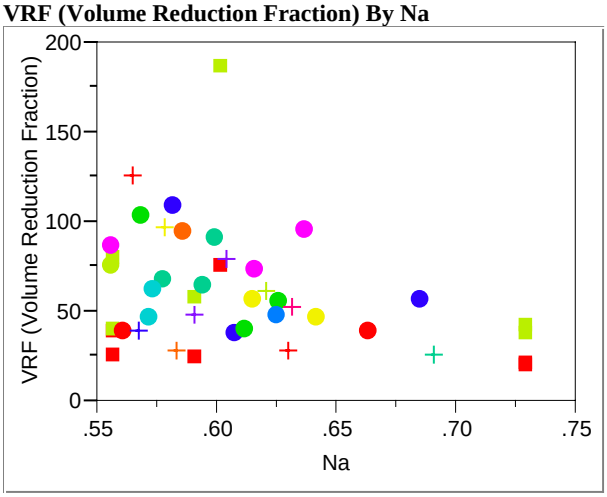

Heat Capacity (cal/g/oC) By K

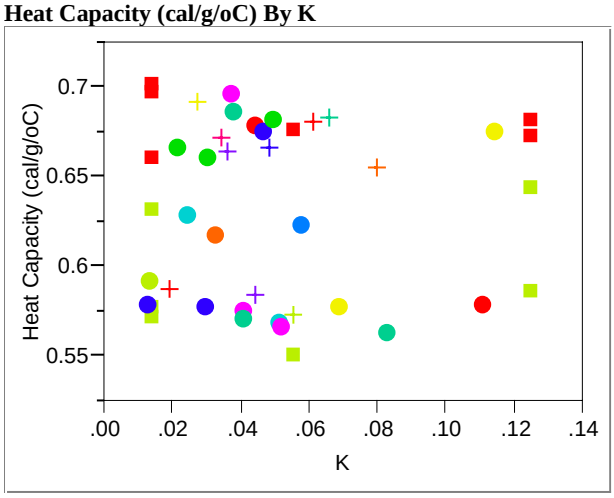

Viscosity (cP) By Na

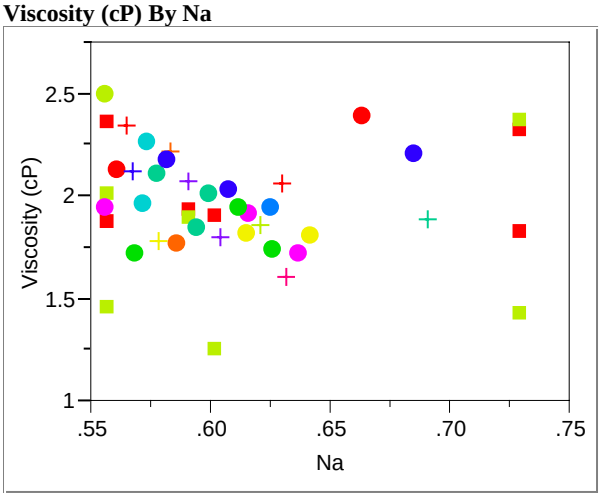

Density (g/mL) By Na

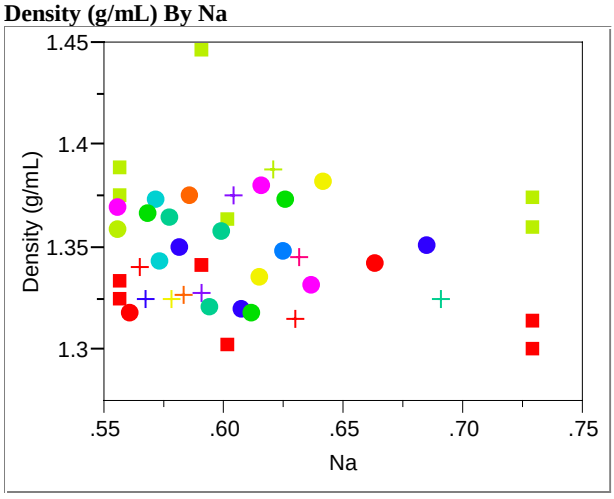

Heat Capacity (cal/g/oC) By Na

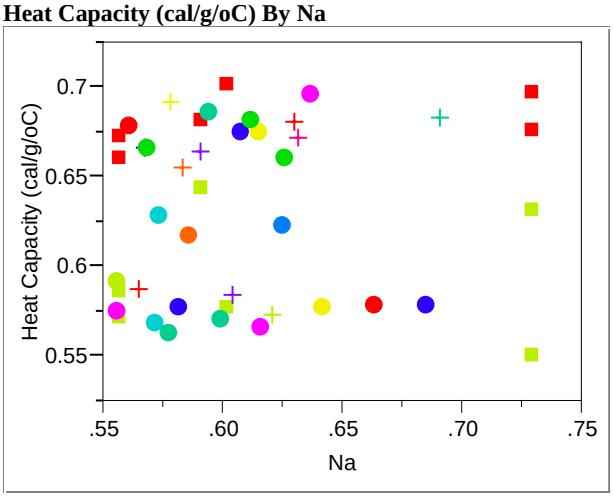

EXHIBIT D-1. Responses of Interest @ 80% Saturation vs. Test Factors *(continued)* (Analyte Concentrations in Scaled Weight Fractions).

Density (g/mL) By Temp (oC)

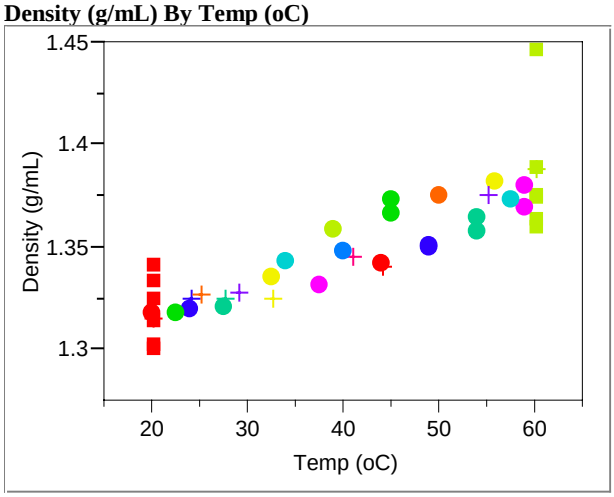

Viscosity (cP) By Temp (oC)

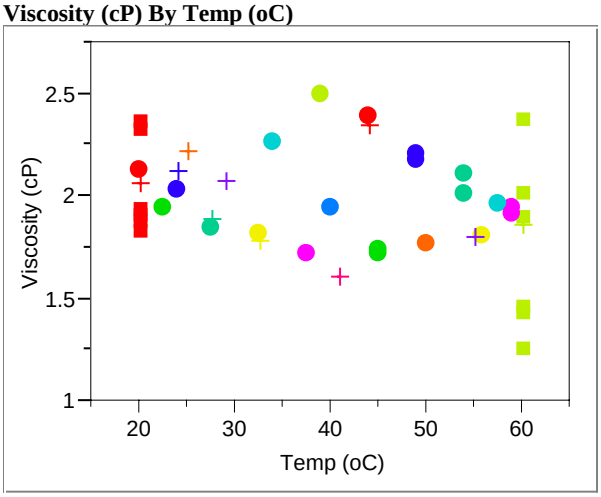

VRF (Volume Reduction Fraction) By Temp (oC)

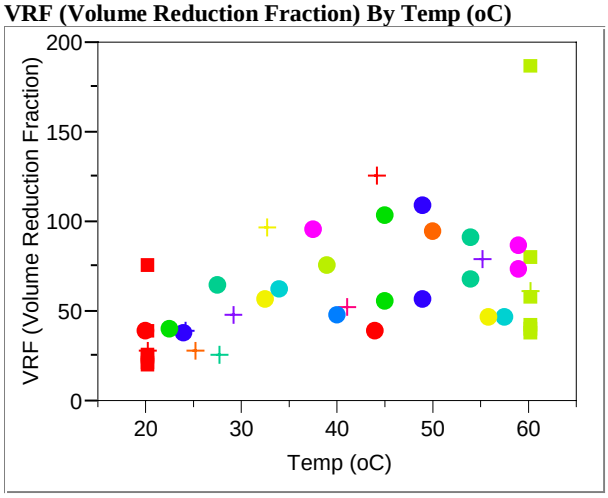

Heat Capacity (cal/g/oC) By Temp (oC)

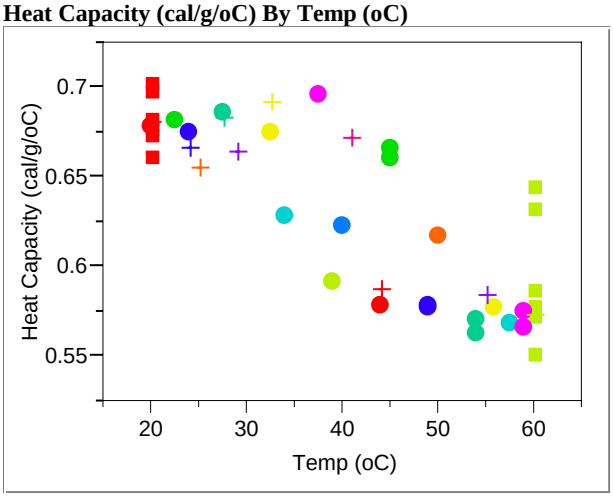

FIGURE D-1. Results from Fitting Density Model Using Phase 1 Data @ 80% Saturation – Actual vs. Predicted Densities (g/ml).

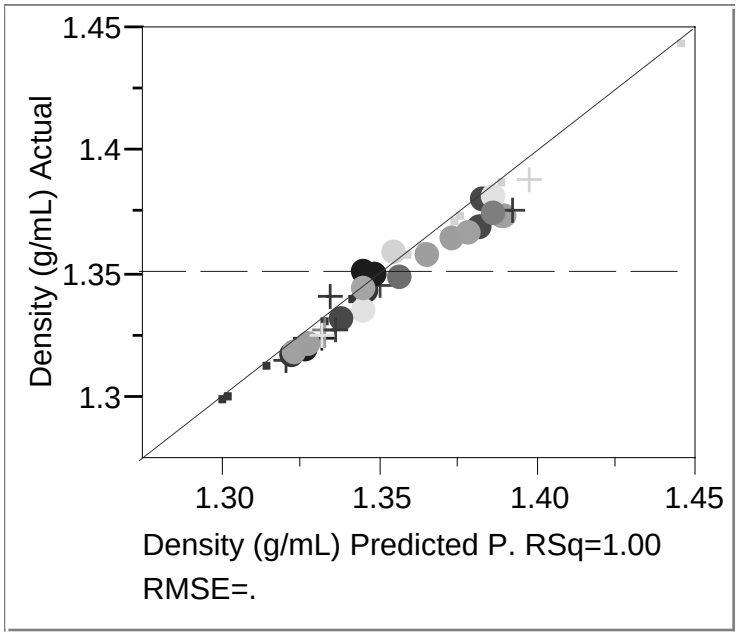

Parameter Estimates

Term		Estimate	Std Error	t Ratio	Prob>|t|
Intercept	Zeroed	0	.	.	.
Al (swf)		1.3254092	.	.	.
Ca (swf)		1.4295801	.	.	.
Cs (swf)		1.3353884	.	.	.
H (swf)		1.3026955	.	.	.
K (swf)		1.3972342	.	.	.
Na (swf)		1.2494043	.	.	.
Al (swf)*Temp (oC)		-0.002045	.	.	.
Ca (swf)*Temp (oC)		-0.001109	.	.	.
Cs (swf)*Temp (oC)		0.0052195	.	.	.
H (swf)*Temp (oC)		0.0008534	.	.	.
K (swf)*Temp (oC)		0.0021992	.	.	.
Na (swf)*Temp (oC)		0.0020157	.	.	.

FIGURE D-2. Results from Fitting Volume Reduction Factor Model Using Phase 1 Data @ 80% Saturation – Actual vs. Predicted VRFs.

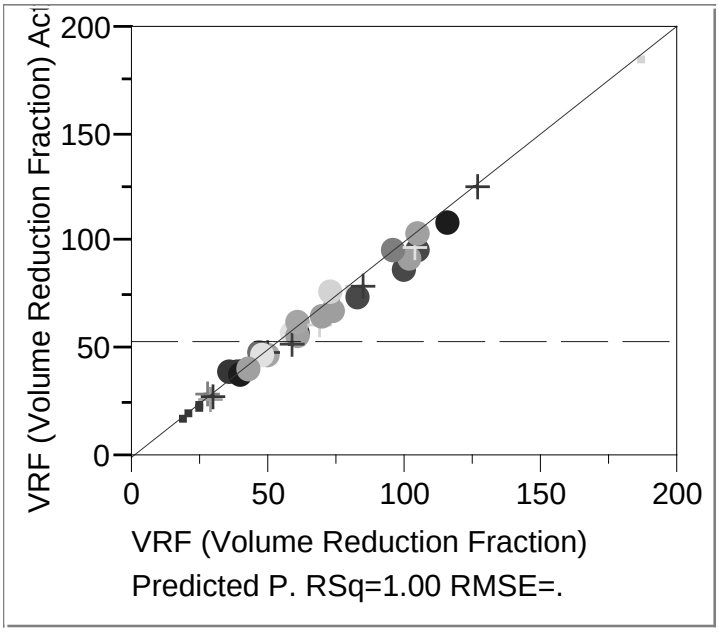

Parameter Estimates

Term		Estimate	Std Error	t Ratio	Prob>|t|
Intercept	Zeroed	0	.	.	.
Al (swf)		80.653324	.	.	.
Ca (swf)		41.9986	.	.	.
Cs (swf)		6.4729349	.	.	.
H (swf)		57.223324	.	.	.
K (swf)		45.163002	.	.	.
Na (swf)		-4.004206	.	.	.
Al (swf)*Temp (oC)		-2.139133	.	.	.
Ca (swf)*Temp (oC)		-0.793947	.	.	.
Cs (swf)*Temp (oC)		1.1784673	.	.	.
H (swf)*Temp (oC)		8.2211619	.	.	.
K (swf)*Temp (oC)		-0.444348	.	.	.
Na (swf)*Temp (oC)		0.3832458	.	.	.

FIGURE D-3. Results from Fitting Viscosity Model Using Phase 1 Data @ 80% Saturation – Actual vs. Predicted Viscosities (cP).

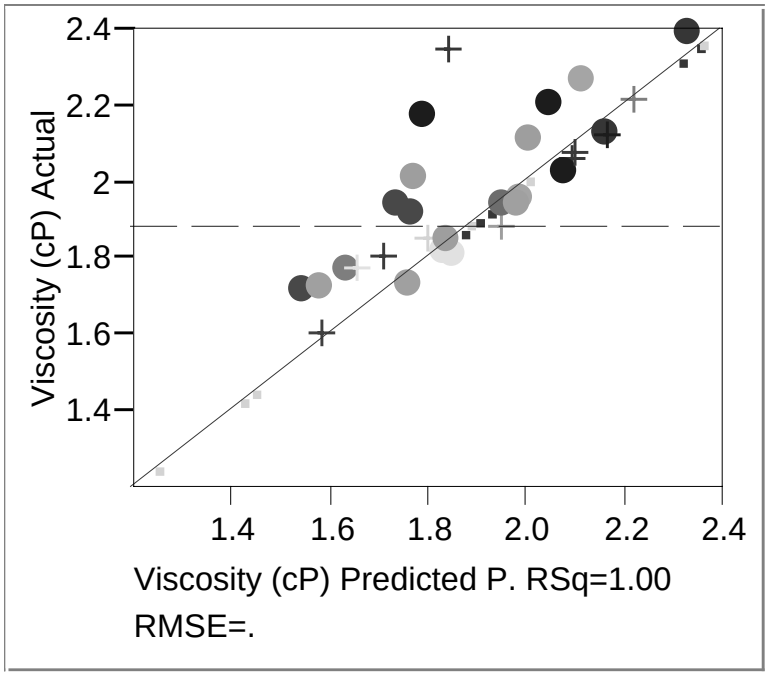

Parameter Estimates

Term		Estimate	Std Error	t Ratio	Prob>|t|
Intercept	Zeroed	0	.	.	.
Al (swf)		5.8709927	.	.	.
Ca (swf)		3.0983094	.	.	.
Cs (swf)		2.554855	.	.	.
H (swf)		2.8620903	.	.	.
K (swf)		1.6350063	.	.	.
Na (swf)		1.7308649	.	.	.
Al (swf)*Temp (oC)		0.0174808	.	.	.
Ca (swf)*Temp (oC)		-0.047406	.	.	.
Cs (swf)*Temp (oC)		-0.009152	.	.	.
H (swf)*Temp (oC)		-0.054186	.	.	.
K (swf)*Temp (oC)		0.0269222	.	.	.
Na (swf)*Temp (oC)		0.0000545	.	.	.

FIGURE D-4. Results from Fitting Heat Capacity Model Using Phase 1 Data @ 80% Saturation – Actual vs. Predicted Heat Capacities (cal/g/^{o}C).

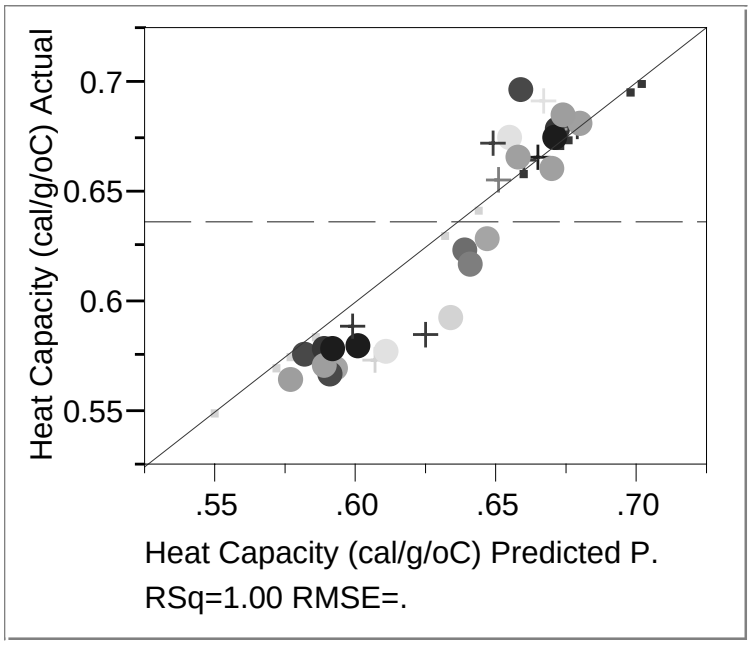

Parameter Estimates

Term		Estimate	Std Error	t Ratio	Prob>|t|
Intercept	Zeroed	0	.	.	.
Al (swf)		0.6546238	.	.	.
Ca (swf)		0.5925133	.	.	.
Cs (swf)		0.5555605	.	.	.
H (swf)		0.7922991	.	.	.
K (swf)		0.6035669	.	.	.
Na (swf)		0.7597277	.	.	.
Al (swf)*Temp (oC)		-0.010985	.	.	.
Ca (swf)*Temp (oC)		-0.000318	.	.	.
Cs (swf)*Temp (oC)		0.0045231	.	.	.
H (swf)*Temp (oC)		-0.00513	.	.	.
K (swf)*Temp (oC)		-0.003778	.	.	.
Na (swf)*Temp (oC)		-0.001728	.	.	.

FIGURE D-5. Overlay Plot of Response versus Model Prediction with ± 15% Error Bands – Density (g/ml) @ 80% Saturation.

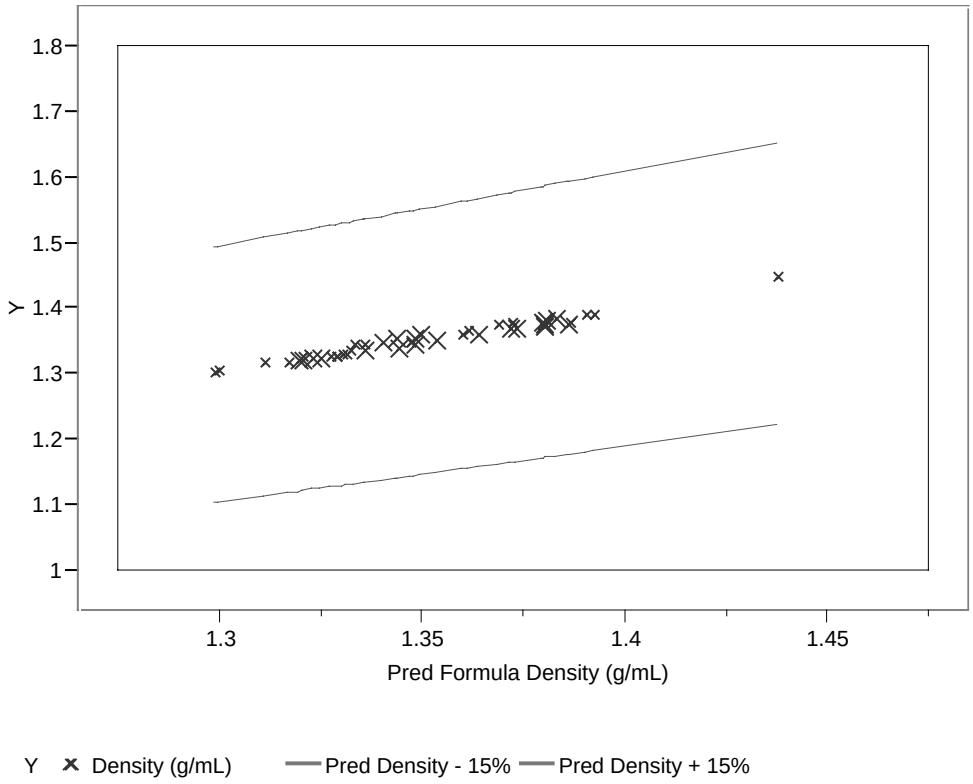

FIGURE D-6. Overlay Plot of Response versus Model Prediction with ± 15% Error Bands – Volume Reduction Factor @ 80% Saturation.

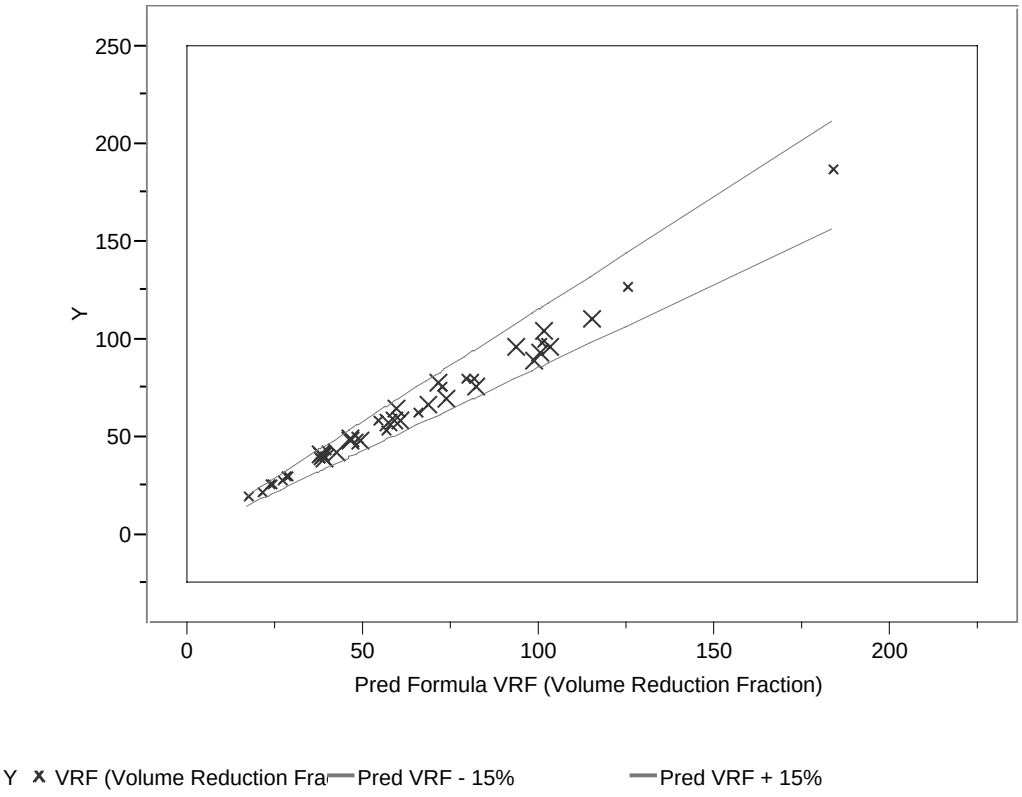

FIGURE D-7. Overlay Plot of Response versus Model Prediction with ± 15% Error Bands – Viscosity (cP) @ 80% Saturation.

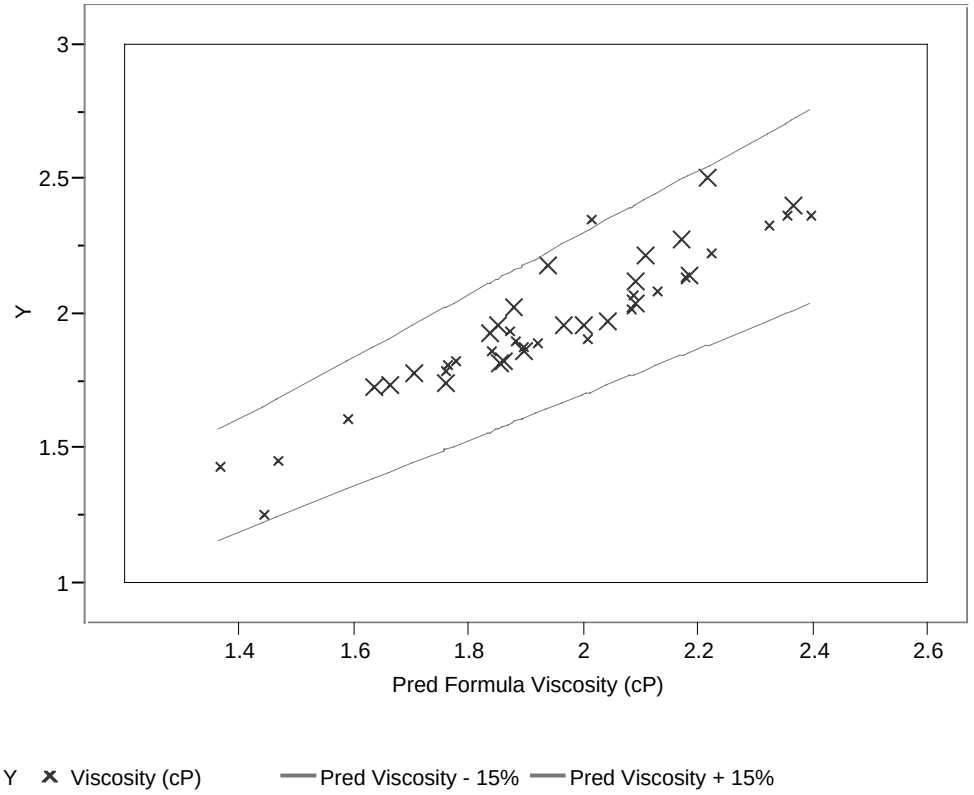

FIGURE D-8. Overlay Plot of Response versus Model Prediction with ± 15% Error Bands – Heat Capacity (cal/g/^{o}C) @ 80% Saturation.

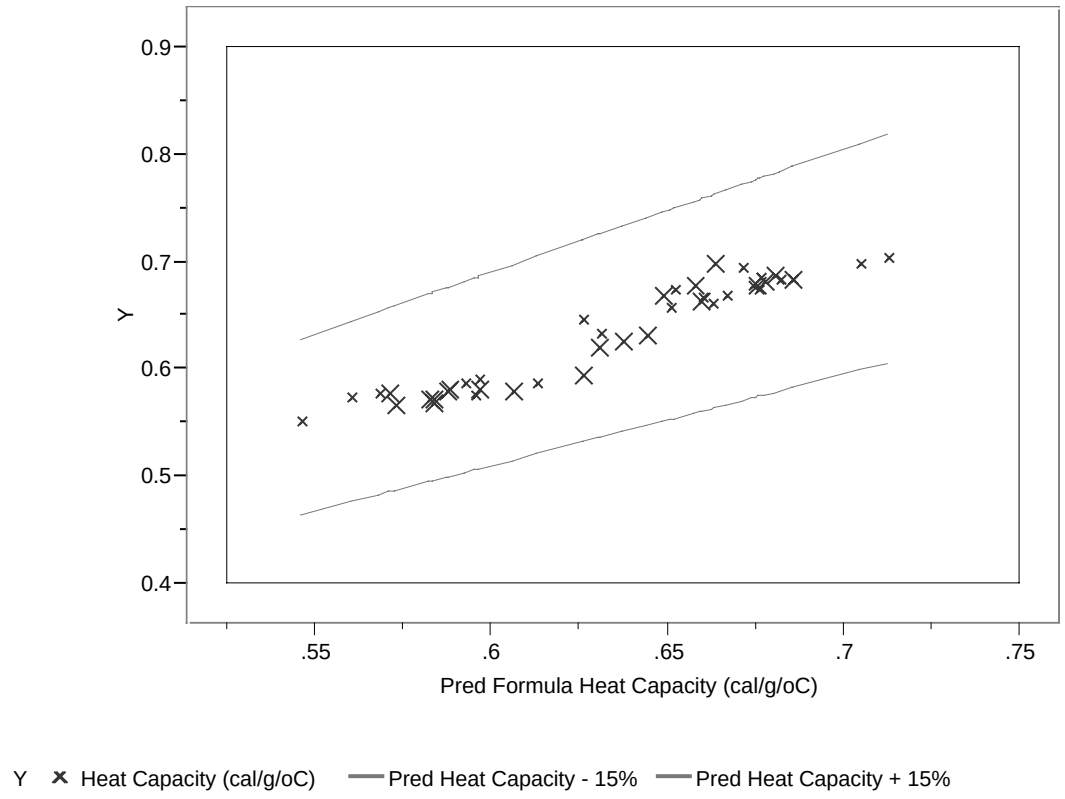

APPENDIX E.

Derivation of Physical Property Models

@ 100% Saturation

EXHIBIT E-1. Responses of Interest @ 100% Saturation vs. Test Factors (Analyte Concentrations in Scaled Weight Fractions).

Solubility (g TS/mL) By Al

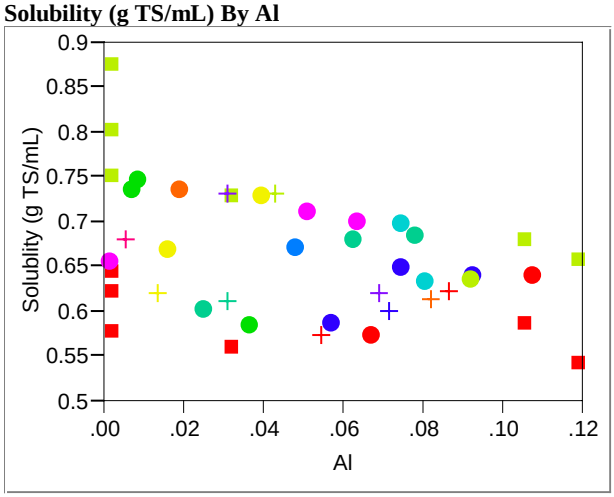

Viscosity (cP) By Al

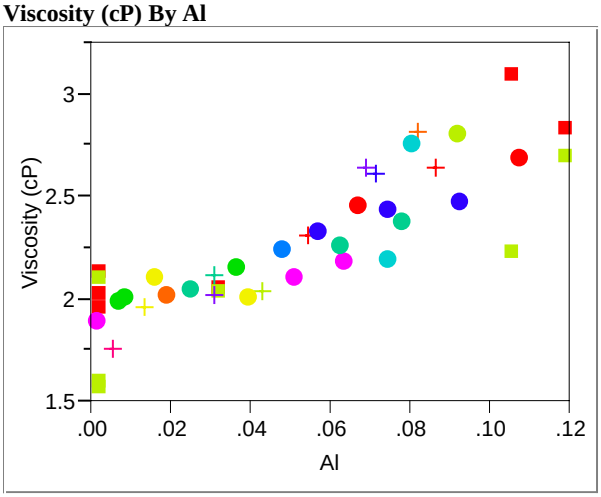

Solubility (g TS/1000 g H2O) By Al

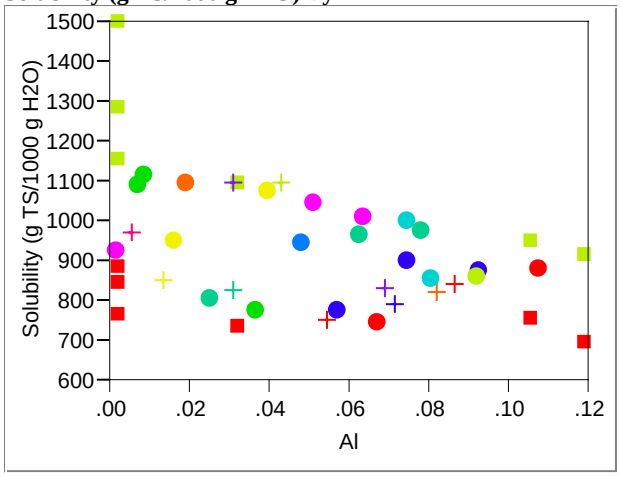

Heat Capacity (cal/g/oC) By Al

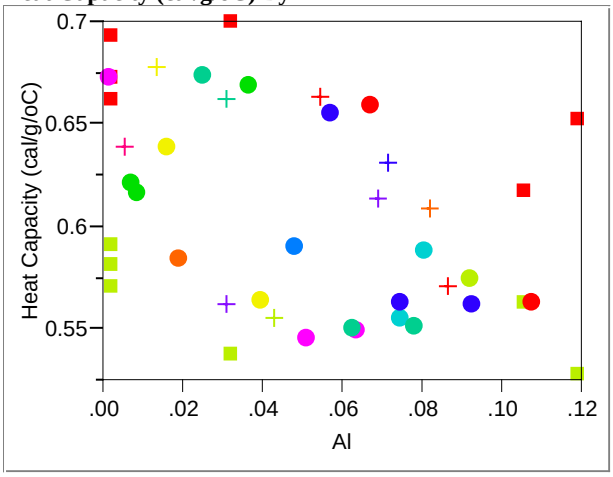

Density (g/mL) By Al

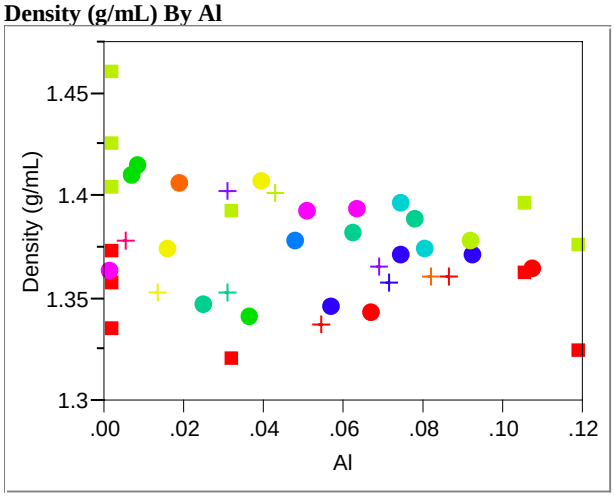

Solubility (g TS/mL) By Ca

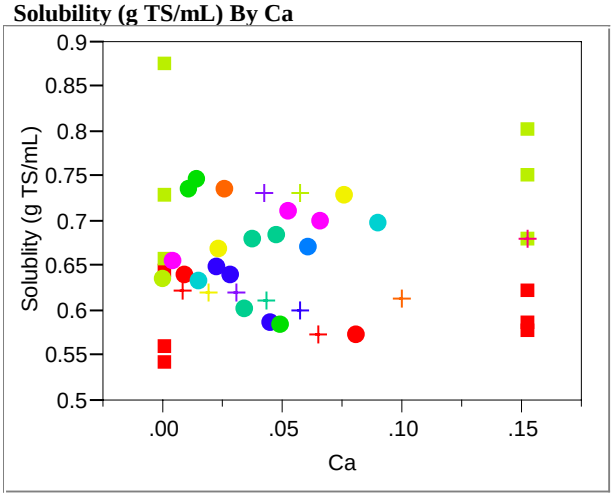

EXHIBIT E-1. Responses of Interest @ 100% Saturation vs. Test Factors *(continued)*
(Analyte Concentrations in Scaled Weight Fractions).

Solubility (g TS/1000 g H2O) By Ca

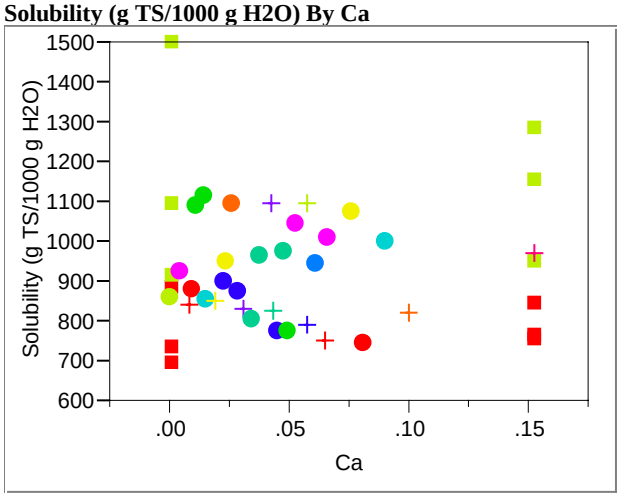

Heat Capacity (cal/g/oC) By Ca

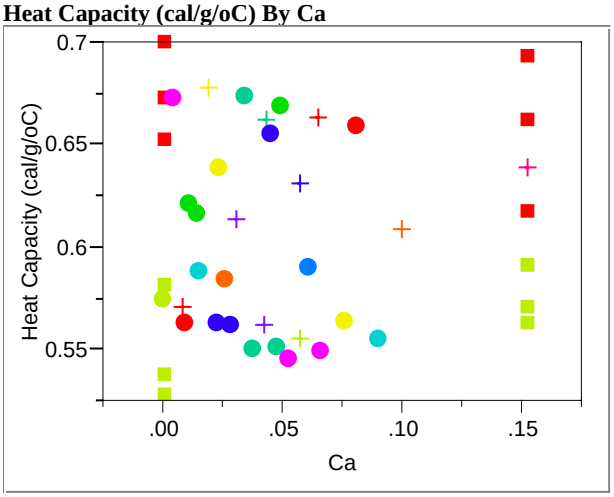

Density (g/mL) By Ca

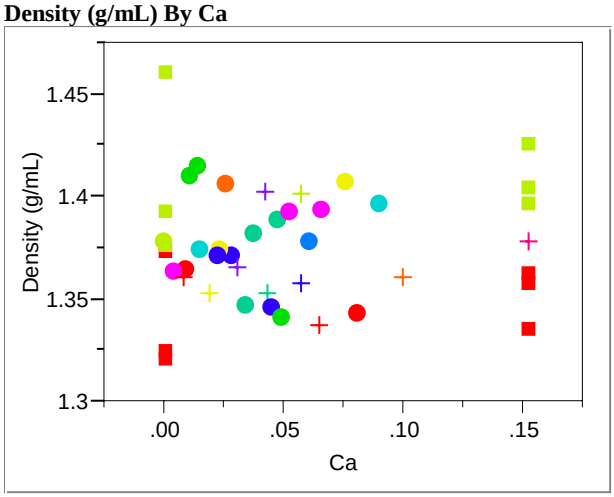

Solubility (g TS/mL) By Cs

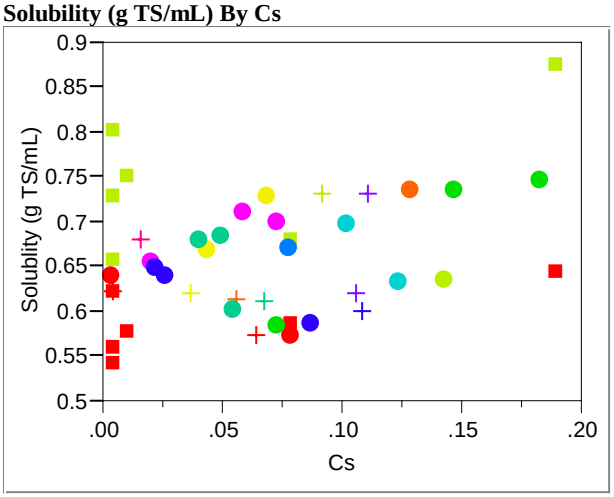

Viscosity (cP) By Ca

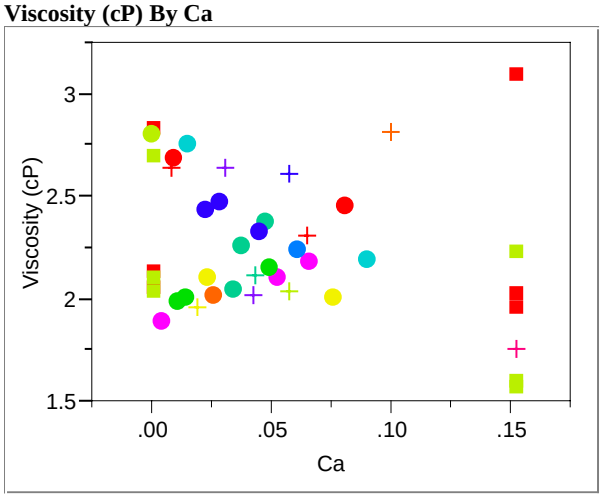

Solubility (g TS/1000 g H2O) By Cs

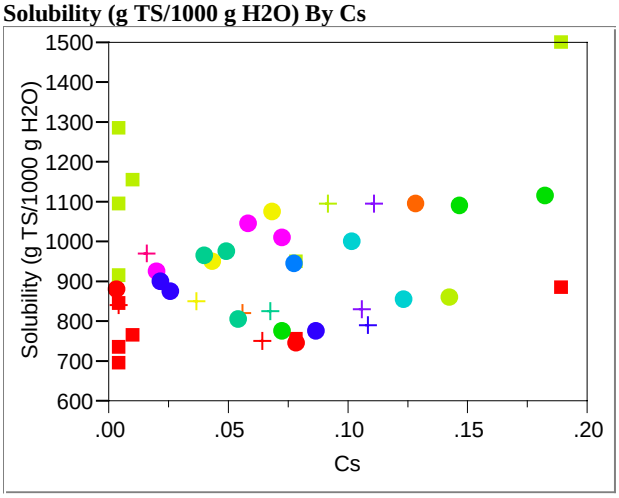

EXHIBIT E-1. Responses of Interest @ 100% Saturation vs. Test Factors *(continued)*
(Analyte Concentrations in Scaled Weight Fractions).

Density (g/mL) By Cs

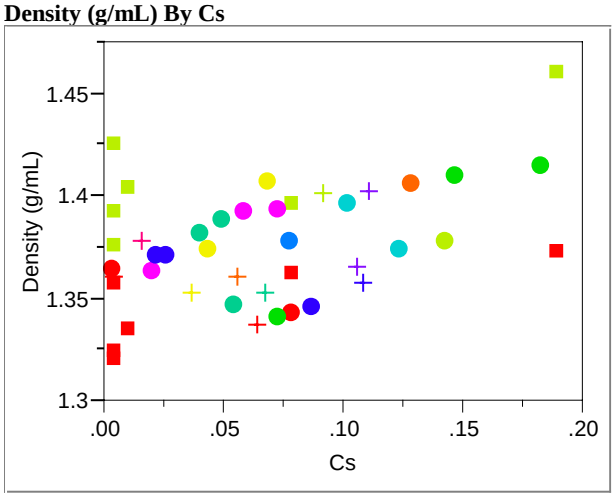

Solubility (g TS/mL) By H

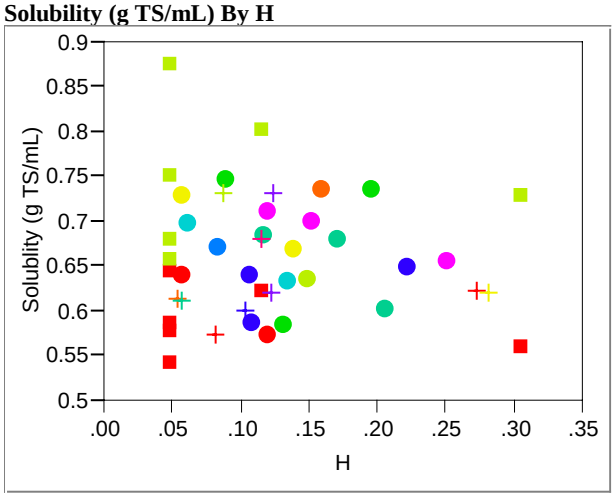

Viscosity (cP) By Cs

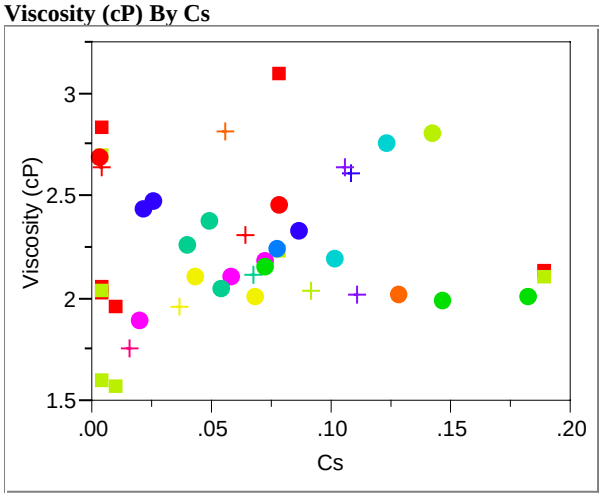

Solubility (g TS/1000 g H2O) By H

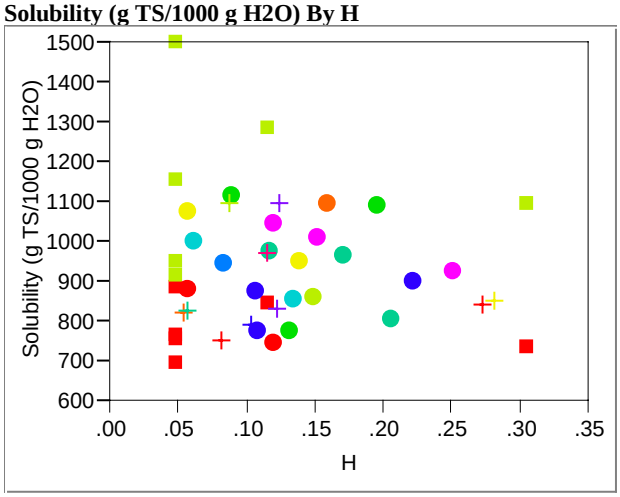

Heat Capacity (cal/g/oC) By Cs

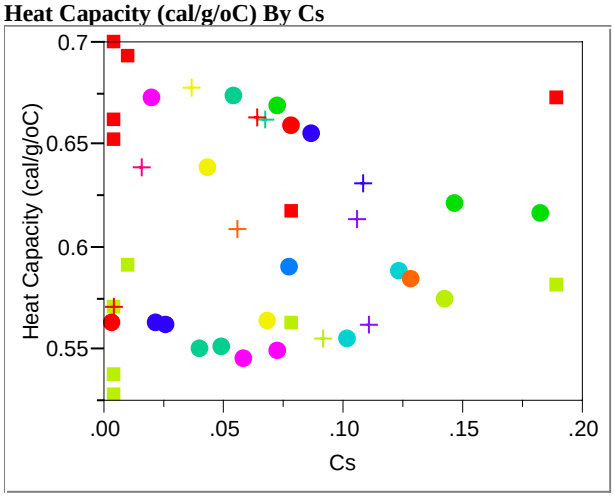

Density (g/mL) By H

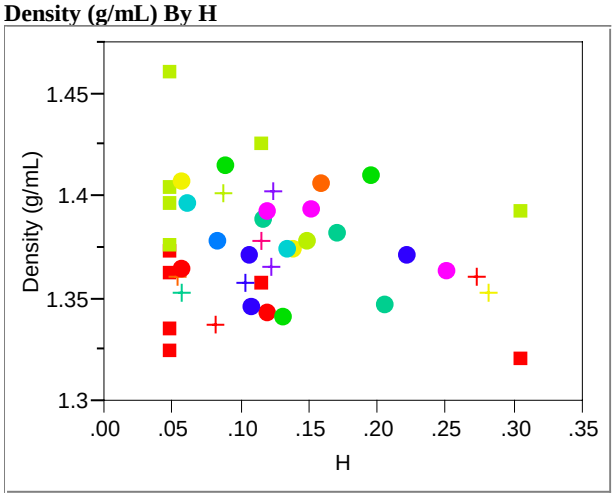

EXHIBIT E-1. Responses of Interest @ 100% Saturation vs. Test Factors *(continued)*
(Analyte Concentrations in Scaled Weight Fractions).

Viscosity (cP) By H

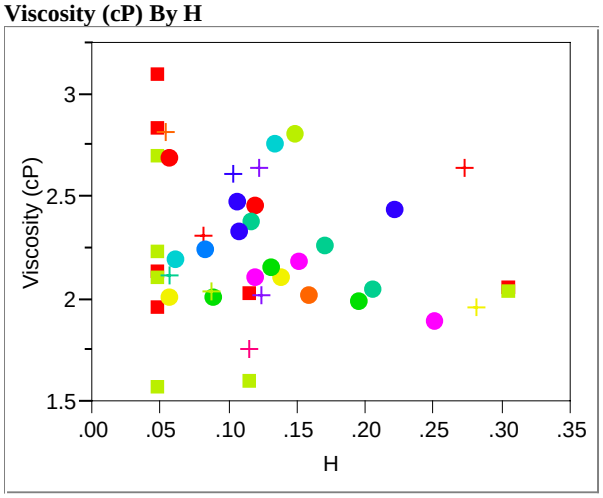

Solubility (g TS/1000 g H2O) By K

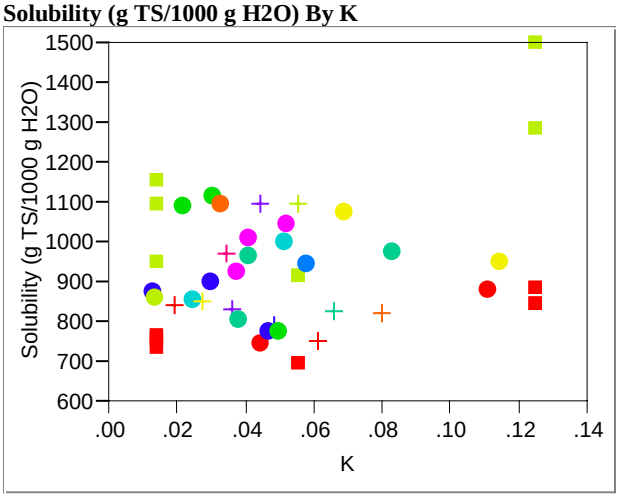

Heat Capacity (cal/g/oC) By H

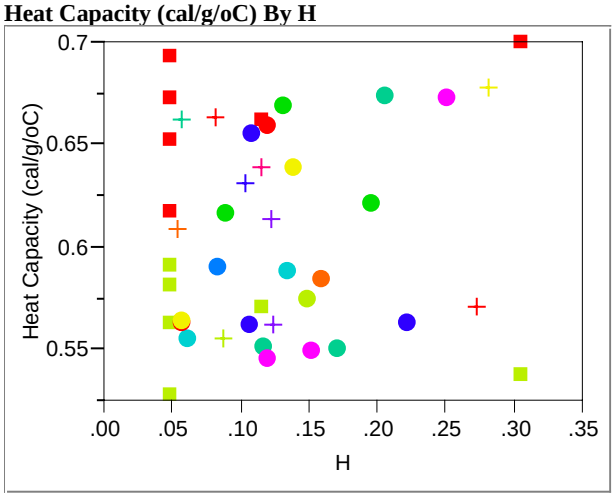

Density (g/mL) By K

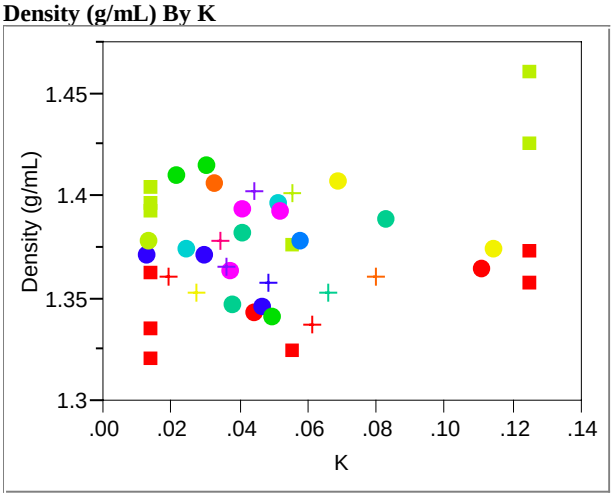

Solubility (g TS/mL) By K

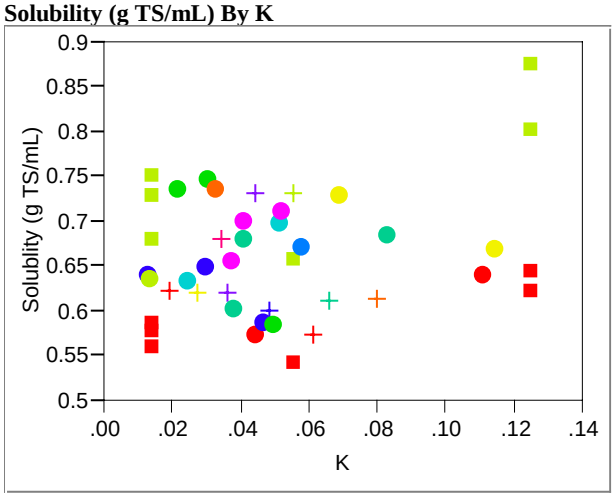

Viscosity (cP) By K

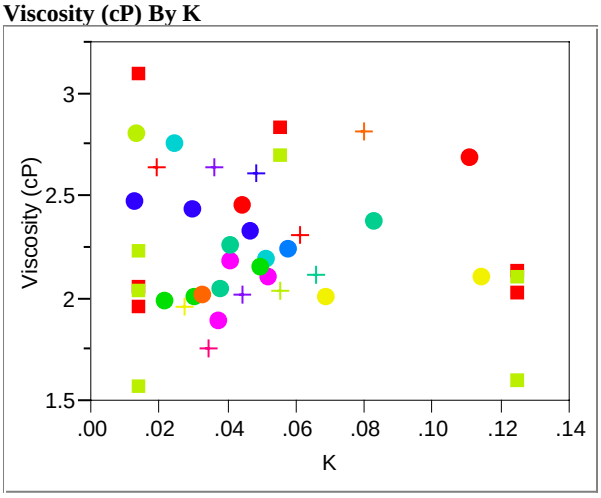

EXHIBIT E-1. Responses of Interest @ 100% Saturation vs. Test Factors *(continued)* (Analyte Concentrations in Scaled Weight Fractions).

Heat Capacity (cal/g/oC) By K

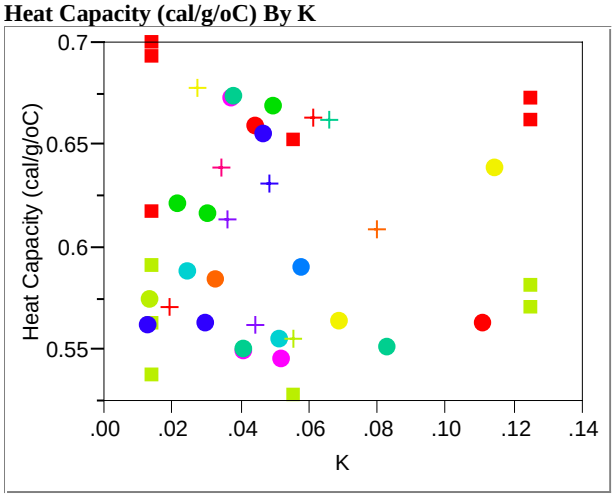

Density (g/mL) By Na

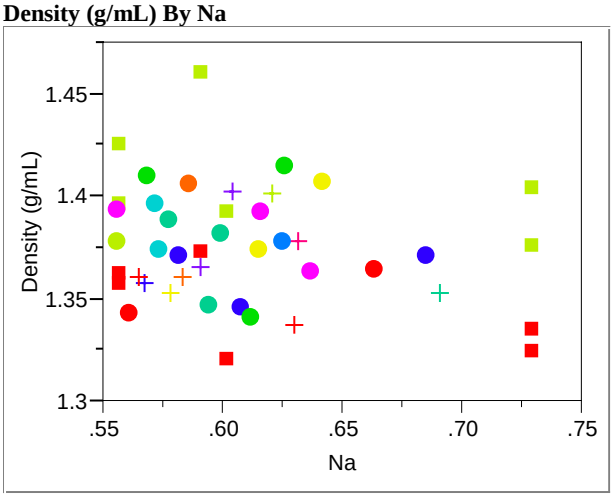

Solubility (g TS/mL) By Na

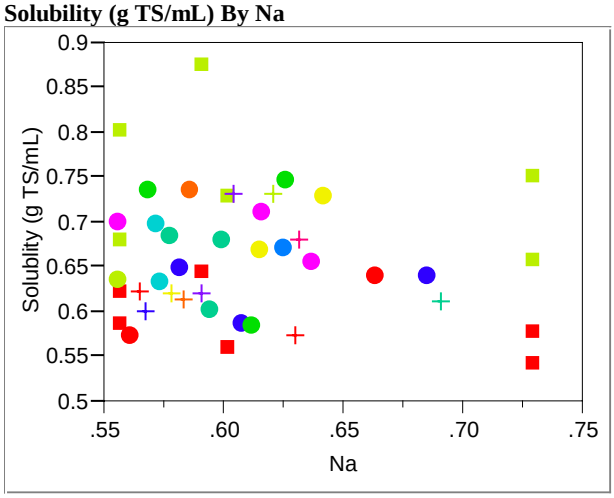

Viscosity (cP) By Na

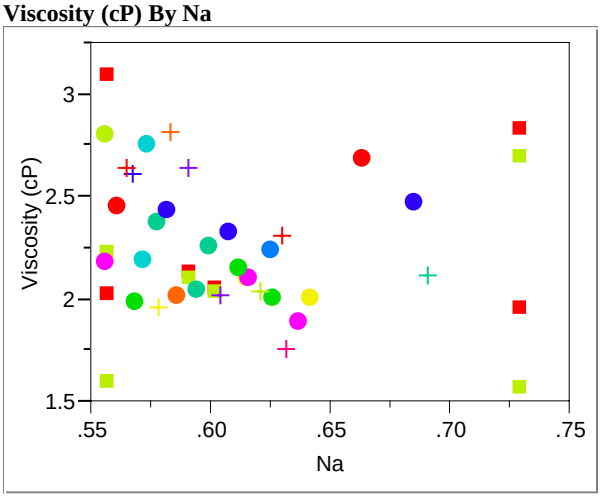

Solubility (g TS/1000 g H2O) By Na

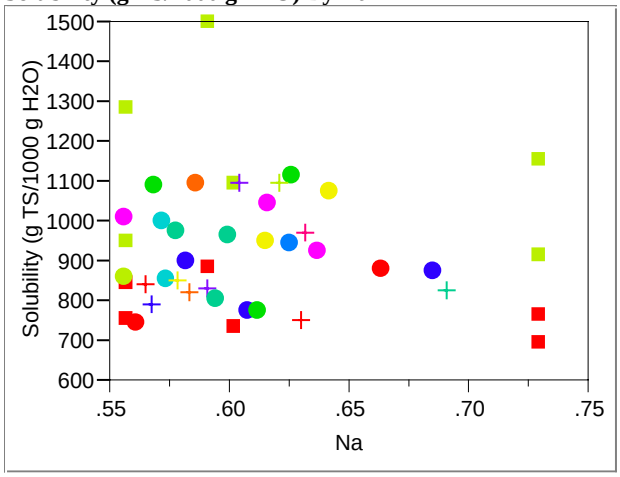

Heat Capacity (cal/g/oC) By Na

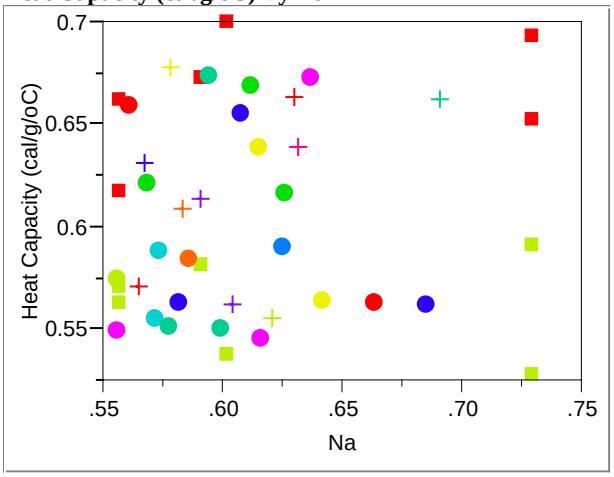

EXHIBIT E-1. Responses of Interest @ 100% Saturation vs. Test Factors *(continued)*
(Analyte Concentrations in Scaled Weight Fractions).

Solubility (g TS/mL) By Temp (oC)

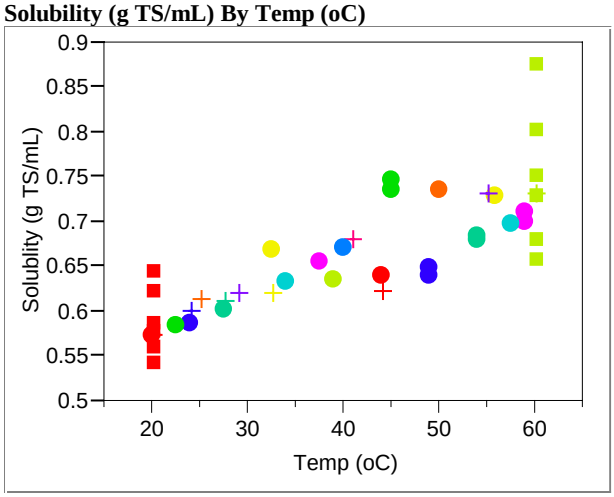

Viscosity (cP) By Temp (oC)

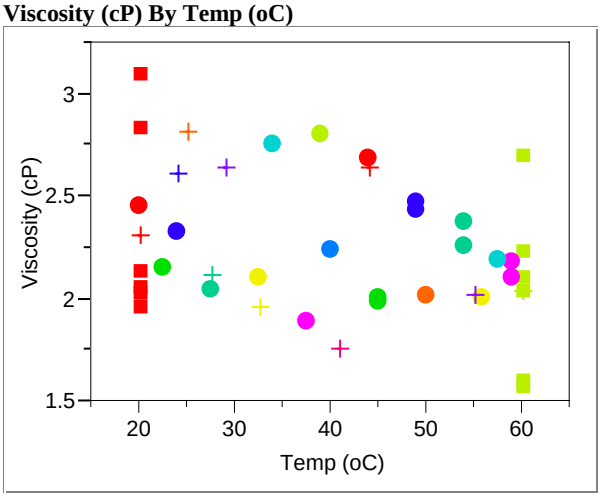

Solubility (g TS/1000 g H2O) By Temp (oC)

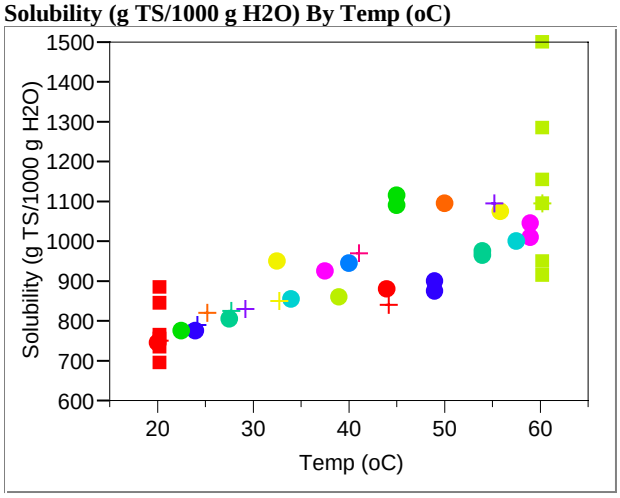

Heat Capacity (cal/g/oC) By Temp (oC)

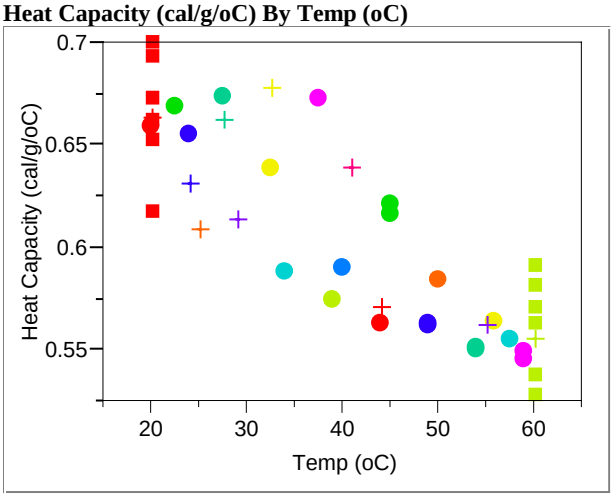

Density (g/mL) By Temp (oC)

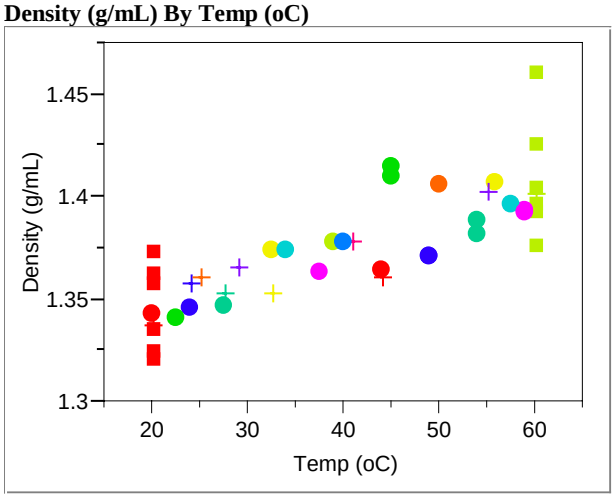

FIGURE E-1. Results from Fitting Solubility Model Using Phase 1 Data @ 100% Saturation – Actual vs. Predicted Solubilities (g TS/ml).

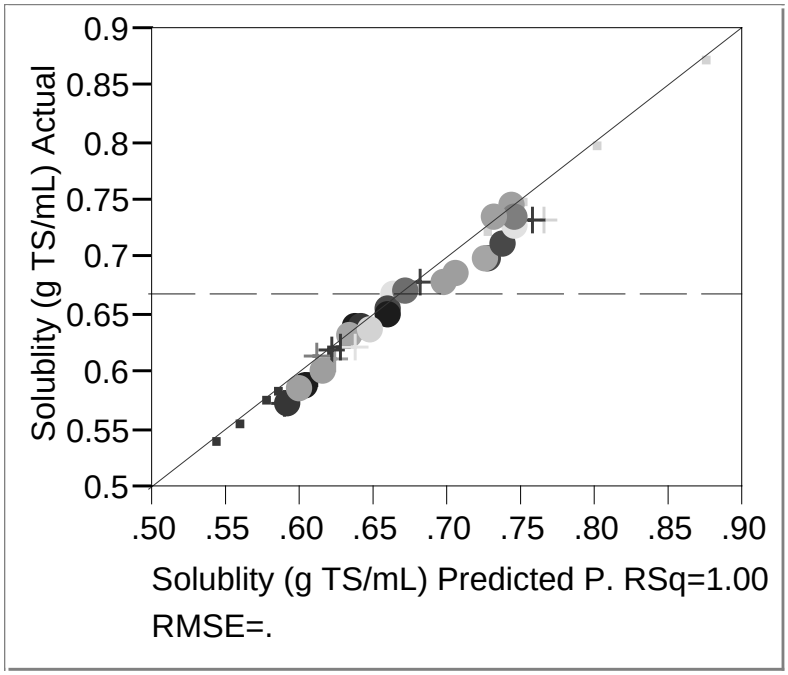

Parameter Estimates

Term		Estimate	Std Error	t Ratio	Prob>|t|
Intercept	Zeroed	0	.	.	.
Al (swf)		0.6909342	.	.	.
Ca (swf)		0.7407277	.	.	.
Cs (swf)		0.6963723	.	.	.
H (swf)		0.5256042	.	.	.
K (swf)		0.7292421	.	.	.
Na (swf)		0.4289797	.	.	.
Al (swf)*Temp (oC)		-0.014424	.	.	.
Ca (swf)*Temp (oC)		-0.000168	.	.	.
Cs (swf)*Temp (oC)		0.0071146	.	.	.
H (swf)*Temp (oC)		0.0039702	.	.	.
K (swf)*Temp (oC)		0.0075014	.	.	.
Na (swf)*Temp (oC)		0.0052366	.	.	.

FIGURE E-2. Results from Fitting Solubility Model Using Phase 1 Data @ 100% Saturation – Actual vs. Predicted Solubilities (g TS/1000 g H2O).

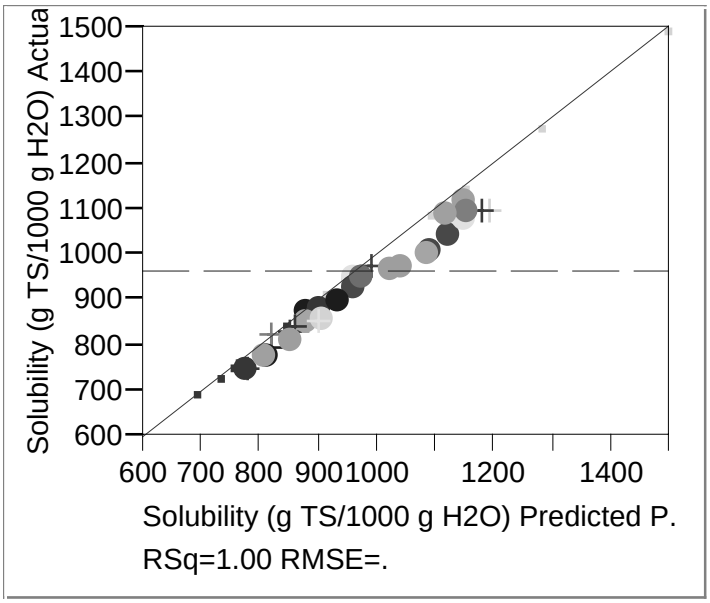

Parameter Estimates

Term		Estimate	Std Error	t Ratio	Prob>|t|
Intercept	Zeroed	0	.	.	.
Al (swf)		1135.2444	.	.	.
Ca (swf)		991.3732	.	.	.
Cs (swf)		690.79906	.	.	.
H (swf)		641.25974	.	.	.
K (swf)		858.75765	.	.	.
Na (swf)		468.17074	.	.	.
Al (swf)*Temp (oC)		-41.64385	.	.	.
Ca (swf)*Temp (oC)		-0.089121	.	.	.
Cs (swf)*Temp (oC)		23.775567	.	.	.
H (swf)*Temp (oC)		8.6191364	.	.	.
K (swf)*Temp (oC)		24.497899	.	.	.
Na (swf)*Temp (oC)		11.452254	.	.	.

FIGURE E-3. Results from Fitting Density Model Using Phase 1 Data @ 100% Saturation – Actual vs. Predicted Densities (g/ml).

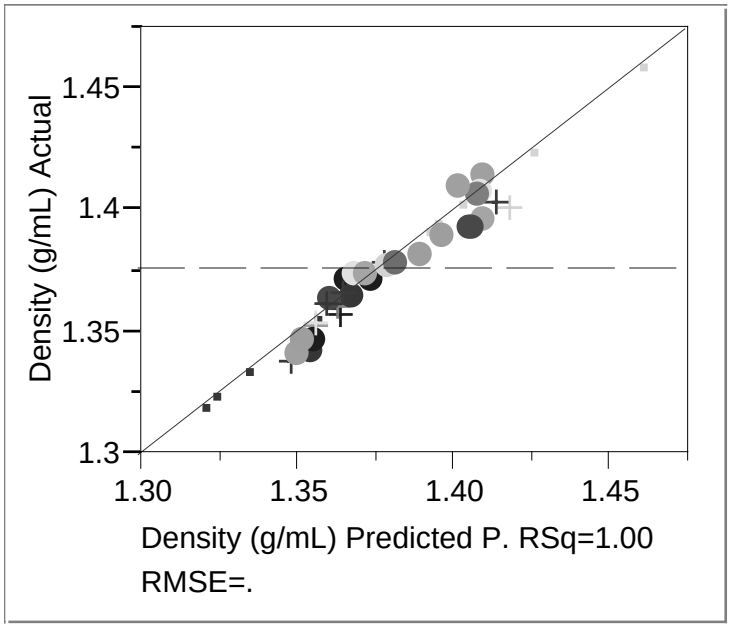

Parameter Estimates

Term		Estimate	Std Error	t Ratio	Prob>|t|
Intercept	Zeroed	0	.	.	.
Al (swf)		1.499099	.	.	.
Ca (swf)		1.4898524	.	.	.
Cs (swf)		1.5039588	.	.	.
H (swf)		1.3135428	.	.	.
K (swf)		1.4194698	.	.	.
Na (swf)		1.2542089	.	.	.
Al (swf)*Temp (oC)		-0.005493	.	.	.
Ca (swf)*Temp (oC)		-0.000876	.	.	.
Cs (swf)*Temp (oC)		0.0018509	.	.	.
H (swf)*Temp (oC)		0.0015725	.	.	.
K (swf)*Temp (oC)		0.002703	.	.	.
Na (swf)*Temp (oC)		0.0022651	.	.	.

FIGURE E-4. Results from Fitting Viscosity Model Using Phase 1 Data @ 100% Saturation – Actual vs. Predicted Viscosities (cP).

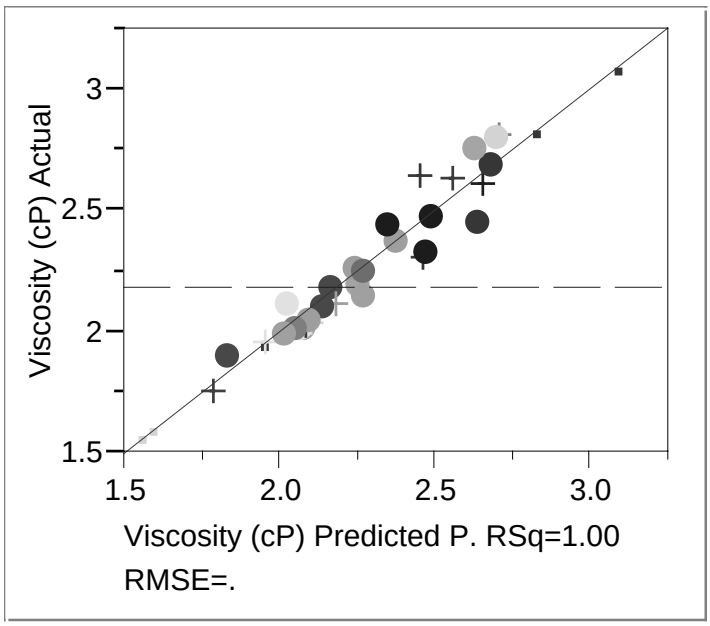

Parameter Estimates

Term		Estimate	Std Error	t Ratio	Prob>|t|
Intercept	Zeroed	0	.	.	.
Al (swf)		12.293764	.	.	.
Ca (swf)		5.1399655	.	.	.
Cs (swf)		4.2544038	.	.	.
H (swf)		2.121379	.	.	.
K (swf)		2.0016051	.	.	.
Na (swf)		1.4741728	.	.	.
Al (swf)*Temp (oC)		-0.075586	.	.	.
Ca (swf)*Temp (oC)		-0.094707	.	.	.
Cs (swf)*Temp (oC)		-0.031712	.	.	.
H (swf)*Temp (oC)		-0.00933	.	.	.
K (swf)*Temp (oC)		0.008471	.	.	.
Na (swf)*Temp (oC)		0.0080326	.	.	.

FIGURE E-5. Results from Fitting Heat Capacity Model Using Phase 1 Data @ 100% Saturation – Actual vs. Predicted Heat Capacities (cal/g/^{o}C).

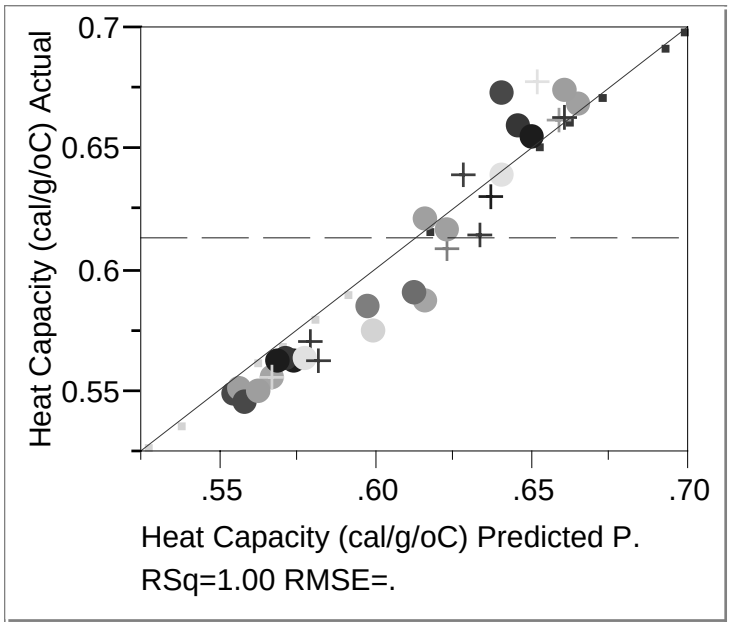

Parameter Estimates

Term		Estimate	Std Error	t Ratio	Prob>|t|
Intercept	Zeroed	0	.	.	.
Al (swf)		0.1210916	.	.	.
Ca (swf)		0.3954999	.	.	.
Cs (swf)		0.5080372	.	.	.
H (swf)		0.7787816	.	.	.
K (swf)		0.5256207	.	.	.
Na (swf)		0.8223346	.	.	.
Al (swf)*Temp (oC)		0.0021022	.	.	.
Ca (swf)*Temp (oC)		0.0048314	.	.	.
Cs (swf)*Temp (oC)		0.0029858	.	.	.
H (swf)*Temp (oC)		-0.004905	.	.	.
K (swf)*Temp (oC)		-0.001046	.	.	.
Na (swf)*Temp (oC)		-0.004036	.	.	.

FIGURE E-6. Overlay Plot of Response versus Model Prediction with ± 15% Error Bands – Solubility (g TS/mL) @ 100% Saturation.

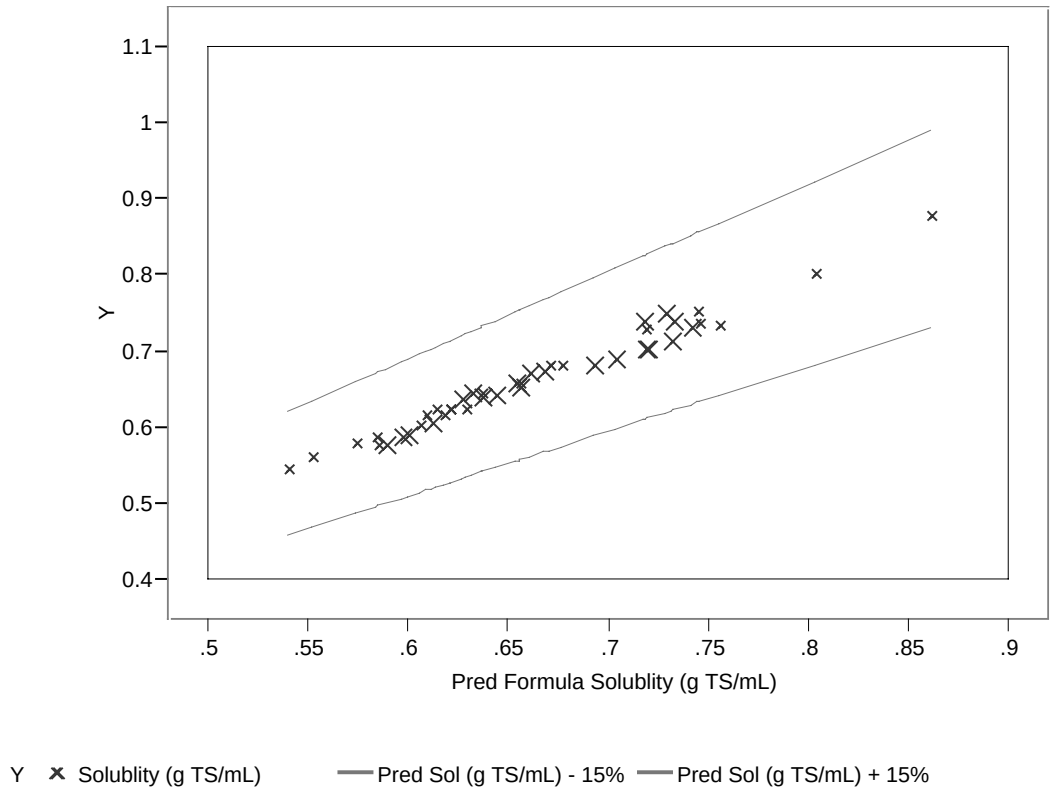

<u>FIGURE E-7</u>. Overlay Plot of Response versus Model Prediction with ± 15% Error Bands – Solubility (g TS/1000 g H_2O)) @ 100% Saturation.

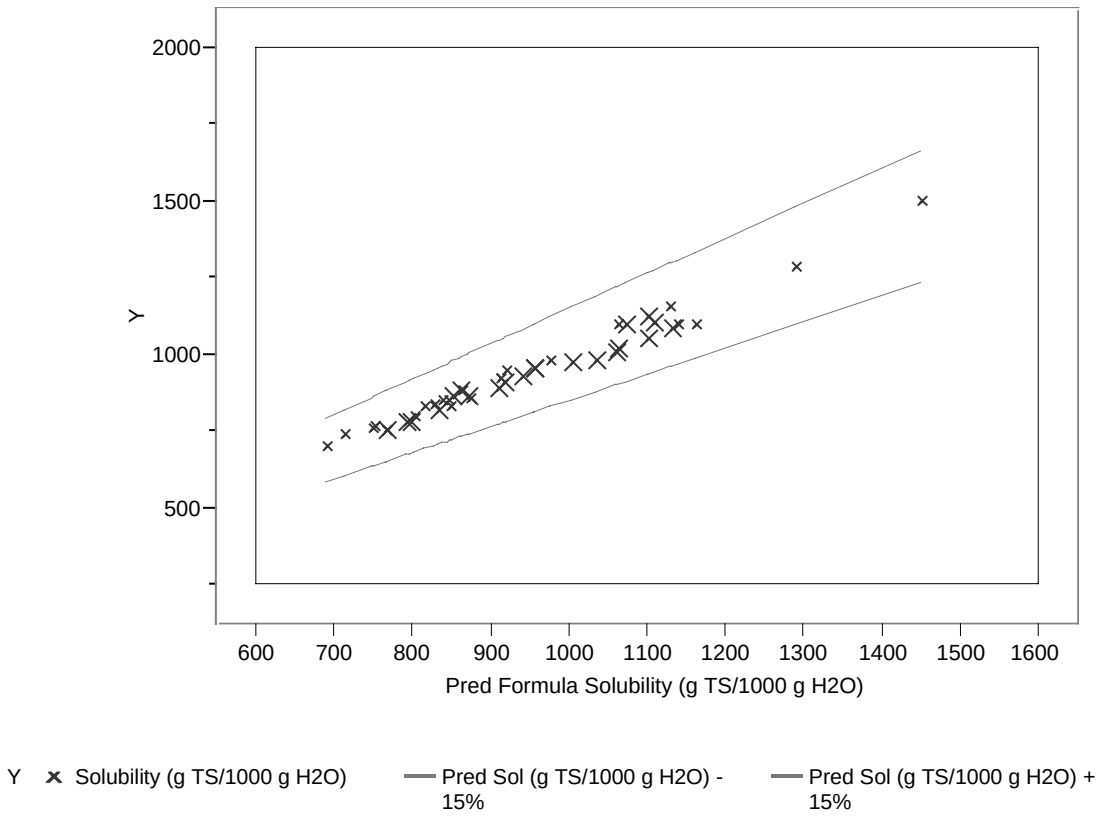

FIGURE E-8. Overlay Plot of Response versus Model Prediction with ± 15% Error Bands – Density (g/mL) @ 100% Saturation.

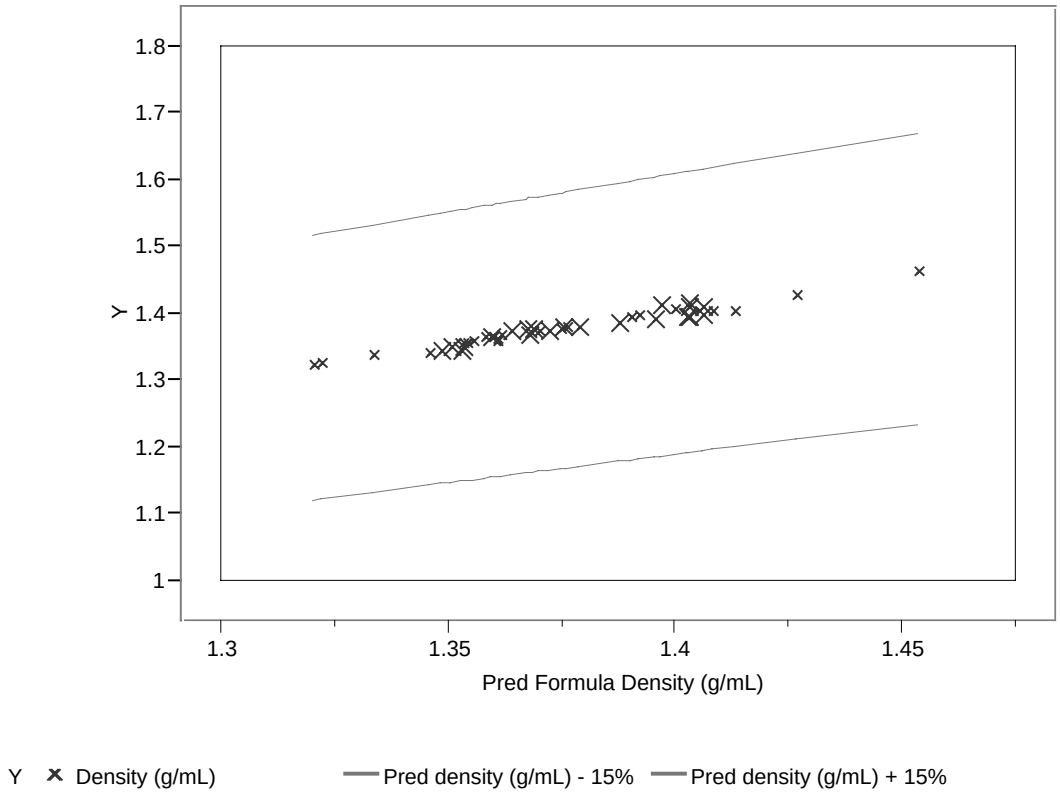

FIGURE E-9. Overlay Plot of Response versus Model Prediction with ± 15% Error Bands – Viscosity (cP) @ 100% Saturation.

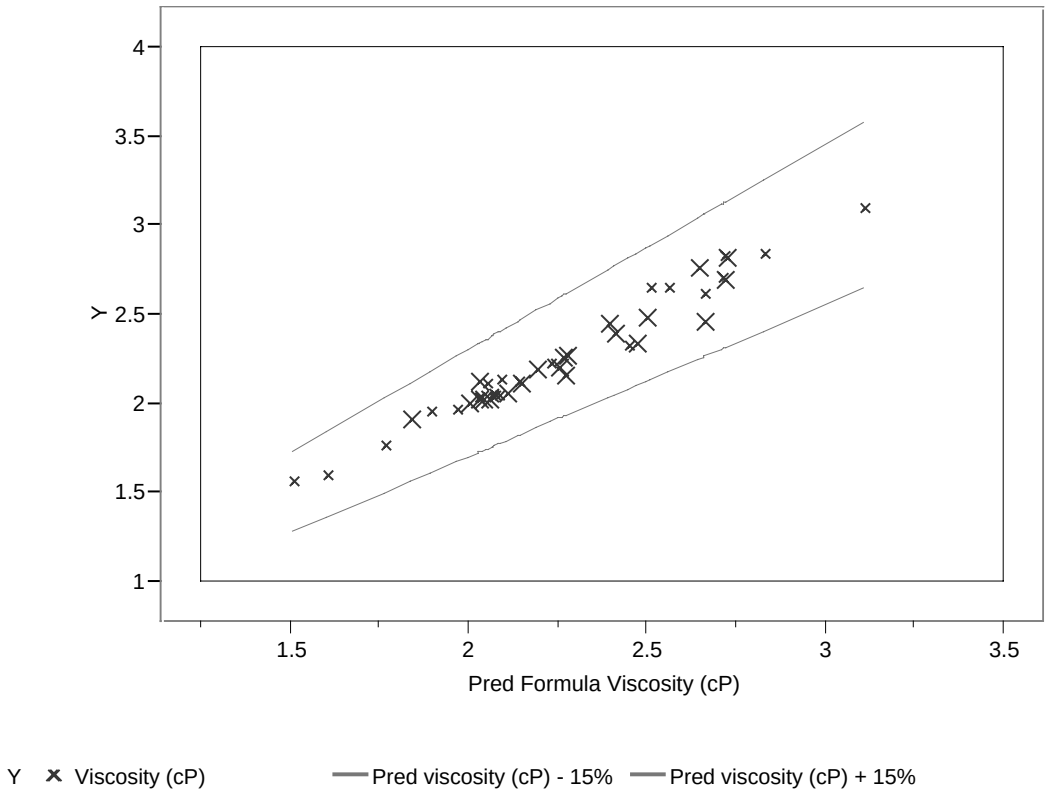

FIGURE E-10. Overlay Plot of Response versus Model Prediction with ± 15% Error Bands – Heat Capacity (cal/g/^{o}C) @ 100% Saturation.

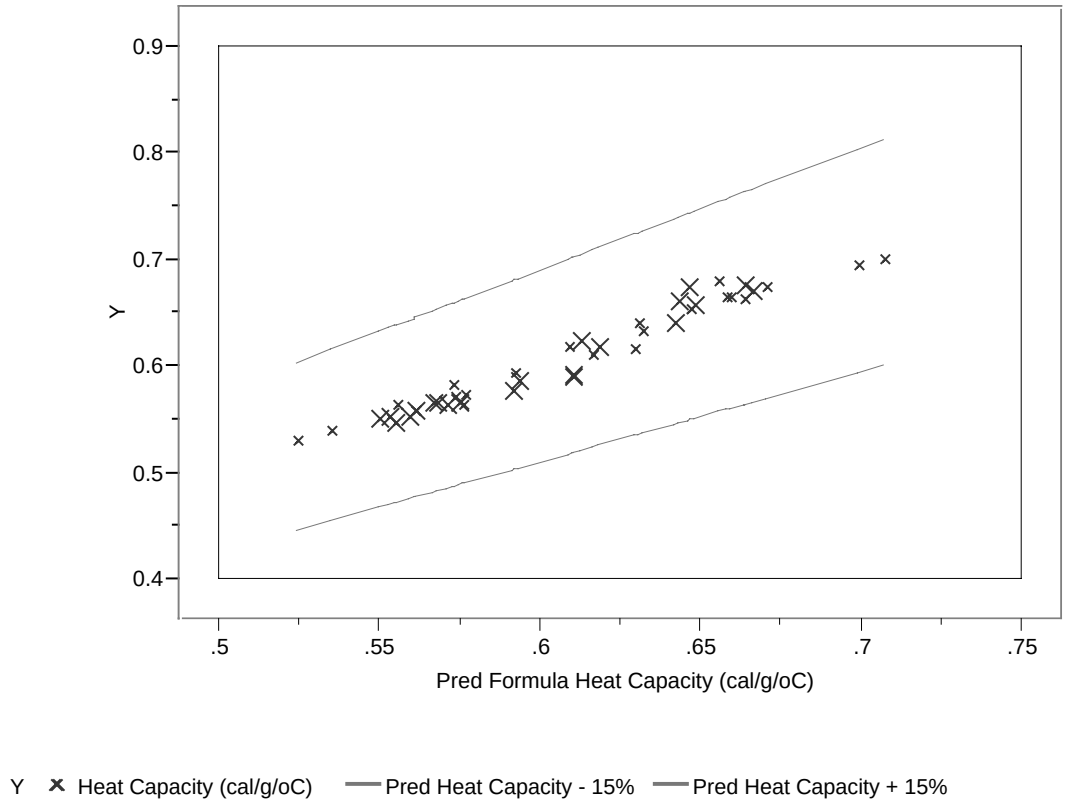

This page left intentionally blank.

APPENDIX F.

Sample Calculations

Application of Table 1.2 for Prediction of the Physical Properties of AZ-102 TFL Cesium Eluate

The composition of AZ-102 cesium eluate produced during the TFL bench-scale IX run is given in Table F-1 [16].

TABLE F-1. Composition of AZ-102 TFL Cesium Eluate

	(mg/L)	Cation mole %			(mg/L)
Na	1520	11.25		S (ICPES)	13.4
Al	3.70	0.01			
Ca	5.43	0.01		NO3	34000
Cr	59.3	0.17		F	<20
Cu	2.88	0.00		Cl	<20
Fe	5.18	0.01		SO4	33
K	25.8	0.11		PO4	<100
Cs	7.41	0.00		C2O4	<100
Total Acid (M)	0.52	88.47		TOC	52.8
Free Acid (M)	0.52			TIC	11.5
Density (g/cc)	1.0198				

The scaled weight fractions (SWF) of the six major cations selected in this study were next calculated from the data given in Table F-1. It is shown in Table F-2 that the resulting concentrations of all six major cations except potassium are within the ranges given in Table 1.1 for the physical property models. However, since the concentration of potassium is still just 12% below the lower bound, which is well within the typical analytical error of ±15%, all the physical property models derived in this study should be equally applicable for potassium.

TABLE F-2. Scaled Weight Fractions of Six Major Cations Selected in this Study.

	(mg/L)	(SWF)	min (SWF)	max (SWF)
Al	3.7	0.00178	0.0017	0.1243
Ca	5.43	0.00261	0	0.1597
Cs	7.41	0.00356	0.0036	0.1983
H	520	0.24972	0.05	0.3188
K	25.8	0.01239	0.0141	0.1309
Na	1520	0.72995	0.5834	0.7641
total major	2082.34	1		
Cr	59.3			
Cu	2.88			
Fe	5.18			
total minor	67.36			
total minor (wt% total cation)		3.13		

The SWF concentrations given in Table F-2 were next substituted into the Eq. (1.1) along with the values of the coefficients given in Table 1.2 for each property.

Volume Reduction Factor at 20 ^{o}C:

$$\begin{aligned} VRF &= (139.01782)(0.00178) + (48.97029)(0.00261) + (27.90272)(0.00356) \\ &= +(63.09169)(0.24972) + (54.90814)(0.01239) - (11.80459)(0.72995) \\ &\quad + \begin{bmatrix} (-3.30647)(0.00178) + (-1.07174)(0.00261) + (0.58164)(0.00356) \\ +(7.73972)(0.24972) + (-0.48689)(0.01239) + (0.52935)(0.72995) \end{bmatrix} (20) \\ &= 54.4 \end{aligned}$$

Density at 100% saturation and 25 ^{o}C :

$$\begin{aligned} \rho_{25\,C}^{sat} &= (1.48886)(0.00178) + (1.47408)(0.00261) + (1.50460)(0.00356) \\ &= +(1.31406)(0.24972) + (1.42237)(0.01239) + (1.25453)(0.72995) \\ &\quad + \begin{bmatrix} (-0.00619)(0.00178) + (-0.00111)(0.00261) + (0.00147)(0.00356) \\ +(0.00142)(0.24972) + (0.00209)(0.01239) + (0.00240)(0.72995) \end{bmatrix} (25) \\ &= 1.3264 \ \ g/ml \end{aligned}$$

Solubility at 25 ^{o}C:

$$\begin{aligned} S_{25\,C} &= (0.73699)(0.00178) + (0.74161)(0.00261) + (0.69789)(0.00356) \\ &= +(0.51292)(0.24972) + (0.77862)(0.01239) + (0.42178)(0.72995) \\ &\quad + \begin{bmatrix} (-0.01693)(0.00178) + (-0.00097)(0.00261) + (0.00599)(0.00356) \\ +(0.00356)(0.24972) + (0.00590)(0.01239) + (0.00559)(0.72995) \end{bmatrix} (25) \\ &= 0.5771 \ \ g\,TS/ml \end{aligned}$$